Development of Microcantilever Biosensing Platforms

Wenxing Wang

Submitted for the degree of Doctor of Philosophy

Heriot-Watt University

School of Engineering and Physical Sciences

April 2013

Abstract

Microcantilever sensor system as a promising field attracted much attention recently. This system has the potential to be applied for a biosensing technology which is parallel reference, label free, sensitive and real time. In this thesis, polyimide has been selected as a material to fabricate cantilever due to its excellent physical, electrical and mechanical properties, on top of its cost advantage. Importantly, we showed it is feasible to microfabricate large array of microcantilever sensors with high-power UV laser directly. It is low cost and rapid, the parameters for laser direct writing fabrication has been studied. The thesis also shows that it is possible to functionalise the polyimide film first and subsequently cut it to functionalised cantilever sensor array.

The unique fabrication and functionalisation process can solve the problem of high-cost microfabrication using silicon and low-efficient functionalisation using capillary tubing all together. In addition, the fabrication process has been further developed to avoid the problem of the cross contamination from receptors on both sides. With this improvement, we developed an internally referenced microcantilever biosensors system for DNA hybridization detection. Different receptors can be coated on each side of the polymer film before fabricating to cantilever biosensors This newly developed capability enables us to coat receptors with similar but slightly different biological properties on each side of the cantilever sensor, a process which is extremely difficult by using conventional capillary tubing methods due to the possibility of thiol exchange on surfaces and hence cross-contamination.

A polyimide microcantilever sensor with embedded microfluidic channel has been developed in this thesis. Photoresist material is used to form the precise microfluidic channel within the microcantilever device. The multilayer polymer film device is still soft enough to operate in static mode. The main advantage of the system presented here is that since the device is made entirely of polymer materials, the fabrication process is simple and low-cost. The magnetic beads have been used to amplify the signal of the biosensing processing; the application of polyimide microfluidic microcantilevers to the

detection of Cryptosporidium and thrombin is reported in this thesis.

Paper based autonomous micocantilever system has also been investigated in this thesis. We build a cantilever system without external pump or force with paper and magnetic field. The limitation of the system is that it takes too much time to pump magnetic beads through the cantilever with capillary. However, we found that it has the potential to develop a long time range timer based on the slowest property. Different methods have been investigated to slow down the speed, when liquid pass through the paper microfluidic. Finally, we demonstrate some timer devices whose ranges are from minutes to month. The devices have the potential to be used as time-based diagnostic assays, food label, etc.

Acknowledgements

I am appreciative for the support and help of my supervisor Dr. Will Shu. He spent much time during these years to teach me how to research, give me feedback and help me to modify the thesis. I also thank Prof. Bob Reuben for his help and suggestions.

I thank Dr Yifan Liu for his help on the Labview, laser fabrication and paper modification. I would like to thank Dr Baixin Chen and Wei Wei for the simulation work for the paper based microfluidic system. I also thank Dr Jining Sun and Marian Millar who spend much time to measure cantilevers by SEM for me. I am grateful to Depack for his assistance during the polyimide based cantilever fabrication. I thank Deppy and Helen for their help on the crypto experiment.

At last, and as always, I am extremely grateful towards my wife and parents, for their continued support and encouragement during these years.

ACADEMIC REGISTRY

Research Thesis Submission

Name:	Wenxing Wang		
School/PGI:	School of Engineering and Physical Sciences		
Version: *(i.e. First, Resubmission, Final)*	Final	Degree Sought (Award and Subject area)	PhD Mechanical Engineering

Declaration

In accordance with the appropriate regulations I hereby submit my thesis and I declare that:

1) the thesis embodies the results of my own work and has been composed by myself
2) where appropriate, I have made acknowledgement of the work of others and have made reference to work carried out in collaboration with other persons
3) the thesis is the correct version of the thesis for submission and is the same version as any electronic versions submitted*.
4) my thesis for the award referred to, deposited in the Heriot-Watt University Library, should be made available for loan or photocopying and be available via the Institutional Repository, subject to such conditions as the Librarian may require
5) I understand that as a student of the University I am required to abide by the Regulations of the University and to conform to its discipline.

*   *Please note that it is the responsibility of the candidate to ensure that the correct version of the thesis is submitted.*

Signature of Candidate:		Date:	

Submission

Submitted By *(name in capitals)*:	WENXING WANG
Signature of Individual Submitting:	
Date Submitted:	

For Completion in the Student Service Centre (SSC)

Received in the SSC by *(name in capitals)*:			
Method of Submission *(Handed in to SSC; posted through internal/external mail):*			
E-thesis Submitted (*mandatory for final theses*)			
Signature:		Date:	

Table of Contents

Abbreviations

AFM	Atomic force microscope
CAD	Computer aided design
CCD	Charge coupled device
COMS	Complementary metal-oxide semiconductor
DNA	Deoxyribonucleic acid
EBEAM	Electron beam
MEMS	Microelectromechanical
NEMS	Nanelectromechanical
NP	Nanoparticle
PBS	Phosphate buffered solution
PEEK	Polyether-ether-ketone
PDMS	Polydimethylsiloxane
PMMA	Poly(methyl methacrylate)
PSD	Position sensitive device
SEM	Scanning electron microscope
SPR	Surface plasmon resonance

List of Publications

J.D. Shephard, D. Varadam, W. Wang, Y. Liu, J.P. Parry, D.P. Hand, W. Shu. Direct Writing Large Arrays of Microcantilevers for bio-MEMS Devices, *Proceedings of LAMP2009 Conference* (2009)

Y. Liu, L. Schweizer, W. Wang, R.L. Reuben, M. Schweizer, W. Shu. Real-time Monitoring of Yeast Cell Growth by the Bending of Polymer Microcantilever

Biosensors, *Sensors and Actuators: Chemical* (Accepted)

W. Wang, Y. Liu, W. Shu, Static Mode Microfluidic Cantilever System, *Lab on a Chip* (Submitted)

Y. Liu, W. Wang, W. Shu. Nanomechanical Cantilever Sensors: Theory and Applications, *Nanosensors: Theory and Applications in Industry, Healthcare, and Defense.* (2010)

List of tables

Chapter 1   Introduction

1.1   Microcantilever sensors

Developing new generation of biosensors is significant for clinic and environmental monitor. Currently,tow types of biosensing tools have been applied for biosensing, i,e. surface plasmon resonance (SPR), quartz crystal microbalances (QCM). However, both of them have some disadvantages, for example no parallel reference. A new technique of cantilever arrays can not only solve these problems but also provide some advantages, such as label free, high sensitive, real time, massive parallelization [1]. Recently, silicon based microcantilever which was traditionally used for atomic force microscopy (AFM), it has been used as a real-time monitoring of biomolecular interaction, such as DNA, protein, etc. Subsequently, I will introduce the basic theory and application of microcantilever biosensors

1.2   Operational principles

The microcantilever sensors can be operated in either static mode or dynamic mode [2,3]. In the static mode, molecular interactions on the surface of the cantilever causes the changes in the surface stress. In dynamic mode, the change of resonant frequency of the cantilever is monitored. The viscous damping limited the application of dynamic mode in biosensing, because most of biosensing will be operated in liquid which viscous damping will decrease the resolution of detection. Therefore, in this thesis, all of the experiments are operated in static mode. The most important theory for the static mode is the Stoney's equation:

$$\overline{} \tag{1.1}$$

Stoney's equation is used to determine the stress in a thin film which is based on simple beam bending formulas.   is the deflection of the cantilever which caused by the stress

difference (   ) between the top and the bottom surfaces. E and   are the Young's modulus and the Posson ratio of the cantilever materials. L and d are the length and the thickness of cantilever.   and   are the surface stress of the top and the bottom of the surfaces [4]. The Young's modulus of polyimide is much smaller than silicon. Therefore the sensitivity of the polyimide cantilever is much higher than the silicon cantilever [5].

1.3   Readout techniques

1.3.1   *Optical*

Readout techniques are most commonly divided into optical [2], piezoresistive [3], capacitance [4], and metal-oxide semiconductor field-effect transistors (MOSFETs) [5] each technology has its advantage and limitation. The optical techniques are the most popular method in microcantilever detection field. In Figure 1a, it is a typical optical based microcantilever system. It combined with three basic parts: the position sensitive detector (PSD) is used to read out the position changes of laser. The laser diode use to produce laser, which can be reflected by the tip of microcantilever. The microcantilever is commonly coated with gold to reflect the laser beam. In Figure 1b, the system has been developed to microcantlevers array. It needs a laser diode array and microcantilevers array. The PSD can be replaced with charge-coupled device (CCD) or complementary metal-oxide semiconductor（ CMOS ）camera chip. The advantage of the multi-microcantilever array system is that it can read multi signal from each cantilever of the array at the same time. It not only increased the efficiency of detection, but also provided a method for the parallel reference experiment. However, the disadvantage of the optical based multi-microcantilever system is that it is not easy to build and manipulate, and it is much more expensive than the common optical based microcantilever system.

(a)   (b)
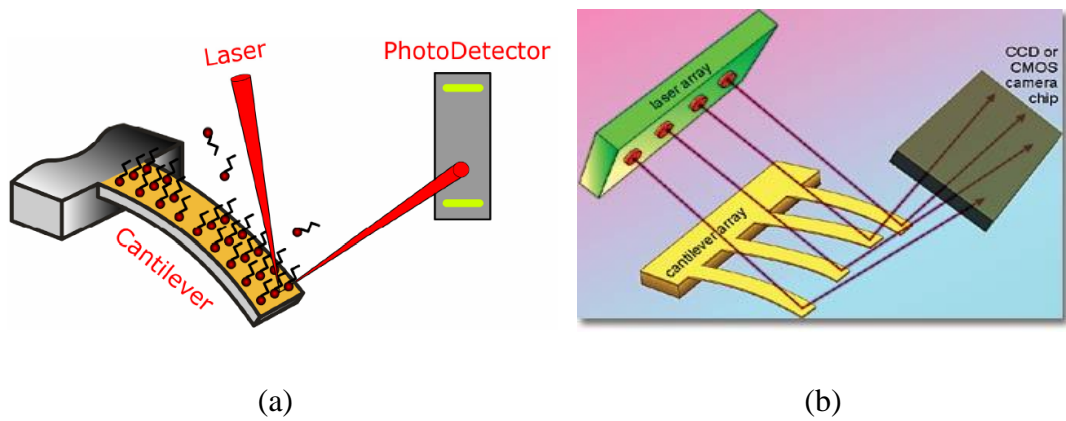
Figure 1: (a) Cantilever sensor (b) Multi-cantilever sensor with an advanced version of the optical lever read-out uses an array of VCSELs for the source and a CCD or CMOS camera as a read detector sensor (Adapted from Shengbo et al. 2013)

1.3.2   Piezoresistive/Piezoelectric

Piezoresistive is one of the most popular methods in the microcantilever readout techniques. It is based on the changes of resistivity of the materials of the cantilever. The advantage of piezoresistive based cantilever system is that it is much easier to build a multi-cantilever array system than the optical deflection method. Another advantage is that the piezoresistive based cantilever system can be much smaller than the optical method, and it need not precise and continuous alignment to make it has the potential to build a portable device. Another advantage which is just the disadvantage of optical based microcantilever system is that it is suitable to the not clear and low opacity liquids.

However, piezoresistive based microcantilever system still has its disadvantage. Firstly, built-in noise affects the resolution and sensitivity of the system. Secondly, even though it can be used in not clear liquid, the isolate is still a problem need to be considered, because of the electrical connections. At last, compared to microcantilever device for optical system, it is not easy to fabricate piezoresistive based microcantilever device.

1.4   Cantilever biodetection

1.4.1   DNA detection
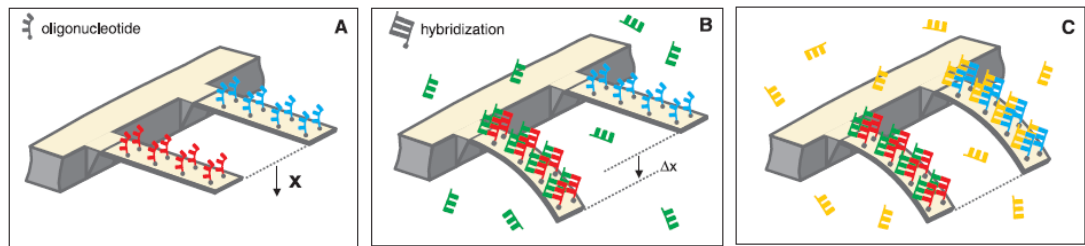
Figure 2: The overview of the hybridization experiment. (a) DNA coated on the surface of cantilever. (b) complementary DNA(green) injected into the system, and it hybridized with DNA(red) on the surface of the cantilever. (c) another complementary DNA(yellow) are injected into the system. (Adapted from Fritz et al. 2000)

Christoph Gerber et al. detected target DNA hybridization with two microcatilevers, so that there is parallel reference detector to compensate for the background. Synthetic 5'thio-modified oligonucleotides with 12-mer and 16-mer oligonucleotide were covalently immobilized on the gold-covered side of the cantilevers (Figure 2a). The functionalization of one cantilever with a 12-mer oligonucleotide (on the right hand) and the other with a 16-mer oligonucleotide was performed in parallel under identical conditions. The arrays were put in hybridization buffer until the differential signal became stable. Then, the complementary 16-mer oligonucleotide solution was injected into the liquid cell (Figure 2b) . Then complementary 12-mer oligonucleotide solution was injected (Figure 2c) [6]. Two years later, Christoph Gerber et al. developed multiple microcantilevers (Figure 3). With this technology, multiple DNA can be detected at the same time [7]. Recently, Jinying Shan et al. offered an energy model for nanomechanical deflection of cantilever-DNA chip chip [6].
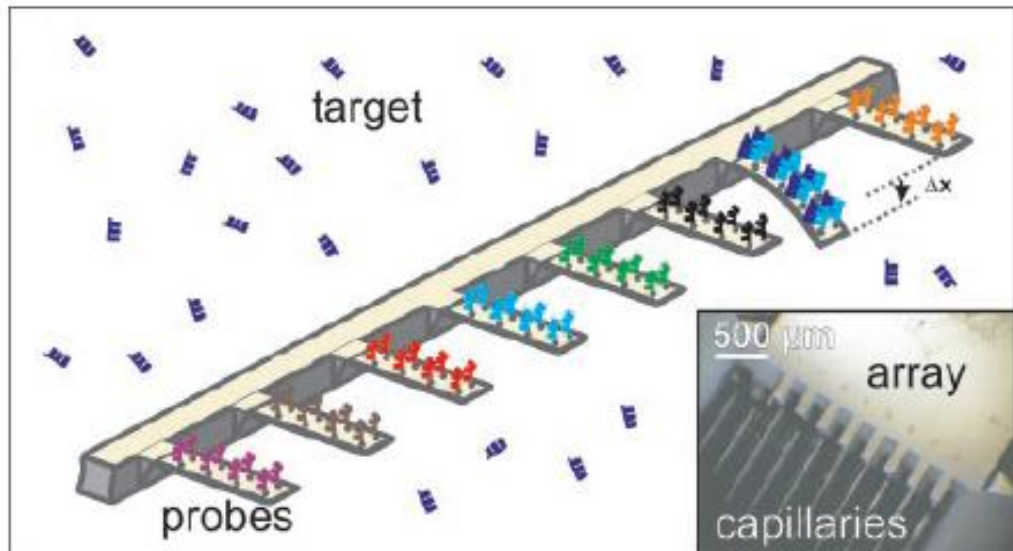
Figure 3: label-free biodetecion and preparation of cantilever biosensor array(Adapted from Christoph et al. 2001)

Thomas Thundat et al have studied the DNA hybridization experiments with microcantilever. They found that the direction of cantilever motion can be changed, by manipulating entropy change during DNA hybridization. The same results can be obtained from protein-ligand binding[8]. This group had discussed the discrimination of DNA single-nucleotide mismatches, by using microcantilever. They employed the rate at hybridization occurs is different to distinguish the complementary DNA and mismatch DNA (Figure 4)[9]. J. Tamayo et al have studied the interaction forces of DNA and complementary nucleic acid on the gold-coated side of a microcantilever. They also studied a self-assembled monolayer of thiolated 27-mer single-stranded DNA on cantilever [10].
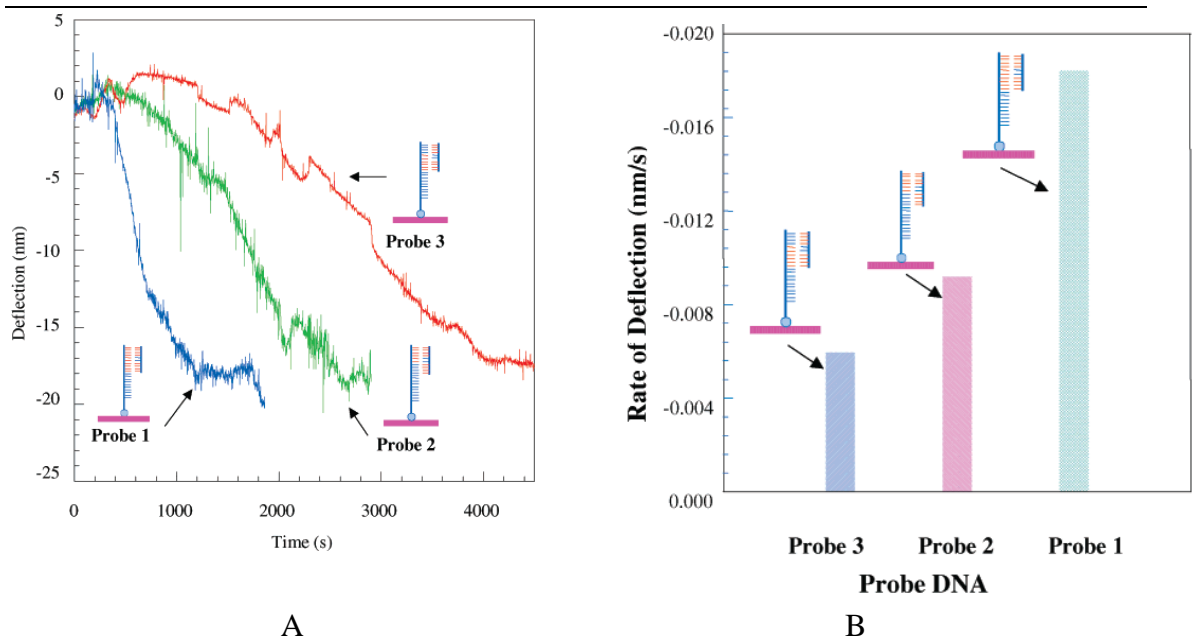
Figure 4: A) Probes 1-3 are used to detect two mismatch target DNA. B) Rate of cantilever deflection (Adapted from Hansen et al. 2001)

DNA hybridization has been studied by Richard Zhang et. al with polymer based microcantilever which has been fabricated with laser. 6-µm-thick polyethylene terephthalate (PET) films has been used to fabricate cantilever with length of 600µm and width of 250µm. An optical beam deflection system has been set up for the single cantilever device. The advantage of the polymer based cantilever is inexpensive, low-cost, and fast fabrication. The device has been used to detect DNA. It is very sensitive that even 0.02 µM DNA can be detected in Figure 5a.
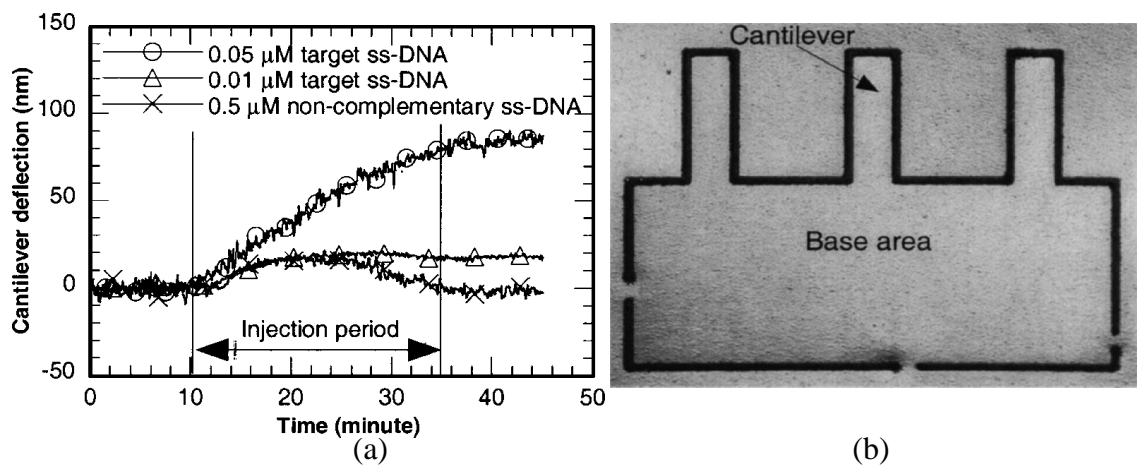
Figure 5: a) results of DNA detection b) laser fabricated polymer cantilever (Adapted from Richard Zhang et al 2004)

1.4.2 *Protein detection*

Label-free detection of biomolecules with cantilever has been demonstrated. A differential surface stress induced nanomechanical bending of the cantilever and the signal has been registered by using a laser deflection system [6] or piezoresistive system [11].These methods have been used for detecting biomolecues, for example antibody-antigen biding [12]. In these experiments, one of the protein was immobilized on the surface of cantilever, and the cantilever will bend when the partner attached to it. Majumdar et al. demonstrated Protein detection experiments using a single cantilever [8]. The adsorption of immoglobulin G (IgG) and albumin (BSA) on a gold surface in buffer solution in terms of surface stress measurements has been studied by single cantilever as well (Figure. 8) [13]. Recently, Gerber present a multiple antibody cantilever array approach that holds promise for biosensing applications, because it can detect multiple proteins in parallel. They have used reference cantilevers to exclude false positive detection, as might occur when using single cantilevers. In particular, the label-free detection of two biomarkers in a background environment of unspecific proteins was demonstrated. Antibody and antigen are significant for diseases treatment and life science research [14]. Antibody and antigen detection are currently the primary detection method for a variety of protein molecules in the environmental and health fields. The detection of it is basic method in diagnosis and environmental control [15]. However, it is a tough work to study proteins. Biochemical is a traditional method and biosensor research seems to be more promising to find a convenient way to detect them [16].

ELISA (Enzyme-linked immunosorbent assay is a traditional antibody/antigen detection method) is not only time consuming but also uses a lot of materials. Fluorescence is not widely used because it needs attachment of labels. Though surface plasmon resonance (SPR) and quartz crystal microbalance (QCM) have some advantages over traditional method ,for example simultaneous analysis , their disadvantage such as reference system are the ACHILLES heel of them [17]. Cantilever is just the method which coped with these problems. The cantilevers are bending, when the surface-stress are changed.

By this means, the instrument can detect if the antibody attached antigen on the surface.

There are two read-out method for protein detection. The first one is the optical beam deflection which is most commonly used. For example scientists have utilized the microcantilever optical deflection assay to determine the sensitivity of cantilevers for detection of prostate specific antigen, which is a biomarker for prostate cancer. Another method is the piezoresistive read-out, the integrated piezoresistor changes its electrical resistance, when the stress of the cantilever changes [18]. This method has some advantages over the optical one, for example, simpler read-out, the antigen/antibody in the blood, for it is not transparent, portable device. Therefore, it is very suitable for antibody and antigen detection. Some scientists attached antibodies to the gold surface via free thiol, to detect antibody-antigen interactions[19].

To amplify the signal, antibody-coated magnetic bead has been used and the concentration of sample are as low as 10^{-18}M (Figure 6) [20]. Bending-plate method with microfabricated cantilevers has been used to transduce the binding of a biological substance to a receptor into a signal. This can be the basis for a new class of biosensors [21].
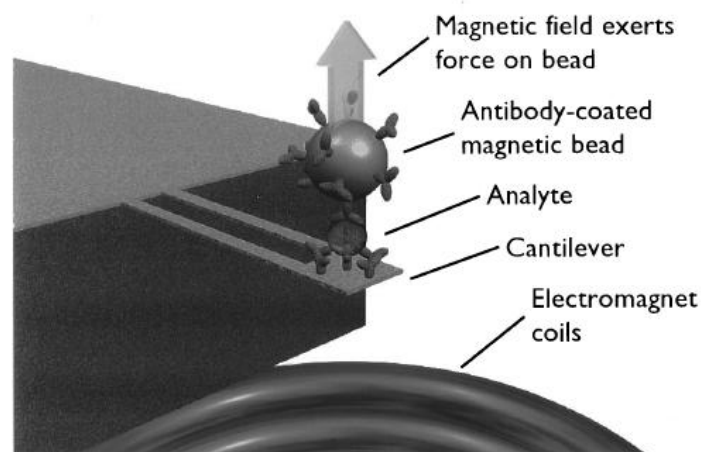
Figure 6: A cantilever-beam force transducer senses the presence of magnetic beads (Adapted from Baselt et al 1996)

FABS concept. A cantilever-beam force transducer senses the presence of magnetic beads, the number of which is proportional to the concentration of analyte in the sample. Not to scale; in general, not one but many beads will attach to the cantilever [20].
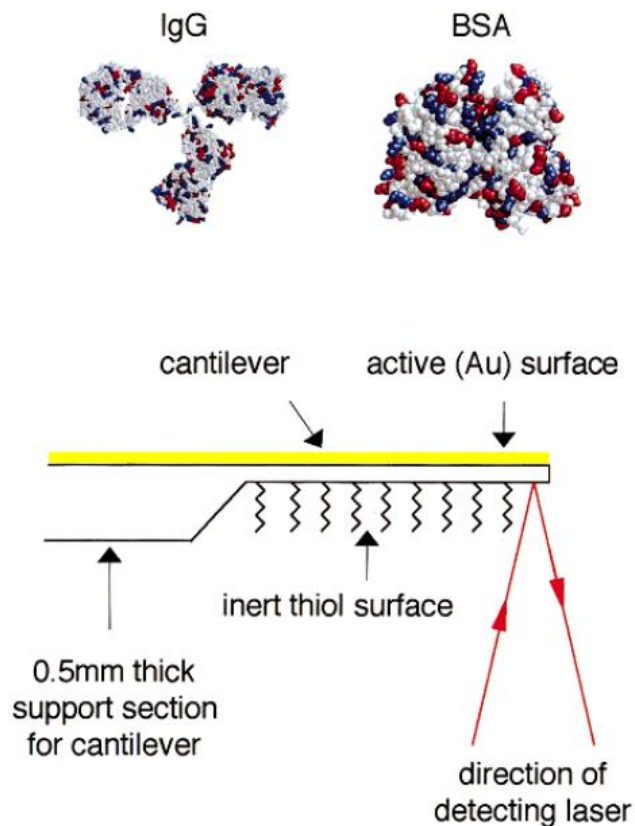
Figure 7: Cantilever has been used to detect protein (Adapted from Mülle et al 1999)

1.4.3 Cell and others

Cell, bacteria, toxin have been studied by cantilever as well [20]. Microscale cantilever beambased resonators have been shown to be extremely sensitive biosensors [22]. To improve the sensitivity of biosensors, microscale cantilever beam based resonators has been deveopled [22]. Craighead'al et al. has detected bacteria with a resonant frequency-based mass detection biological sensor. They used bulk micromachining techniques to fabricate an array of low-stress silicon-nitride cantilever beams. Mass change after bacteria binding will cause the change in resonant frequency of the cantilever. This method even can detect single bacterial cells [23]. Amit Gupta and Demir Akin further developed this technology; so it is not only ultrasensitive but also energy and time efficient. The advantage of Demir's method is better than traditional

diagnosis system such as oligonucleotide based assays and Enzyme-Linked Immunosorbent Assay [24].
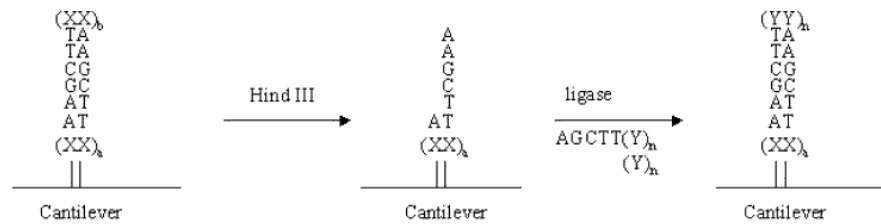
Figure 8: Illustration for ligation and digestion work. (Adapted from Gupta et al 2004)

DNA - microcantilevers system has been studied by many groups and the purpose of this system has not been limited. This system has been used to study enzyme. Thomas Thundat et al. first studied the mechanical motion of Hind III restriction endonuclease and Ligase manipulate immobilized DNA on gold/silicon microcantilevers (Figure 8). (DNA XAAGCTT XX AAGCTTX was first cut with Hind III. Then DNA XAAGCTT XX AAGCTTX was ligated to a longer one. X's and Y's haven't showed here.)[25]. Itamar Willner et al use DNA –microcantilevers system (magnetic particles involved) to detect activities of endonucleases. They discussed ApaI and MseI and the scheme is shown in Figure 9 [25]. Quadruplex DNA has been induced to this system as well. Rachel A. Shu, W et al have used DNA Molecular Motor Driven Micromechanical Cantilever Arrays (Figure 10) [26].
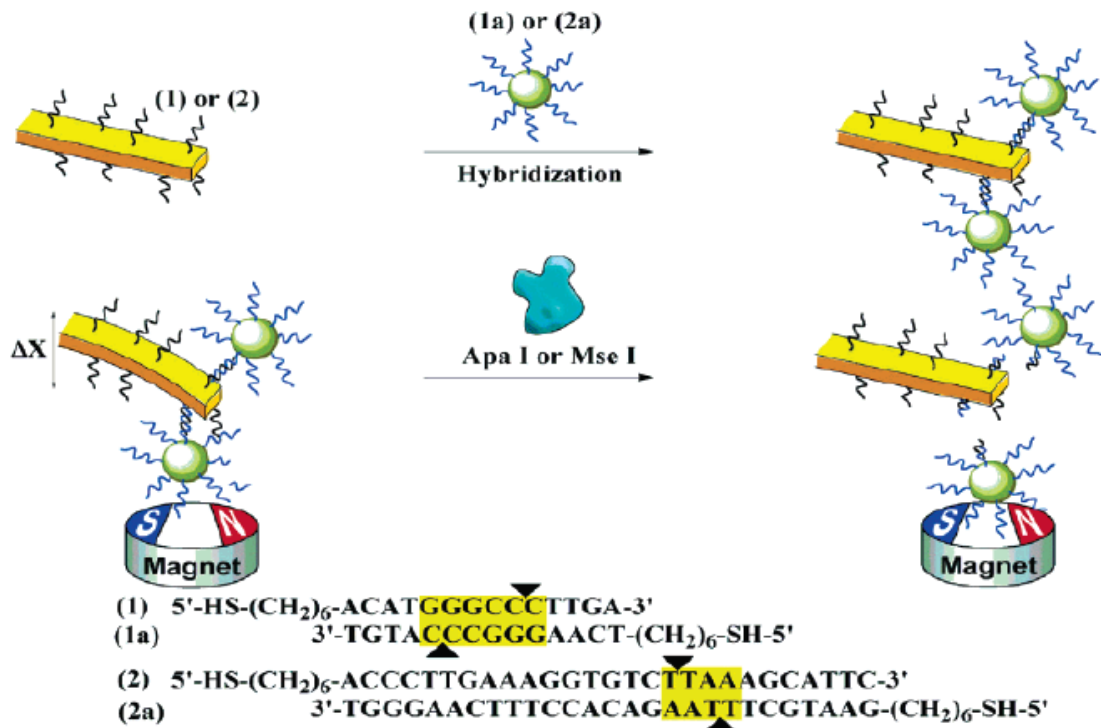
Figure 9: Scheme of magnetic particles involved to detect activities of endonucleases. (Adapted from Stevenson et al 2002)
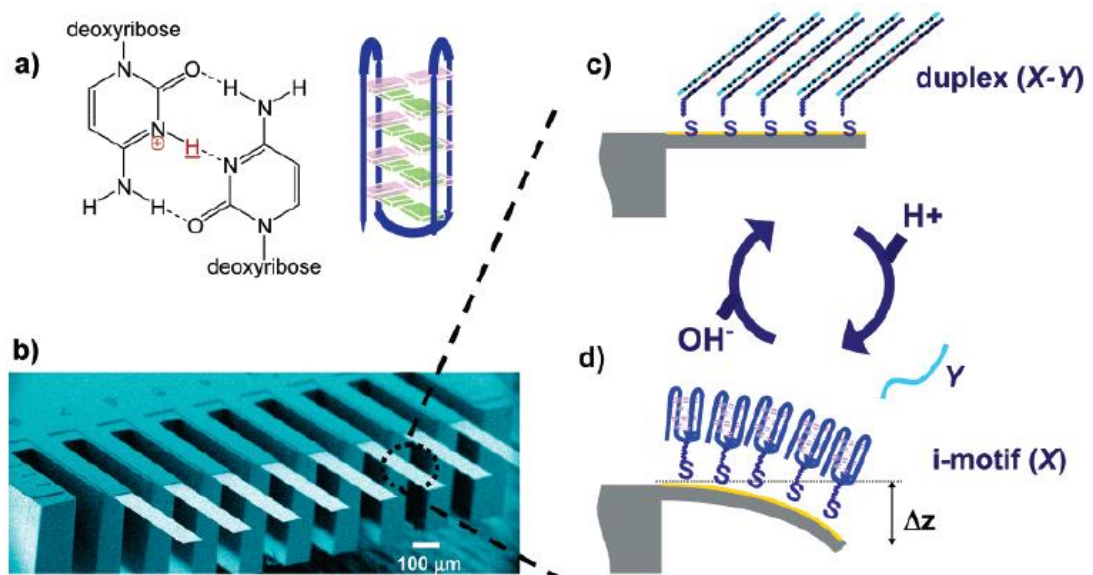
Figure 10: DNA molecular motor driven microcantilever arrays. (Adapted from Shu W et al 2005)

1.5 Fabrication of microcantilevers

Microfabrication are the processes of fabrication of micrometer sizes and smaller.

Microfabrication has been used in physics, material science, chemistry, and computer

11

science, whose major concepts are microlithography, micromaching, laser technology and micromechatronics [27]. Traditionally, cantilevers are made of silicon. In this process, DRIE (deep reactive ion etching), PECVD (plasma enhanced chemical vapor deposition), CPD (critical point drying), and electron gun metal evaporation are used for silicon microfabrication. A process is given as a simple overview (Figure 11) [27].
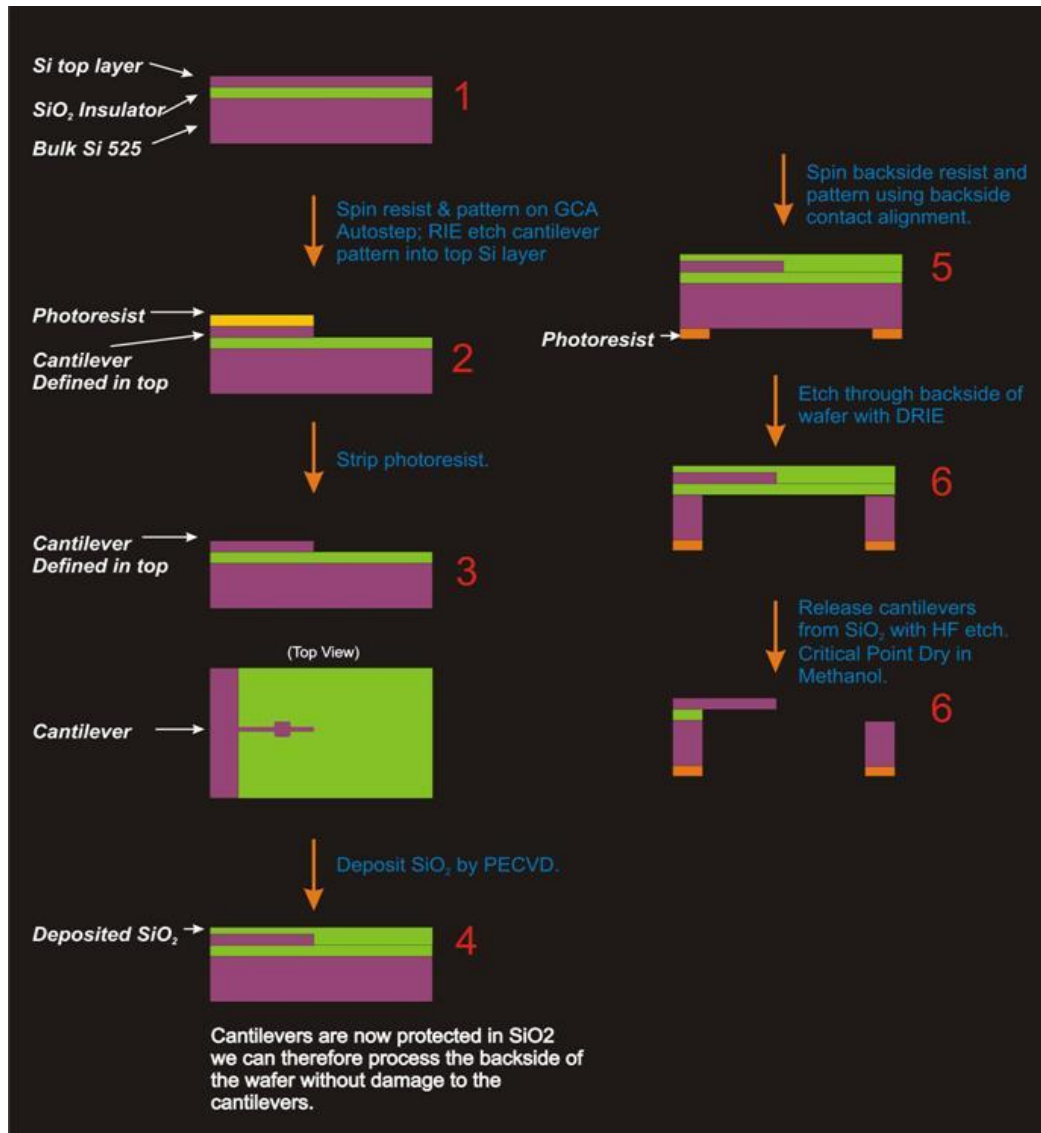
Figure 11: A process of cantilever fabrication (Adapted from Raimondi, F., et al 2000)

Laser micromachining technology is a good alternative to silicon machining for polymer based microfluidic system and MEMS (Micro Electro Mechanical systems) [1,2]. Polymer based microfjuidic or MEMS system can produce from hot embossing and injection molding, [3,4] which are relatively complex and expensive compared to

laser direct fabrication. Both UV and CO_2-laser have been tried to fabricate microfluidic system and MEMS with polymer. [9,10]

1.6 Microfluidics technology

1.6.1 Traditional Microfludics system

Microfludics is a promising technology, which may revolutionize biological analysis in the future [28]. The advantage of microfluidics is that even tiny volumes of sample can be analyzed with this technology, which is very useful for biological detection, for example DNA, protein, and cell[29]. Microfluidic system is generally fabricated with two layers, one layer is with mcrostructure on the surface and the other layer is a channel layer. PDMS is a very popular materials to fabricate microfluidic channels, because it has fantastic mechanical properties and it is easy to process [30]. However, the weakness of PDMS is non-specific binding, which may affect the results of detection if the reagent is very tiny [31]. To solve the problem, polyethylene glycol(PEG) has been involved in the system, which is a non-biofouling materials [32-37]. Another problem followed this method is that PEG on the surface is not long-term stable. [30] To cope with this problem, UV-assisted molding cause cross-linked polyethylene glycol (PEG) has been developed [38]. There are two lithographic methods, which used to fabricate micropatterns within a microfluidic channel: contact printing and capillary molding, which has been compared in table1 [38]. The advantage of the contact printing is that it is easy to manipulate and prevent cross contamination, but the limitations of this technology is that swelling of the stamp may increase the pattern size. Capillary molding can fabricate two dimensional structure, which has the potential to cell biology studies [39, 40].
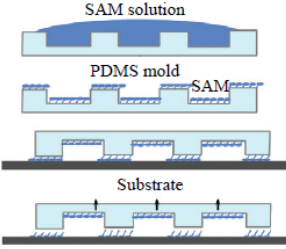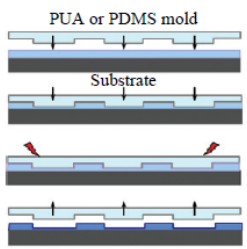
	Contact printing	Capillary molding
Mold	Soft mold Poly (dimethylsiloxane) (PDMS) Hard PDMS (h-PDMS)	Poly (dimethysiloxane) (PDMS) Rigiflexible mold (PUA)
Resolution	~500 nm ~50 nm with h-PDMS	~50 nm with PUA mold
Application	1. Channel fabrication 2. Direct printing of biological molecules (1D chemical modification)	1. Channel fabrication 2. Fabrication of micro/nanostructures (2D structure)
Process		

Table 1: comparison between contact printing and capillary molding (Adapted from Andersson, et al 2003)

1.6.2   Paper Microfludics

Paper-based microfluidic technology has significant capabilities in developing low-cost devices for biosensing, water analysis and environmental monitoring[12-15]. This thesis presents a new method to control time with paper microfluidic device. The advantage of this method is that time period can be controlled from seconds to months. Examples of the application with this method are given in this study.   A device which can control concentration and time for biochemical reaction kinetic assay will be demonstrated in this thesis.

Paper-based microfludics has gained more attention recently, which can use as substrate to pattern microstructure on it, and it is easy to fabricate. The advantage of paper-based microfludics is simple, easy to use, low cost, and portable [41-43]. It has the potential to be used in less-industrialized countries, emergency situations, and health-care settings [41].

(a) (b)
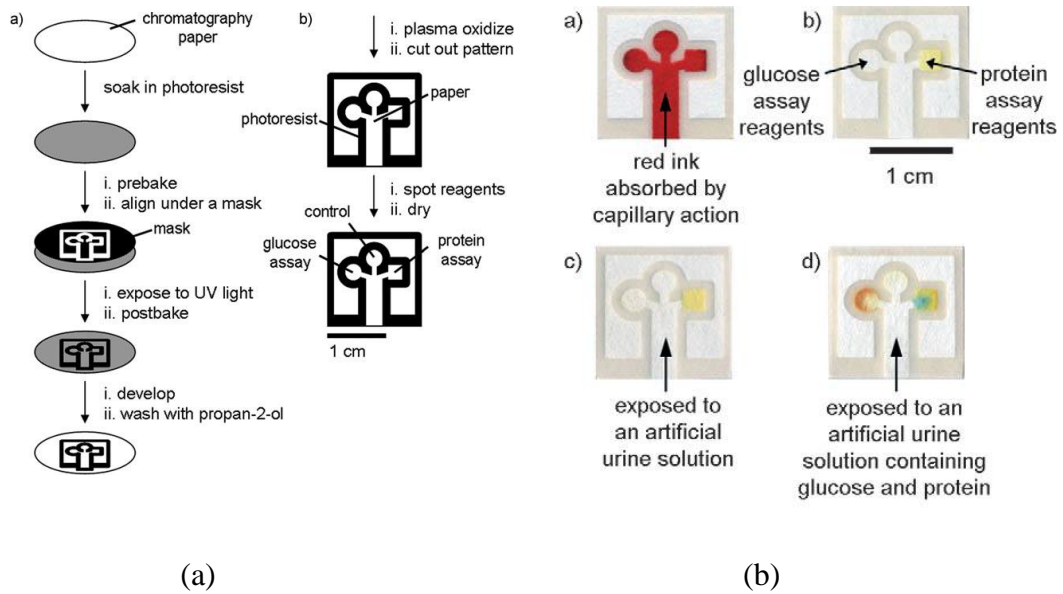
Figure 12: Fabrication process for SU-8 paper microfluidic device (Adapted from Martinez, et al 2007)

In Figure 12, Whitesides and co-workers use paper and SU-8 to fabricate a microfluidic device, which was used to detect glucose, and protein.A chromatography paper was soaked in SU-8 2010 photoresist. Subsequently, a mask with a channel and three pads will be covered on it. Then it is exposed to UV light to form a microfludic structure. Enzymatic oxidation of iodide to iodine reaction has been used to detect glucose and tetrabromophenol blue(TBPB) has been used to detect protein. Both of the two reactions can cause color change. In Figure 12b, it show the control and positive results of the experiment [41].
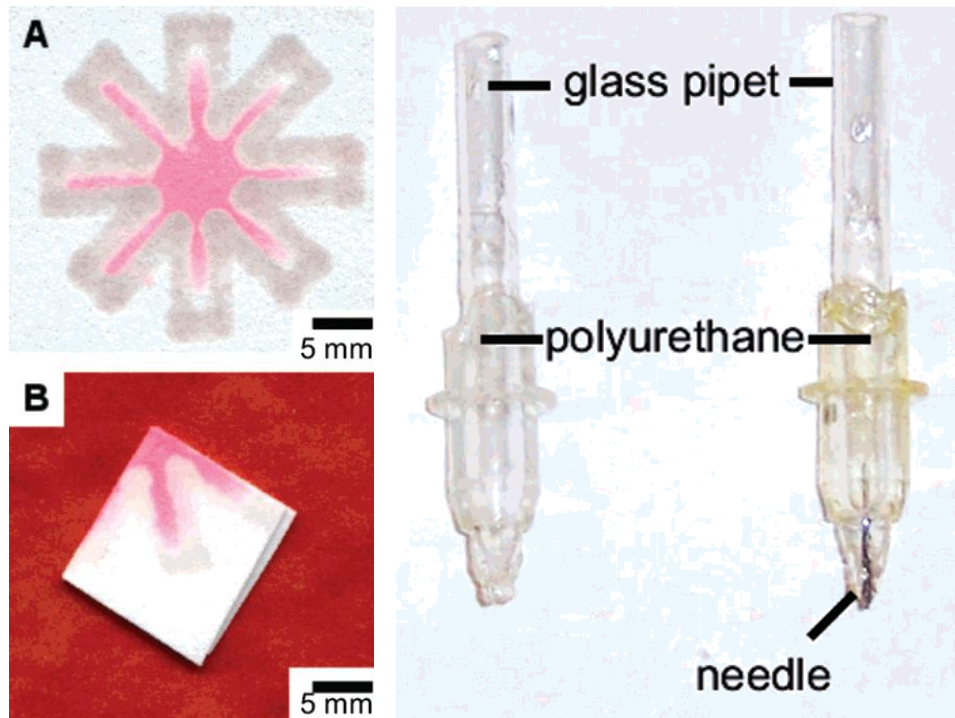
Figure 13: PDMS paper microfluidic device (Adapted from Martinez, et al 2008)

Recently, the paper SU-8 based microfludics device has been updated with paper-PDMS based microfludics. The advantage of PDMS is that PDMS is elastomer, and it is more flexible than photoresist in paper. Figure 13 shows that it even can be folded without destroying the channel. The process to fabricate the device is different to the paper SU-8 based microfludics. A pen has been designed to print PDMS and ink, and it is the picture of the pen in Figure 13 [44].

1.7 Aim and objectives

The main objective of this thesis is to amplify the signal of microcantilever biosensors for DNA, protein, and bacteria detection. Some mechanical methods have been investigate to amplify the signal, such as: polyimide and paper as material have been studied, microfluidic-microcantilever has been tried. This approach will need to overcome many challenges, such as low cost, internally referenced, highly sensitive, multiplexed arrays, etc.

This thesis has four main research objectives:

- To develop polymer based microcantilever biosensors for amplification of the signal for DNA detection. The signal of DNA detection is very low with silicon cantilever, and the Yong's module of polymer is lower than silicon, therefore, polymer based cantilever has the potential to amplify the signal for DNA detection.

- To investigate an internal referenced microcantilever system, the receptor for target and the receptor as reference can be immobilized on both the top and the bottom of the microcantilever evenly.

- To investigate whether microfluidics fits onto a microcantilever surface system can amplify the signal for crypto and thrombin detection.

- To investigate whether paper microfluidic based microcantilever can amplify the signal for bio detection. At the same time, to investigate whether it is suitable to develop a timer.

1.8   Structure of the thesis

This thesis will be presented in seven chapters:

Chapter 1 presents the introduction and literature review of microcantilever and microfluidic research for biosensing.

Chapter 2 describes experimental techniques and method in this thesis, for example, the microcantilever system, laser fabrication, and gold coating.

Chapter 3 presents the details of polyimide based microcantilever fabrication. The parameters for fabrication have been optimized in this chapter.

Chapter 4 reports an internally referenced polyimide based microcantilever system. One base mismatch DNA has been detected with this system.

Chapter 5 demonstrates a microcantilever-microfluidic system, magnetic beads and magnetic field used to amply the signal of detection. Detection of Crypto and thrombin as examples will be carried by using the system. The potential of using this system as a density sensor will be also discussed.

Chapter 6 summarizes a paper microfluidics based micro cantilever system and a paper microfluidics based timer system. A microfluidic based device which can use to trigger the system has also been investigated.

Chapter 7 summarizes the work and results of the thesis and recommend the future work.

1.9   References for Chapter 1

1.   Lavrik, N.V. and P.G. Datskos, *Femtogram mass detection using photothermally actuated nanomechanical resonators.* Applied physics letters, 2003. **82**(16): p. 2697-2699.

2.   Ilic, B., Y. Yang, and H. Craighead, *Virus detection using nanoelectromechanical devices.* Applied physics letters, 2004. **85**(13): p. 2604-2606.

3.   Lee, J.H., et al., *Immunoassay of prostate-specific antigen (PSA) using resonant frequency shift of piezoelectric nanomechanical microcantilever.* Biosensors and Bioelectronics, 2005. **20**(10): p. 2157-2162.

4.   Zhou, F., et al., *Highly reversible and multi-stage cantilever actuation driven by polyelectrolyte brushes.* Journal of the American Chemical Society, 2006. **128**(16): p. 5326-5327.

5.   Shekhawat, G., S.H. Tark, and V.P. Dravid, *MOSFET-embedded microcantilevers for measuring deflection in biomolecular sensors.* Science, 2006. **311**(5767): p. 1592-1595.

6.   Fritz, J., et al., *Translating biomolecular recognition into nanomechanics.* Science, 2000. **288**(5464): p. 316-318.

7.   McKendry, R., et al., *Multiple label-free biodetection and quantitative DNA-binding assays on a nanomechanical cantilever array.* Proceedings of the National Academy of Sciences, 2002. **99**(15): p. 9783.

8.   Wu, G., et al., *Origin of nanomechanical cantilever motion generated from biomolecular interactions.* Proceedings of the National Academy of Sciences, 2001. **98**(4): p. 1560-1564.

9.   Hansen, K.M., et al., *Cantilever-based optical deflection assay for discrimination of DNA single-nucleotide mismatches.* Analytical Chemistry, 2001. **73**(7): p. 1567-1571.

10.   Carrascosa, L.G., et al., *Nanomechanical biosensors: a new sensing tool.* TrAC Trends in Analytical Chemistry, 2006. **25**(3): p. 196-206.

11.   Mukhopadhyay, R., et al., *Nanomechanical sensing of DNA sequences using piezoresistive cantilevers.* Langmuir, 2005. **21**(18): p. 8400-8408.

12.   Arntz, Y., et al., *Label-free protein assay based on a nanomechanical cantilever array.* Nanotechnology, 2003. **14**: p. 86.

13. Moulin, A., et al., *Measuring surface-induced conformational changes in proteins.* Langmuir, 1999. **15**(26): p. 8776-8779.

14. Ciordia, S., V. Ríos, and J.P. Albar, *Contributions of advanced proteomics technologies to cancer diagnosis.* Clinical and Translational Oncology, 2006. **8**(8): p. 566-580.

15. Andreotti, P.E., et al., *Immunoassay of infectious agents.* BioTechniques, 2003. **35**(4): p. 850-861.

16. Murphy, L., *Biosensors and bioelectrochemistry.* Current opinion in chemical biology, 2006. **10**(2): p. 177-184.

17. Boozer, C., et al., *Looking towards label-free biomolecular interaction analysis in a high-throughput format: a review of new surface plasmon resonance technologies.* Current opinion in biotechnology, 2006. **17**(4): p. 400-405.

18. Boisen, A., et al., *Environmental sensors based on micromachined cantilevers with integrated read-out.* Ultramicroscopy, 2000. **82**(1): p. 11-16.

19. Warner, M.G., S.M. Reed, and J.E. Hutchison, *Small, water-soluble, ligand-stabilized gold nanoparticles synthesized by interfacial ligand exchange reactions.* Chemistry of materials, 2000. **12**(11): p. 3316-3320.

20. Baselt, D.R., G.U. Lee, and R.J. Colton, *Biosensor based on force microscope technology.* Journal of Vacuum Science & Technology B: Microelectronics and Nanometer Structures, 1996. **14**(2): p. 789-793.

21. Müller, K., S. Sainov, and S. Mittler-Neher, *Raiteri, R.; Nelles, G.; Butt, HJ; Knoll, W.; Skladal, P. Sensing of Biological Substances Based on the Bending of Microfabricated Cantilevers.* Sensors and Actuators B, 1999. **61**: p. 213-217.

22. Ilic, B., et al., *Mechanical resonant immunospecific biological detector.* Applied physics letters, 2000. **77**(3): p. 450-452.

23. Ivnitski, D., et al., *Nucleic acid approaches for detection and identification of biological warfare and infectious disease agents.* BioTechniques, 2003. **35**(4): p. 862-869.

24. Gupta, A., D. Akin, and R. Bashir, *Detection of bacterial cells and antibodies using surface micromachined thin silicon cantilever resonators.* Journal of Vacuum Science & Technology B: Microelectronics and Nanometer Structures, 2004. **22**(6): p. 2785-2791.

25. Stevenson, K.A., et al., *Nanomechanical effect of enzymatic manipulation of*

DNA on microcantilever surfaces. Langmuir, 2002. **18**(23): p. 8732-8736.

26.   Shu, W., et al., *DNA molecular motor driven micromechanical cantilever arrays.* Journal of the American Chemical Society, 2005. **127**(48): p. 17054-17060.

27.   Raimondi, F., et al., *Quantification of polyimide carbonization after laser ablation.* Journal of Applied Physics, 2000. **88**(6): p. 3659-3666.

28.   Andersson, H. and A. Van den Berg, *Microfluidic devices for cellomics: a review.* Sensors and Actuators B: Chemical, 2003. **92**(3): p. 315-325.

29.   Kim, P., et al., *Soft lithography for microfluidics: a review.* 2008.

30.   Duffy, D.C., et al., *Rapid prototyping of microfluidic systems in poly (dimethylsiloxane).* Analytical Chemistry, 1998. **70**(23): p. 4974-4984.

31.   Ocvirk, G., et al., *Electrokinetic control of fluid flow in native poly (dimethylsiloxane) capillary electrophoresis devices.* Electrophoresis, 2000. **21**(1): p. 107-115.

32.   Popat, K.C., R.W. Johnson, and T.A. Desai, *Characterization of vapor deposited poly (ethylene glycol) films on silicon surfaces for surface modification of microfluidic systems.* Journal of Vacuum Science & Technology B: Microelectronics and Nanometer Structures, 2003. **21**(2): p. 645-654.

33.   Popat, K.C. and T.A. Desai, *Poly (ethylene glycol) interfaces: an approach for enhanced performance of microfluidic systems.* Biosensors and Bioelectronics, 2004. **19**(9): p. 1037-1044.

34.   Lahann, J., et al., *Reactive polymer coatings: a first step toward surface engineering of microfluidic devices.* Analytical Chemistry, 2003. **75**(9): p. 2117-2122.

35.   Stark, M.B. and K. Holmberg, *Covalent immobilization of lipase in organic solvents.* Biotechnology and bioengineering, 2004. **34**(7): p. 942-950.

36.   Gingell, D., et al., *Adsorption of a novel fluorescent derivative of a poly (ethylene oxide)/poly (butylene oxide) block copolymer on octadecyl glass studied by total internal reflection fluorescence and interferometry.* Journal of biomedical materials research, 2004. **28**(4): p. 505-513.

37.   Malmsten, M., K. Emoto, and J.M. Van Alstine, *Effect of chain density on inhibition of protein adsorption by poly (ethylene glycol) based coatings.* Journal of colloid and interface science, 1998. **202**(2): p. 507-517.

38.   Kim, P., et al., *Fabrication of non-biofouling polyethylene glycol micro-and nanochannels by ultraviolet-assisted irreversible sealing.* Lab on a Chip, 2006. **6**(11): p. 1432-1437.

39.   Kim, D.H., et al., *Guided three-dimensional growth of functional cardiomyocytes on polyethylene glycol nanostructures.* Langmuir, 2006. **22**(12): p. 5419-5426.

40.   Kim, P., et al., *Fabrication of nanostructures of polyethylene glycol for applications to protein adsorption and cell adhesion.* Nanotechnology, 2005. **16**(10): p. 2420.

41.   Martinez, A.W., et al., *Patterned Paper as a Platform for Inexpensive, Low‐ Volume, Portable Bioassays.* Angewandte Chemie International Edition, 2007. **46**(8): p. 1318-1320.

42.   Martinez, A.W., et al., *Simple telemedicine for developing regions: camera phones and paper-based microfluidic devices for real-time, off-site diagnosis.* Analytical Chemistry, 2008. **80**(10): p. 3699-3707.

43.   Martinez, A.W., et al., *FLASH: A rapid method for prototyping paper-based microfluidic devices.* Lab Chip, 2008. **8**(12): p. 2146-2150.

44.   Bruzewicz, D.A., M. Reches, and G.M. Whitesides, *Low-cost printing of poly (dimethylsiloxane) barriers to define microchannels in paper.* Analytical Chemistry, 2008. **80**(9): p. 3387-3392.

45.   Zhang, X.R. and X. Xu, *Development of a biosensor based on laser-fabricated polymer microcantilevers.* Applied physics letters, 2004. **85**(12): p. 2423-2425.

46.   Burg, T.P., et al., *Weighing of biomolecules, single cells and single nanoparticles in fluid.* Nature, 2007. **446**(7139): p. 1066-1069.

Chapter 2   Experimental Techniques

2.1 Introduction

In this chapter, the experimental techniques used in this thesis have been summarized. YVO4 and O2 laser system have been used to fabricate polyimide, PMMA, and paper. Cantilever system has been introduced in this chapter which used to detect DNA, crypto. The optical cantilever system was improved in this thesis. Polyimide cantilevers array have been investigated, which has been fabricated with laser directly. Thousands of cantilevers can be fabricated in a few minutes. Polyimide based double sided gold coated cantilevers have been demonstrated. A rotary motor was used to thermally coat the both sides of the cantilever simultaneously. Magnetic amplified microcantilever microfluidic system has been set-up, which use to detect crypto and thrombin in this thesis. A special holder was fabricated with PMMA, which use to set the magnet in the holder and can remove it when the magnetic field does not need. Paper based microfluidic mcirocantilever system has been pumped with electrophoresis and chromatography. Different kind of microscope has been used to observe the results of the experiment. UV Ultraviolet spectrum and electrophoresis has been used to detect DNA.

2.2 Laser system

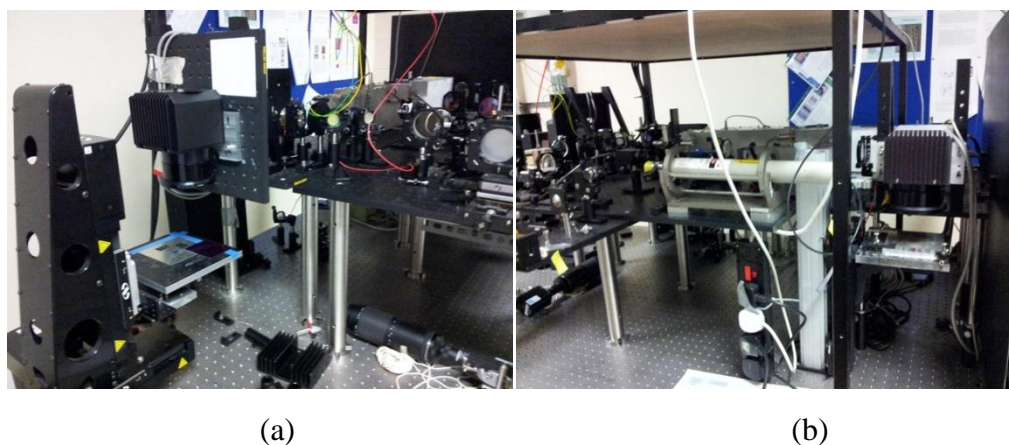(a)   (b)

Figure 14: Laser System used for fabrication of microcantilever (a) front side of the laser system (b) the back side of the laser system.

The laser used to fabricate the polyimide is the INAZUMA solid state diode pumped laser build by Spectra-Physics Lasers, Inc. The laser used here is Nd: YVO4 (Neodymium- doped Yttrium ortho Vanadate) that is optically pumped by laser diodes. The frequency of the laser ranges from 15 kHz to 100 kHz. The laser can operate at three different wavelengths with the help of two scan heads and the dismountable harmonic modules. Its actual wavelength is in the near infrared at 1064 nm (head2) and by using the doubler module, the laser can lase in the visible (green) at 532 nm (head2) which is transformed lateral into UV wavelength, lasing at 355 nm (head1). The sample is moved underneath the beam using a x–y–z-translation stage with an accuracy of 0.1 mm. Light from this laser was coupled to a galvanometer scan head (XLR8-10, Nutfield Technology, Windham, NH).

Type	Wavelength	Pulse width	Pulse energy	Rep rate
Excimer	193-308nm	20ns	to 500 mJ	to 500 Hz
nωNd:YAG	266-532nm	10ns	a few mJ	to kHz
fs Ti:Sapphire	775nm	150fs	~1mJ	to kHz
Nd:YAG	1.064μm	10ns	10mJ	to kHz

Table 2: Comparison of laser system for microfabrication

(a)   (b)

(c)   (d)
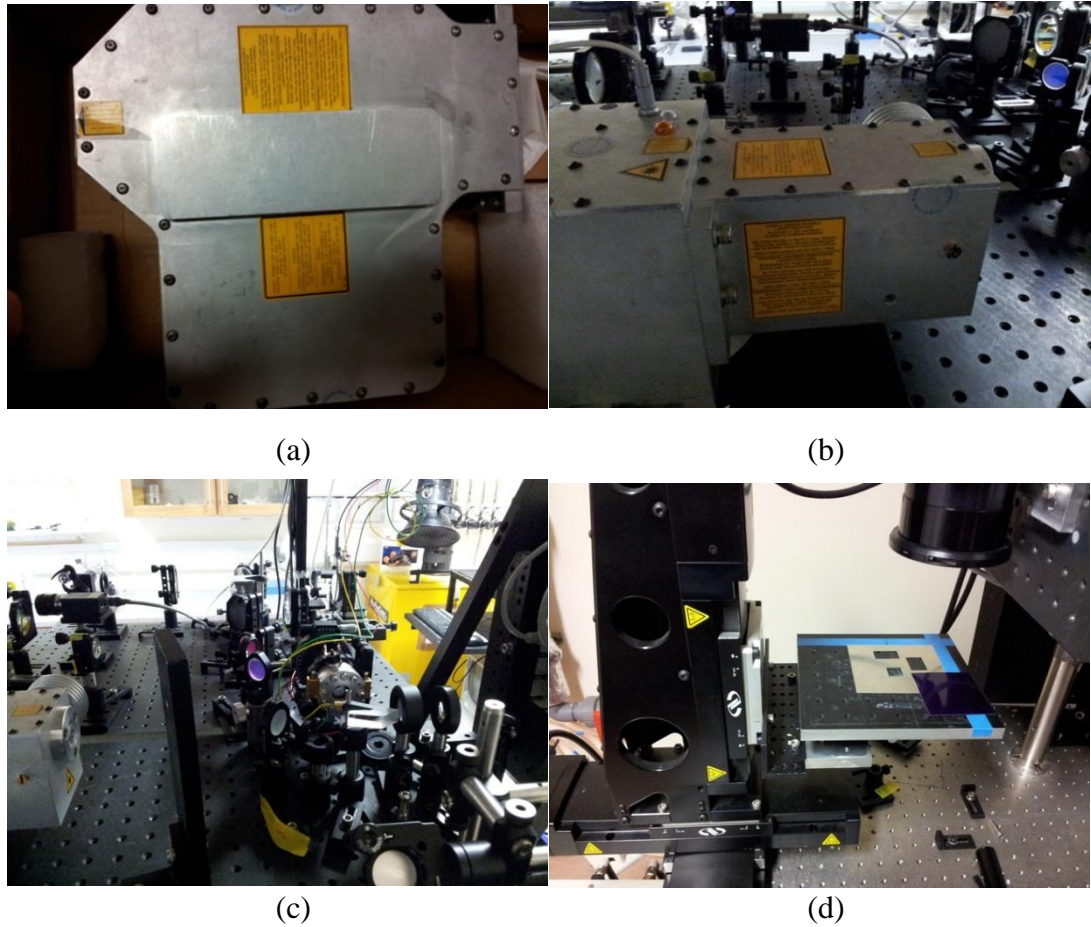
Figure 15: The component of laser system (a) The generator of 355nm laser beam. (b) The generator for 1064nm and 532nm laser beam. (c) A series of mirrors of the laser system. (d) The working stage for laser fabrication.

The system contains a series of mirrors, which use to redirect the laser beam to different laser head (Figure 15abc). In Figure 15d, it is the platform for laser fabrication. The platform can be adjusted by software to set it on the focus of the laser.
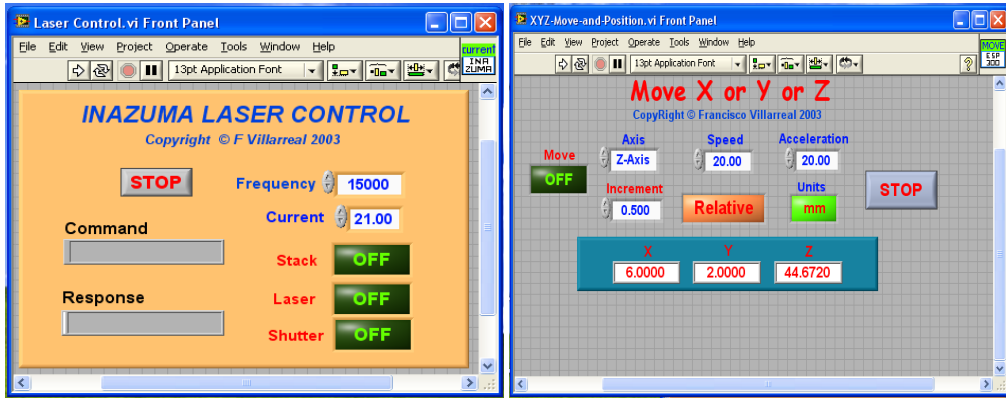
(a)   (b)
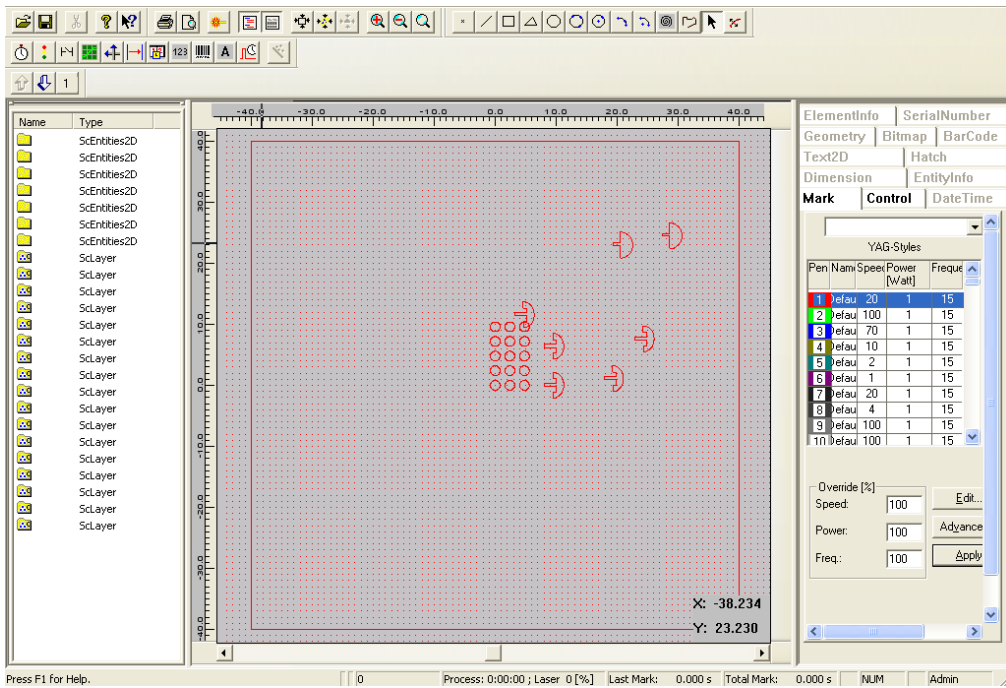
(c)

Figure 16: The software of laser system (a) The panel for the power laser beam. (b) The panel for the platform. (c) The panel for laser fabrication

2.3 CO$_2$ laser system

(a)   (b)

(c)   (d)
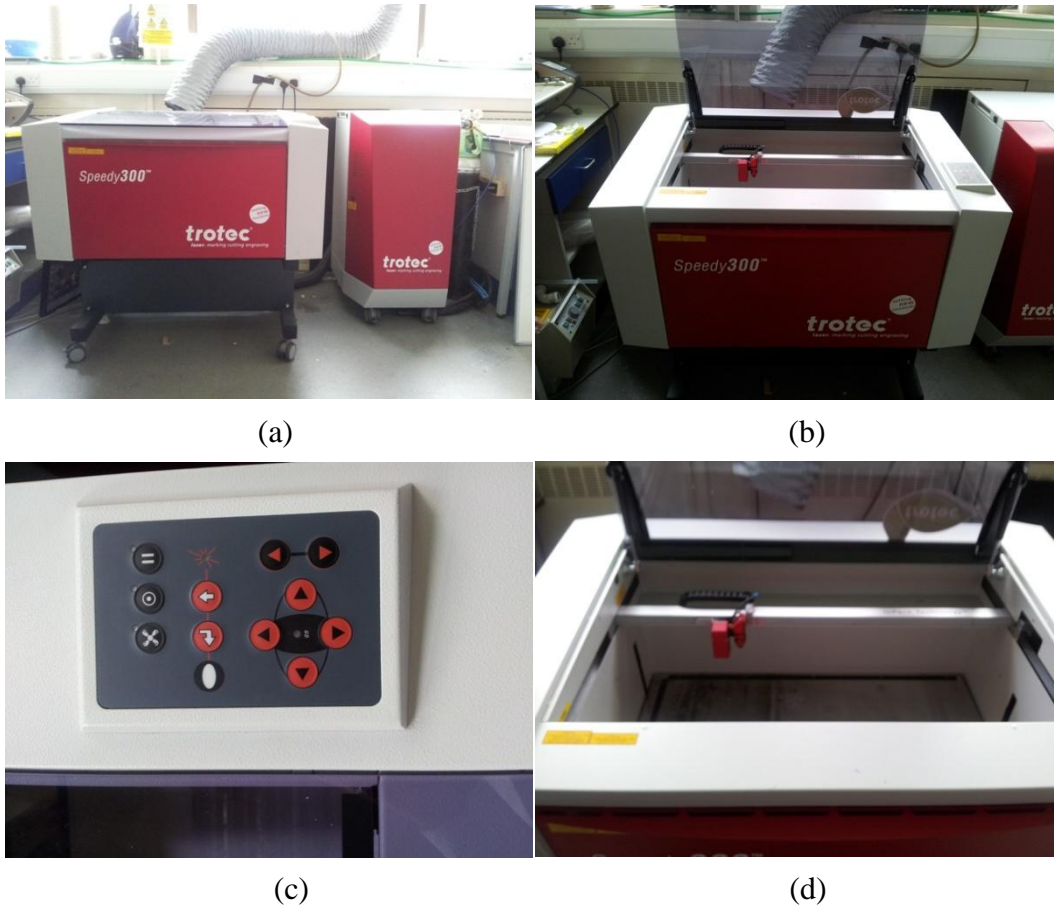
Figure 17: CO$_2$ Laser system (a) Trotec speedy300 laser system. (b) and (d) The inside of the laser. C) The control panel of the system.

The Trotec Speedy 300 CO$_2$ laser system include air assist, air-flushed optics, Bi-directional communication, exhaust unit control, Ferro-magnetic work table, Focus lenses, InPack technology, laser pointer, software autofocus and trolley table. The laser has been used to engrave and cut PMMA, paper, and membrane, etc. in this thesis. It is not as accurate as the UV laser, but the fabricating area of this laser is much larger.

2.4 Microcantilever system
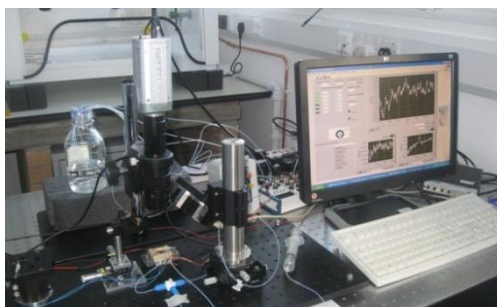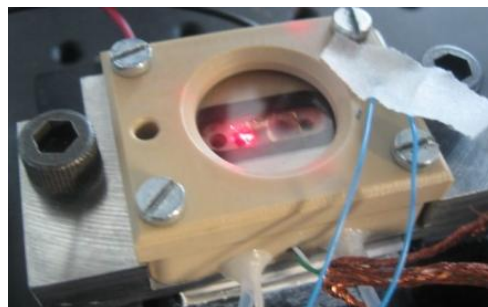
(a)　　　　　　　　　　　　　(b)

(c)　　　　　　　　　　　　　(d)
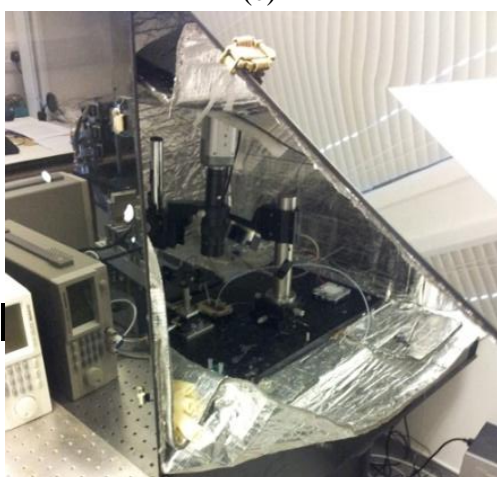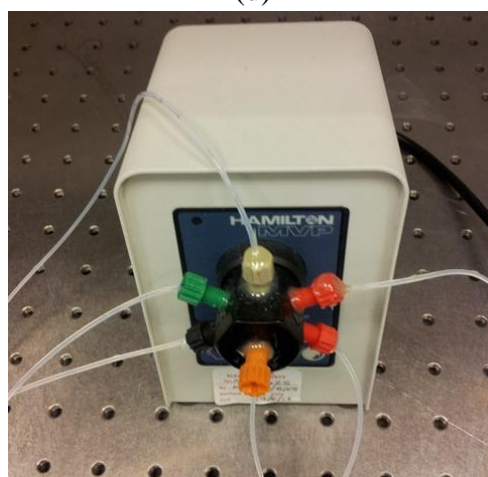
(e)　　　　　　　　　　　　　(f)
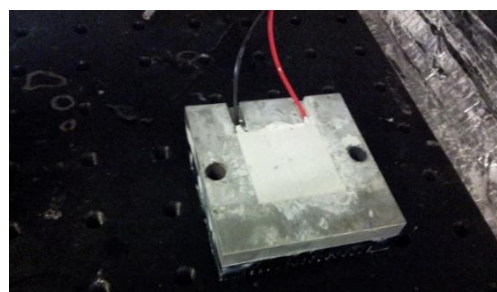
(g)　　　　　　　　　　　　　(h)

Figure 18: Microcantilever system (a) Microcantilever system type I. (b) The holder for microcantilever (type I). (c) Microcantilever system type II. (d) The holder for microcantilever (type II). (e) The thermal insulated box. (f) Rotary valve. (g) Temperature control system. (h) Digital CCD camera

28

The cantilever optical readout system developed in this thesis includes a fluid cell, laser diode, position-sensitive detector (PSD), microscope with digital CCD camera, temperature control system, non-transparent box, and rotary valve. There are two types of fluid cells in this thesis: type I is microcantilever inside fluid cells and type II is microfluidics- microcantilever system. The fluid cell of type I is fabricated from PEEK, and sealed with a sapphire cover due to them both being inert to all chemicals involved in this experiment. Type II which is microfluidics in microcantilevers is fabricated with polyimide and photoresist.

The cantilever system is set up on an optical table (Newport Laminar Flow isolator) to reduce vibrations. The system is mounted in a non-transparent box made of PMMA (5mm thickness), with thermal insulated materials (10mm thickness), which reduces the external disturbance from air flow, background light, and temperature variations in the lab. If the samples are temperature sensitive, a temperature control system can be set. The system combined with a temperature sensor and a temperature control device. The rotary valve switch device communicates via RS-232 and is used to flow different liquids into the fluid cell. The fluid cell is fabricated from PEEK, and sealed with a sapphire cover due to them both being inert to all chemicals involved in this experiment.

The optical resolution of the microscope is 5 m, which used to confirm that the laser beam is on the tip of the cantilever. The laser beam reflected by the cantilever is aligned on to a position-sensitive detector (PSD) and an amplifier was used to amplify the current signal from the PSD and convert into voltage signals. A National Instrument data acquisition card was then used to record data in LabView. There are four windows which shows temperature, differential, normal, and sum signal. The temperature and valve can be controlled with the software.
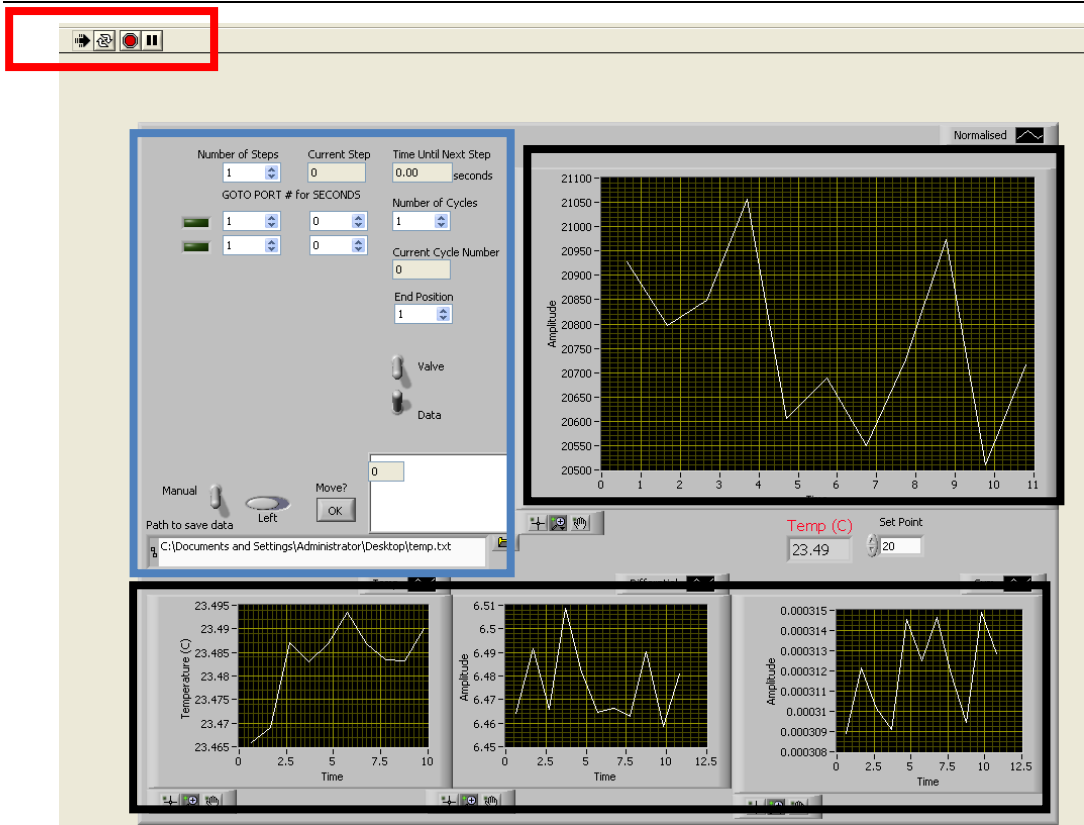
Figure 19: Software of the Microcantilever the red area used to switch on/off the system. The blue area used to control the rotary valve. The black area is the display area which is used to display the signal.

2.5 Gold coated chamber
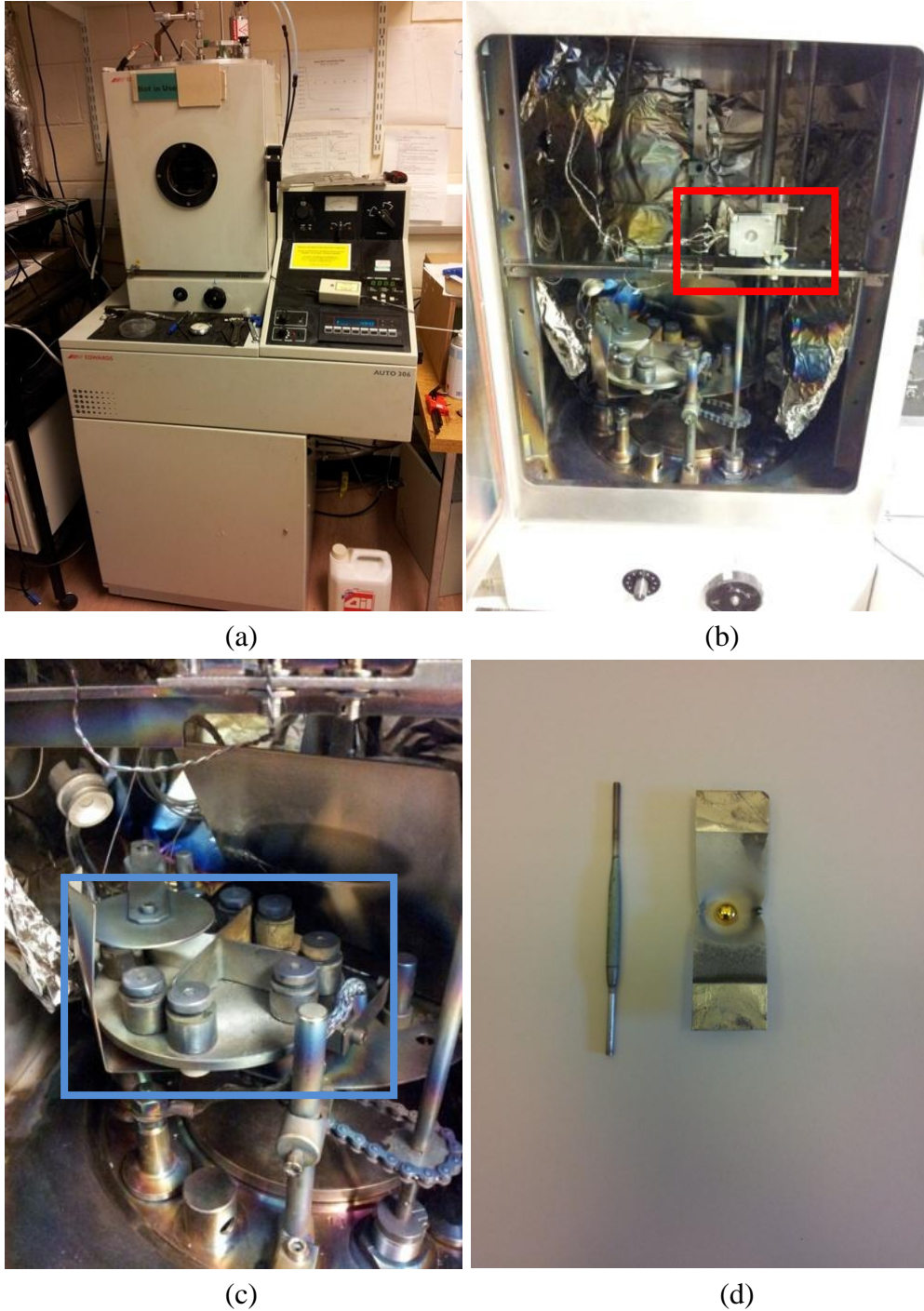
Figure 20: Gold evaporation system. (a) BOC Edwards Auto 500 system. (b) The motor for double sided gold coating. (c) The turnplate for gold or chromium. (d) The chromium rod and boat for gold.

A gold evaporation system (BOC Edwards Auto 500, U.K.) has been used to coat gold on the surface of polymer. For example, if gold need to coat on polyimide, A chromium film need to evaporate on one side of the polyimide film in advance. Subsequently, the gold will be evaporated on the polyimide film with the required

thickness. The parameter of the evaporation is that the base pressure is 1×10^{-7} mbar and the thermal evaporation rate is 0.4 nm/s. If the device is used to detect DNA, DNA immobilized on one side of the polyimide film after gold coating on it. (10 M DNA in a buffer containing 1.0M potassium phosphate) The polyimide was subsequently immersed in 1mM 2-mercaptoethanol (Sigma Aldrich) for 1 hour, to remove non-specifically adsorbed DNA. The polyimide films were then rinsed by water (18.2 M Ohms, Elga Maxima), and dried with a stream of nitrogen.

2.6 Microscope

(a)   (b)

(c)   (d)
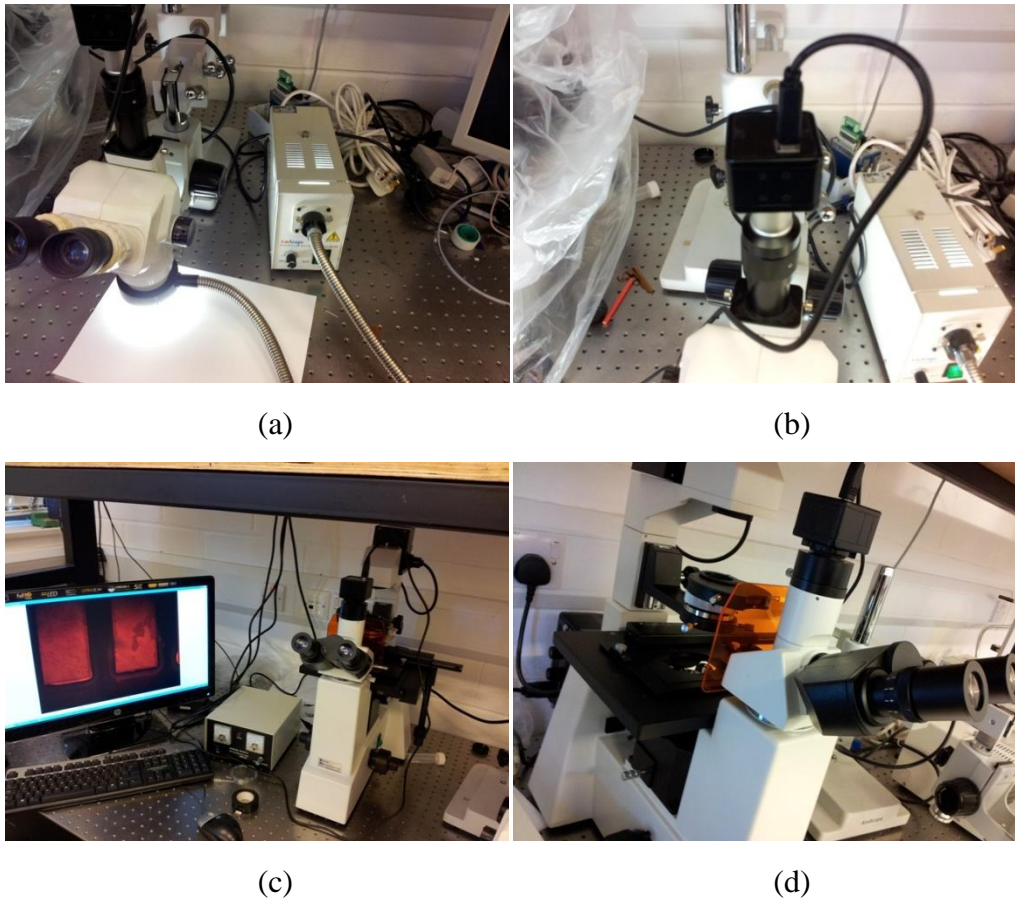
Figure 21: Optical and Fluorescence Microscope (a) and (b) are Optical Microscope. (c) and (d) are Fluorescence Microscopes.

Microscope is a necessary tool for the research, and different type of microscopes have been used, for example, optical microscope, fluorescence microscope, scanning electron microscope (SEM) in this thesis.

2.7 Electrophoresis
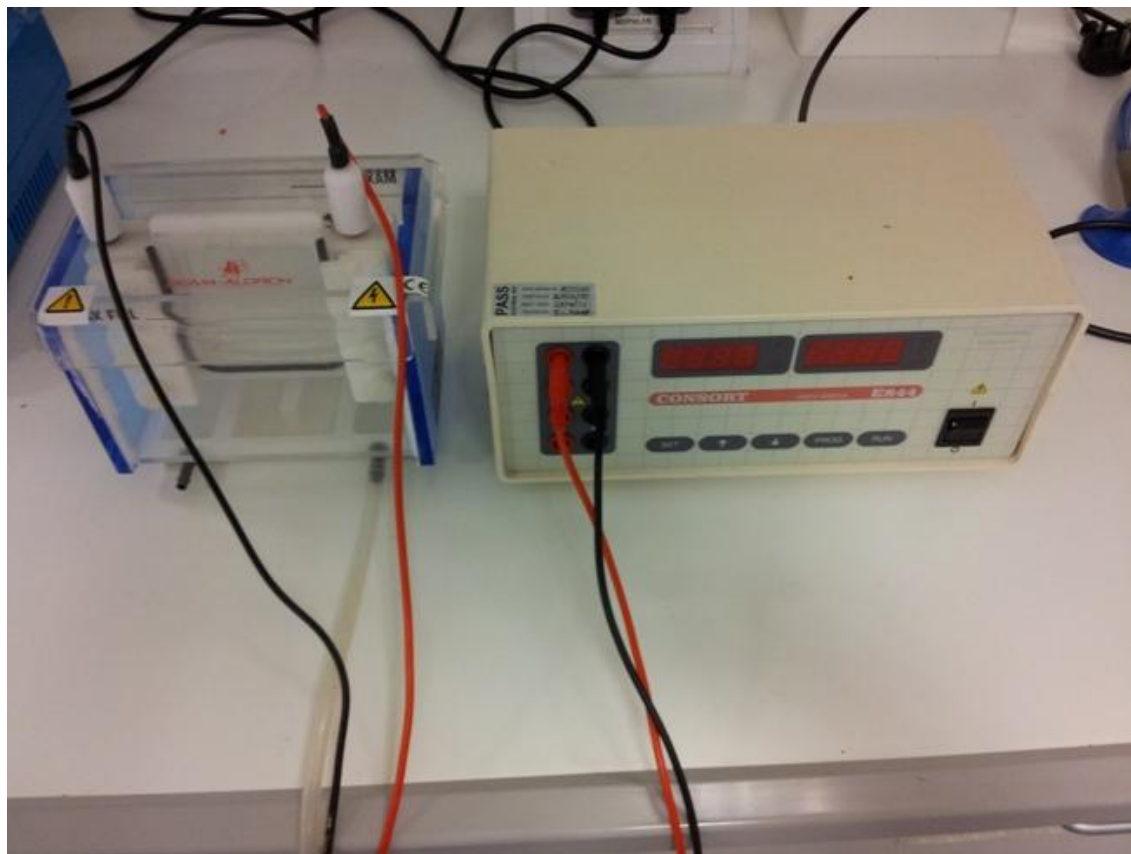
Figure 22: the electrophoresis system the left side is electrophoresis chamber, the right side is electrophoresis power supply.

In Figure 22, electrophoresis system included electrophoresis power supply and electrophoresis chamber, and the electrophoresis chamber can be classified into vertical one and horizontal one. Generally the vertical electrophoresis is used for polyacrylamide gel electrophoresis, which resolution is enough to separate one base of DNA. Most of the horizontal electrophoresis is used for Agarose gel electrophoresis, which can be used to separate big segment of DNA.

In this thesis, a polyacrylamide gel electrophoresis system which is a vertical one has been used to separate duplex strand DNA and single strand DNA. The voltage is 250V and the temperature is 25℃. 50mM Tris-HCl has been used as buffer, which pH is 7.5. The electrophoresis system includes power supply and chamber are purchased from sigma.

2.8 Ultraviolet spectrum

Figure 23: Varian Ultraviolet spectrum

The Ultraviolet spectrum is purchased from the Varian company, whose model is Cary 300. A temperature control system has been set up to control the temperature of the sample, which make the equipment not only can detect the scan spectrum of the sample at one point of temperature, but also can detect temperature changed spectrum of the sample at one point of UV spectrum. Even three dimension graph of time, temperature and wavelength can be obtained.

In this thesis, DNA (5uM) was dissolved in 1xTris buffer with a pH of 7.5. The variation of UV absorption in the DNA solution was recorded from the temperature ranges of 20 to 55℃, using a scan rate of 1℃/min with a constant UV wavelength of 260nm to find the melting point of each sequence.

Chapter 3   Rapid Laser Micromachining of highly Functionalised Microcantilever Biosensor Array

3.1 Introduction

There is a growing demand for biological Micro-Electro-Mechanical-Systems or bio-MEMS, which can directly interface with biological species in a wide variety of potential applications such as disease diagnostics, personalized treatment and novel drug delivery systems. Microcantilevers can form one type of bio MEMS device where specific molecular interactions occurring on the microcantilever surface will bend the cantilever beam, as a result of surface stress change, thereby translating molecular interactions into a mechanical response, which can be detected either optically or electronically [1].

Traditionally, microcantilevers are made of silicon, which involves a time consuming, multi-step, and high-cost vacuum fabrication processes [2]. This process is limited to the number of viable materials and requires flat surfaces for micromechanical devices [3]. Polymer is a good alternative to silicon in machining microfluidic system and MEMS (Micro Electro Mechanical systems) [4,5]. Polymer based microfluidic or MEMS system can be produced by hot embossing and injection molding [6, 7], which is relatively complex and expensive compared to laser direct fabrication. Lasers have been widely used as a rapid and flexible tool for machining novel materials and devices in the macro-world. It is able to be used in a variety of conditions including: tough materials, thick materials, and curved surfaces [8-10]. Recently, a variety of lasers were used for micromachining from nanosecond lasers to ultrafast lasers as well as IR lasers to UV lasers, depending on the materials to be fabricated and the desired applications [11-13]. On the other hand, laser ablation of polyimide has been investigated, as polyimides are known for their thermal stability, good chemical resistance, and excellent mechanical properties [14-16]. Therefore, the polyimide film has been selected as material for microcantilever in this thesis.

However, while potential applications are wide the technology is only feasible if a relatively rapid and low cost method for fabricating the components can be developed. For example, microcantilevers have been fabricated from silicon, but this involves time consuming multistage lithography and mask based etching and deposition processes in a high-cost clean room fabrication facility [17]. In addition, suspending microcantilever beams made of crystalline silicon materials are mechanically fragile, requiring great care of handling. However, polymer materials can be used as alternative candidates for fabricating microcantilevers which can be integrated with sensing or actuation to form microsensors or microactuators. In particular, polyimide films with excellent physical, electrical and mechanical properties are very suitable to the proposed applications; most importantly they are considerably cheaper than silicon.

If these polyimide devices are to be used for a large variety of applications then the ability to micro fabricate large arrays of differing cantilever geometries is appealing. This fabrication process should be flexible, low-cost and be simple to adapt for mass production. Laser machining of polyimide is well understood [14-16, 18] and good results have been demonstrated particularly using UV Excimer lasers.

Cantilevers have a important applications as sensor, which need to coat with specific sensor layers on their surfaces as receptor, for example DNA, or Protein. This layer used to respond to the analyte, which can react with the receptor. Generally, one side of the cantilever is coated with gold, which can reflect the laser beam to improve the optical readout. Another advantage of it is that the thiol can be bound to the gold-coated surface to form H-S covalent bond [19]. Reliably and efficiently functionalise each suspending microcantilever beam is a main challenge in cantilever biosensing field. Mcirocapillaries has been used to functionalise each cantilever on an array [19, 20]. The disadvantage of it is that it will functionalise the top and bottom at the same time, therefore, one side need to be with inert coating and the other side is functionalised with receptors layers. Another efficient method of functionalizing large microcantilever array

is to use chemical inkjet printing technique [19, 21]. The inkjet printing has an advantage over the capillary method that the speed is high and only one side of a cantilever will be coated to prevent the contamination of the backside.

The main challenge for the inkjet printing method is that it need precisely align the nozzle for the 3-dimentional cantilever structure, because the reproducibly functionalise the flexible suspending beams with of the curved shaped.

In this chapter, we have introduced a Q-Switched (60 ns pulse width) Diode Pump Solid State (DPSS) Nd:YVO4 laser (Spectra-Physics) operating at 355 nm in conjunction with a high speed scanning galvanometer stage. Whilst Excimer lasers have proven to be excellent lasers for mask type processing of MEMS devices [22]. The DPSS system offers a different approach and in particular, much more flexibility. The high beam quality of the DPSS system allows a small focused spot to be generated at the work place, which can then be scanned rapidly across the work place surface using a scanning galvanometer. This direct writing provides a very powerful and flexible micromachining device particularly for 2D geometries. DPSS laser systems are now widespread in industry and have a proven track record becoming an industrial standard for many micromachining applications offering a relatively straightforward turnkey system. A rapid laser micromachining highly functionalised microcantilever biosensor arrays has been described. The polyimide film has been functionalised before it is fabricated to microcantilever array with laser. It can not only use to functionalise single receptor layer on all cantilevers rapidly, but also combine with inkjet printing method to functionalise different receptor on each cantilever, which can cope with the curved shaped of the cantilevers.

3.2 Materials and Method

Kapton polyimide has many advantages, such as excellent electrical, physical, and mechanical properties, which has been applied in many different industries. (DuPont High Performance materials with ISO 9002). A wide temperature range for physical, chemical, and electrical properties: -269ºC-+400ºC. It can be used in wire and cable

tapes, motor slot liners, Tubing, Fiber optics cable, Etching, and Shims. Polyimide film (DuPont) are purchased from RS components Ltd, The thickness of the polyimide are 7.8μm, 12.5μm, 25μm, 50μm and 75μm.

3.3 Laser cutting parameters for clear cut

(a)   (b)
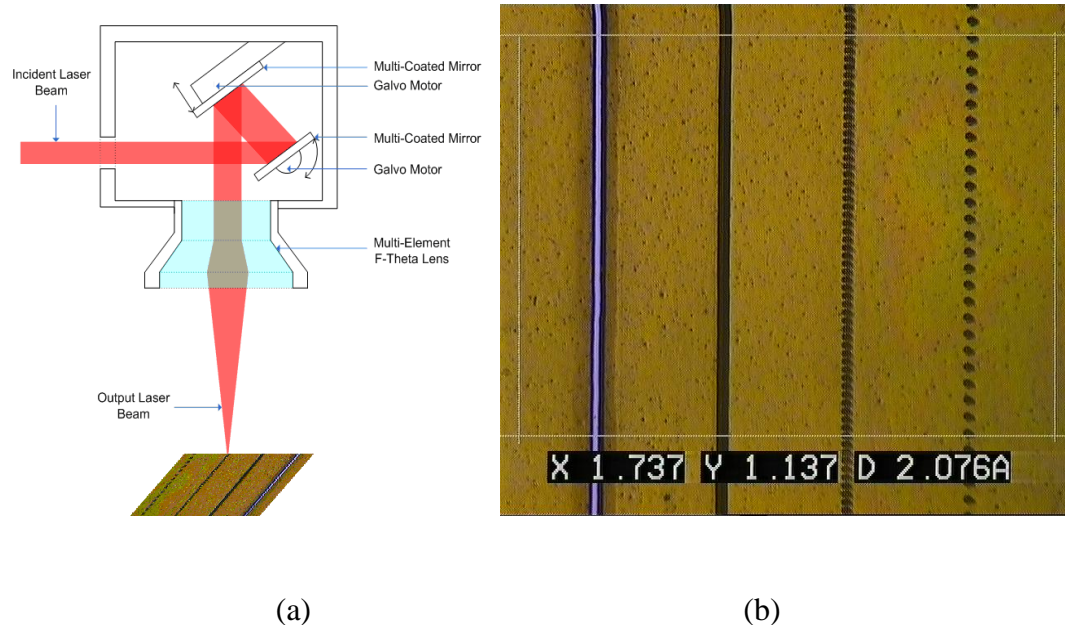
Figure 24: (a) Schematic for an optical scanner (b) Laser fabricated polyimide

Wavelength (355nm), power, and the impulse width were fixed, while the speed and frequency were adjusted to optimize the conditions. In Figure 1b, It can be seen that laser fabrication is some points on a line. If frequency increases or the scan velocity decreases, the density of the points will increase. To characterize the laser cutting effect, the relationship of frequency, velocity, average power and Pl was correlated with an equation : Pl=fPa/v (Pa is average power which is obtained from the meter, f and v are frequency of the laser and scan velocity of the laser, respectively, Pl is power divided by line).

It was then shown how the results responded to the PI, especially when v or f was changed to increase PI.   In Table 3, the velocity was decreased to increase Pl. In Table 4, and the frequency was increased to increase Pl. Both of their average powers are 1W.

Pl(W/m)	A(mm/s)	B(mm/s)	C(mm/s)
200000	60	140	220
225000	53.3	124.4	195.6
250000	48	112	176
275000	43.6	101.8	160
300000	40	93.3	146.7
400000	30	70	110
500000	24	56	88
600000	20	46.7	73.3
700000	17.1	40	62.9

Table 3: The frequency of column A, B and C are 15000Hz, 35000Hz and 55000Hz.

Pl(W/m)	D(Hz)	E(Hz)	F(Hz)
200000	15000	17500	20000
225000	16875	19687.5	22500
250000	18750	21875	25000
275000	20625	24062.5	27500
300000	22500	26250	30000
400000	30000	35000	40000
500000	37500	43750	50000
600000	45000	52500	60000
700000	52500	61250	70000

Table 4: The speed of column D, E and F are 15000Hz, 35000Hz and 55000Hz.

In Table 3, the frequency of column A is 15000Hz. The frequency of column B is 35000Hz.The frequency of column C is 55000Hz. In Table 4, the speed of column D is 50mm/s. The speed of column E is 60mm/s. The speed of column F is 70mm/s

Average power is 1W
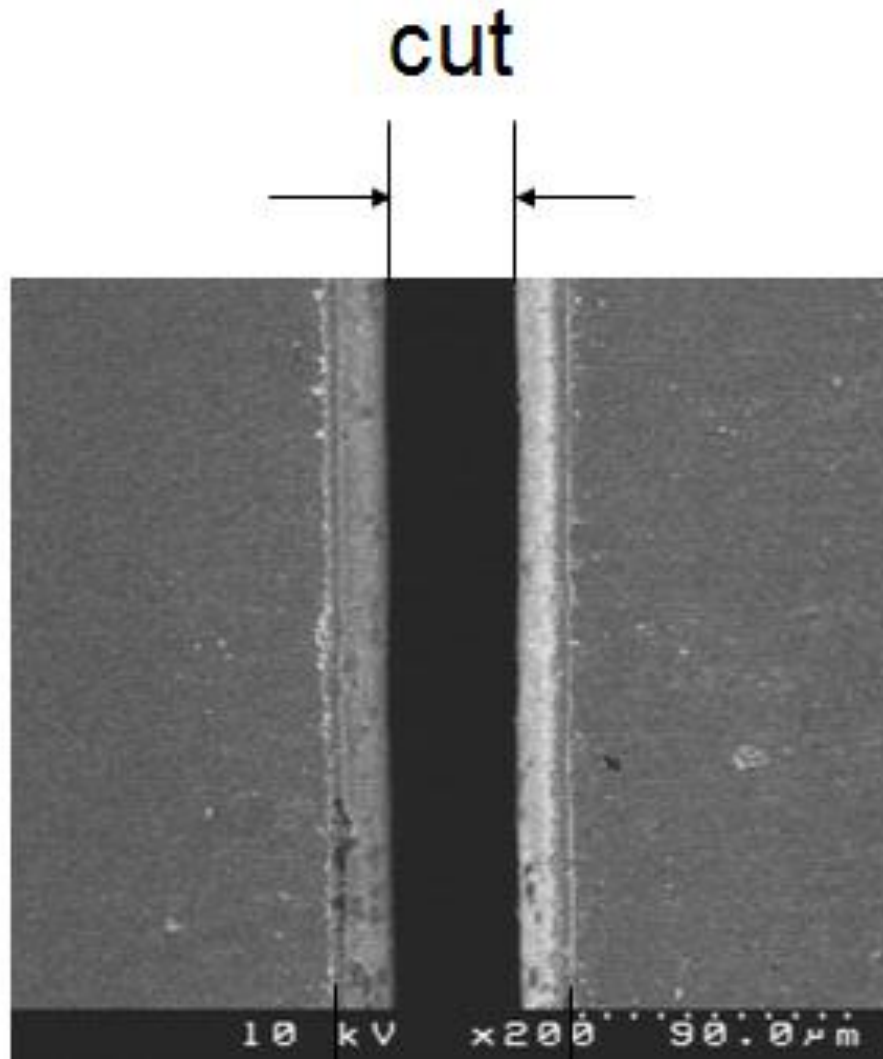
Figure 25: The polyimide was ablated through by laser, and it was defined cut region.

In Figure 25, this is the polyimide which was ablated by laser with a defined cut region. The conditions of the width of cut regions are shown in Table 3 and Table 4 from Figure 26: . Each point has been repeated for three times, and the curve of the graph has been drawn with the middle of the data. Other two data is used for the errors bar. The cut region increased with Pl, and it was caused by the change of v or f. From these results, the laser cutting conditions can be optimized. The cut region decreased when the Pl decreased. When the Pl is near 250000, the cut region is very narrow.
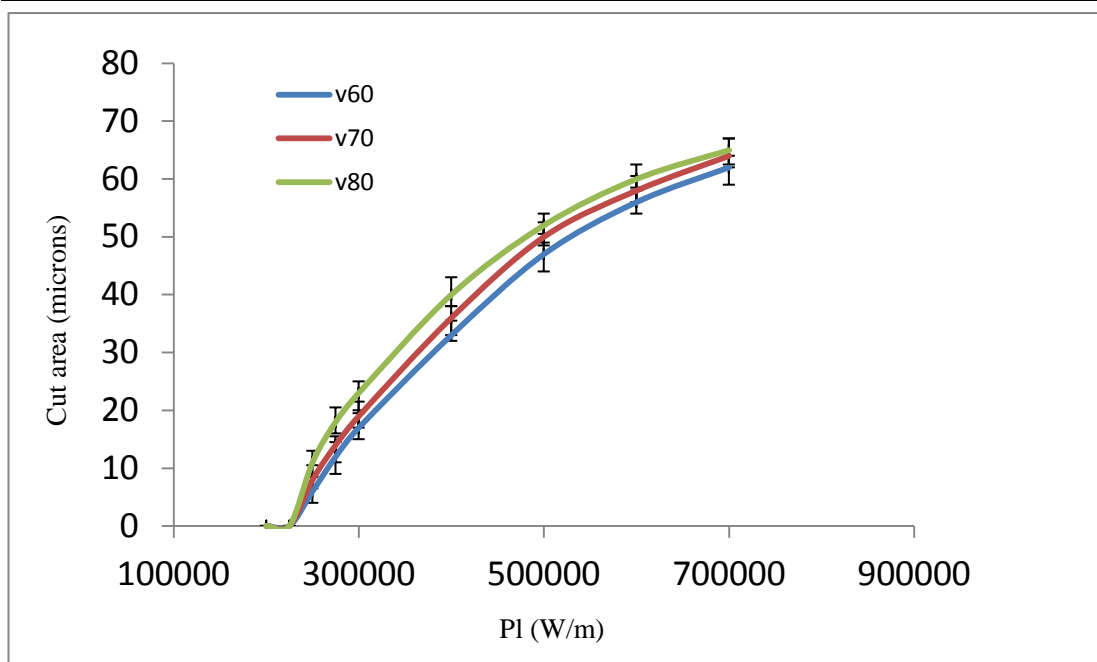
(a)
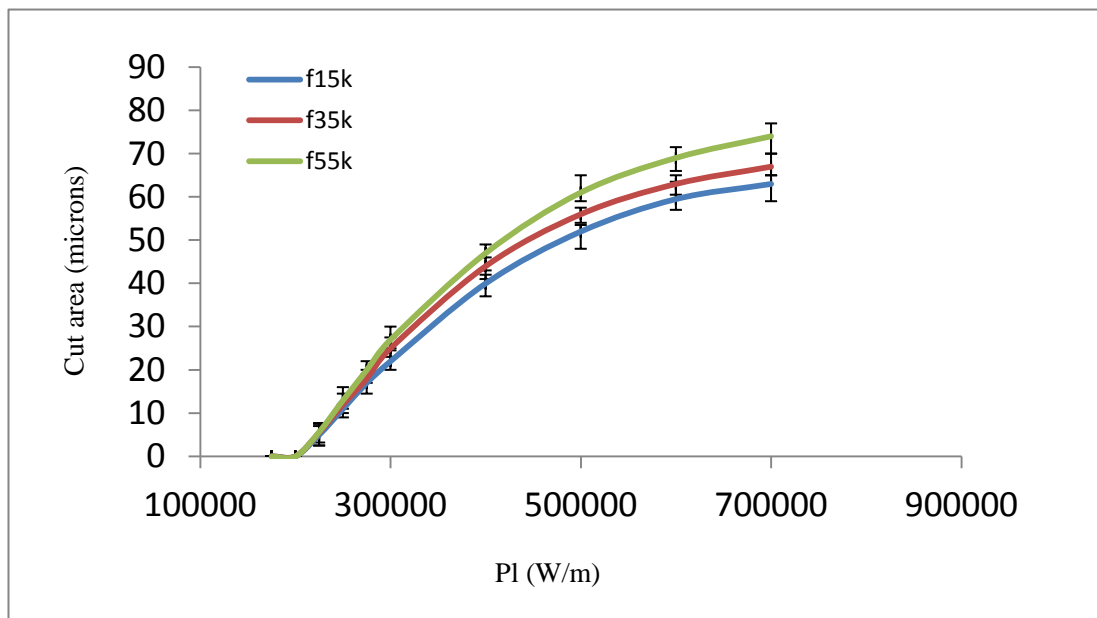
(b)

Figure 26: It is the data of cut regions of the polyimide. (a) The velocity are increased from 60 to 80mm/s, and (b) the frequency are increased from 15k to 55k.

3.4 Gold and chromium coated and Functionalization

A chromium film of 5nm and gold film of 50nm are evaporated on one side of the 25μm thickness polyimide film. (BOC Edwards Auto 500, U.K.; base pressure, 1 x 10^{-7} mbar; a thermal evaporation rate, 0.4 nm/s).If the device is used to detect DNA, DNA immobilized on one side of the polyimide film after gold coating on it. (10μM DNA in a buffer containing 1.0M potassium phosphate) The polyimide was subsequently immersed in 1mM 2-mercaptoethanol (Sigma Aldrich) for 1 hour., to remove non-specifically adsorbed DNA.[23, 24] The polyimide films were then rinsed by water (18.2 M Ohms, Elga Maxima), and dried with a stream of nitrogen.

3.5 Fabrication of microcantilever
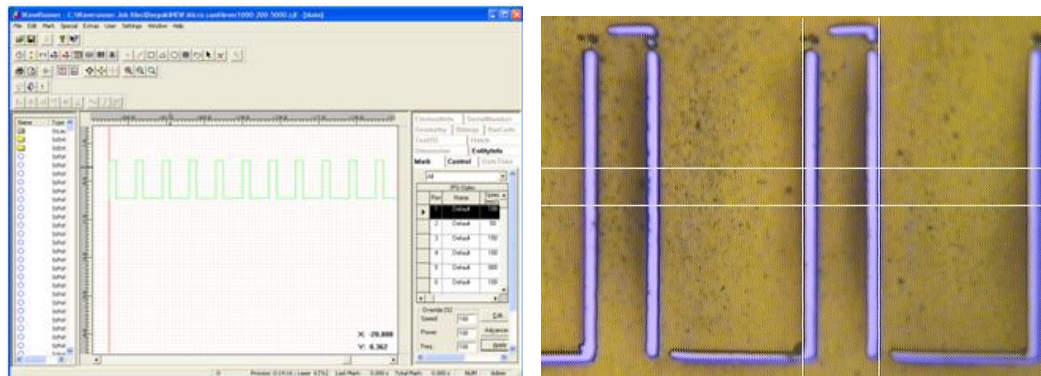
(a)   (b)

Figure 27: Polyimide cantilever fabrication (a) The design on the software. (b) Polyimide based cantilever fabricated with laser.

Figure 26 is used to find better parameter for fabricating polyimide with laser, and the cantilevers has been fabricated with the following the parameters: frequency 15kHz, current 85%, speed 45mm/s. The cantilever has been designed as shown in Figure 27a, and in Figure 27b, it is the results the of the cantilevers. The corner of the cantilevers is not cut through. It means that the laser beam delayed the line drawn on the software.

| (a) | (b) |
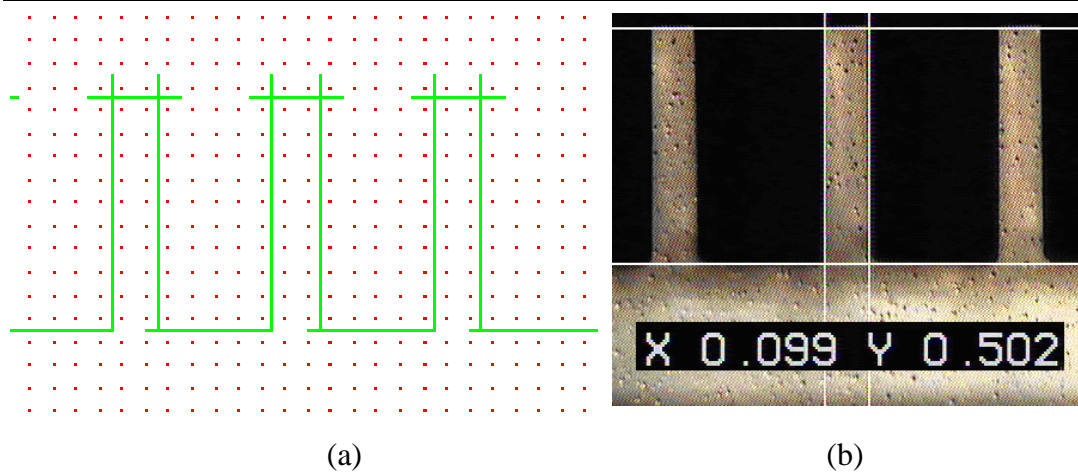
Figure 28: (a) Cantilever designed on software (b) Polyimide based cantilever fabricated with laser

To solve this problem, the structure of the microcantielver designed on the software has been updated, which is shown in Figure 28. The line didn't start from the end of each line. With this design, the cantilever can be fabricated as the designed shape shown in Figure 28b. Another method to solve the laser beam delay problem is that the whole cantilever has been drawn with one line. As shown in Figure 29, it is the cantilever, which is used to mount on cantilever system.

| (a) | (b) |

Figure 29: Polyimide cantilever under microscope. (a) Cantilevers under camera. (b) Cantilevers under microscope

(a)   (b)

Figure 30: Polyimide cantilever array (a) The structure of microcantilever designed on the software and (b) The polyimide based cantilever array, which is fabricated with laser.

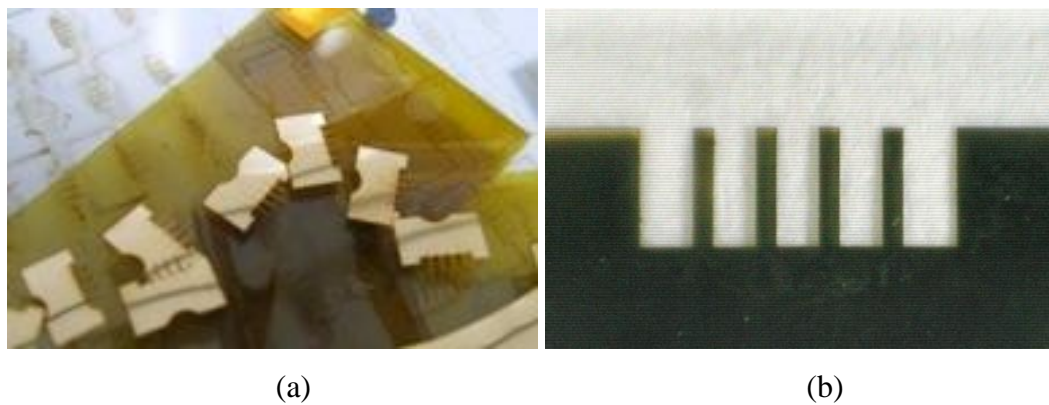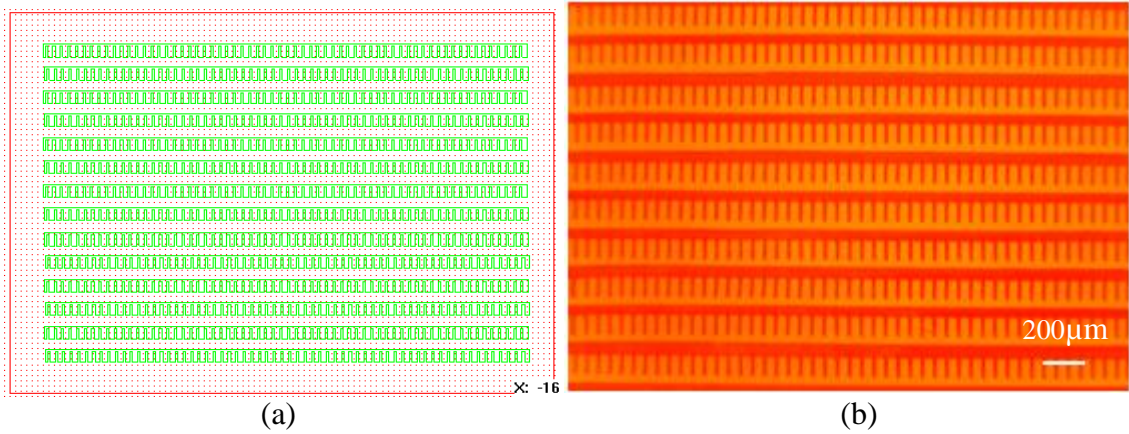With the parameters for laser fabrication, we found, microcantilevers were fabricated. A shown in Figure 30, the conditions for fabrication are frequency (15kHz), speed (45mm/s), and power (560mW). The size of the cantilever is 1000μm x200μm and it can produce hundreds of cantilevers in Figure 30b. The conditions are scanning speed: 45mm/s, power :500mW, frequency: 30kHz. A cantilever array has been designed in Figure 30a, and in Figure 30b it has been fabricated to cantilevers. About 600 cantilevers can be fabricated in few minutes, which is much faster than silicon cantilever fabrication. Each cantilever is fabricated with 25μm thickness polyimide.

3.6 Fabrication of other kind of microcantilever

In this section a series of microstructures has been fabricated, for example microcantilever on cycle, microcantilever with rectangle. The structure has been designed on computer by the Waverunner software. The polyimide is 25μm in thickness, and the parameter to fabricate is discussed before. The shapes have the potential to apply for BioMEMS, cell culture and other field.
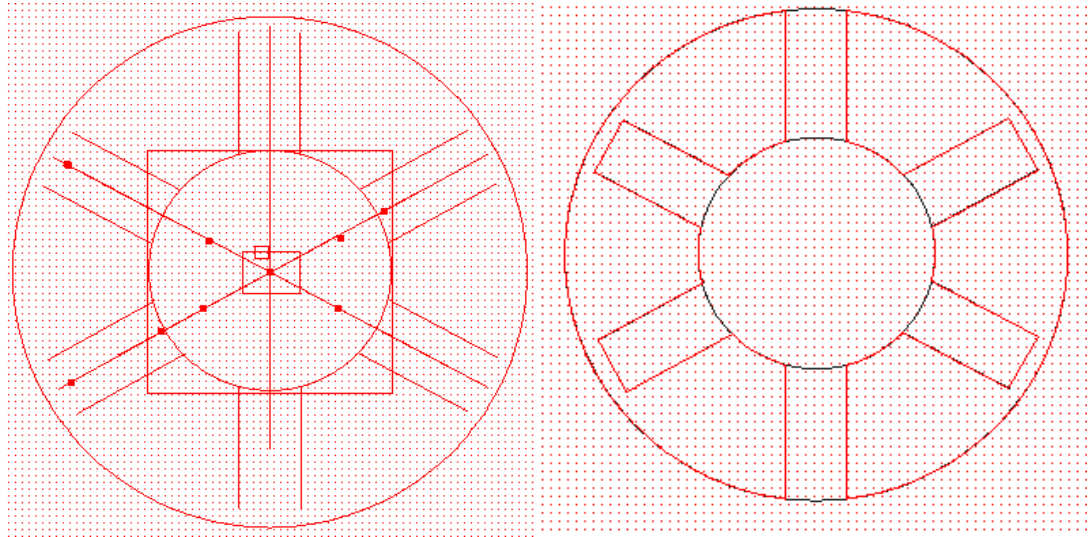
Figure 31: laser fabricated polyimide cantilever on cycle

A microcantilever designed with Waverunner software: circle is 200µm, fingers are 100µm and the whole cantilever size is nearly 500µm.

(a)   (b)
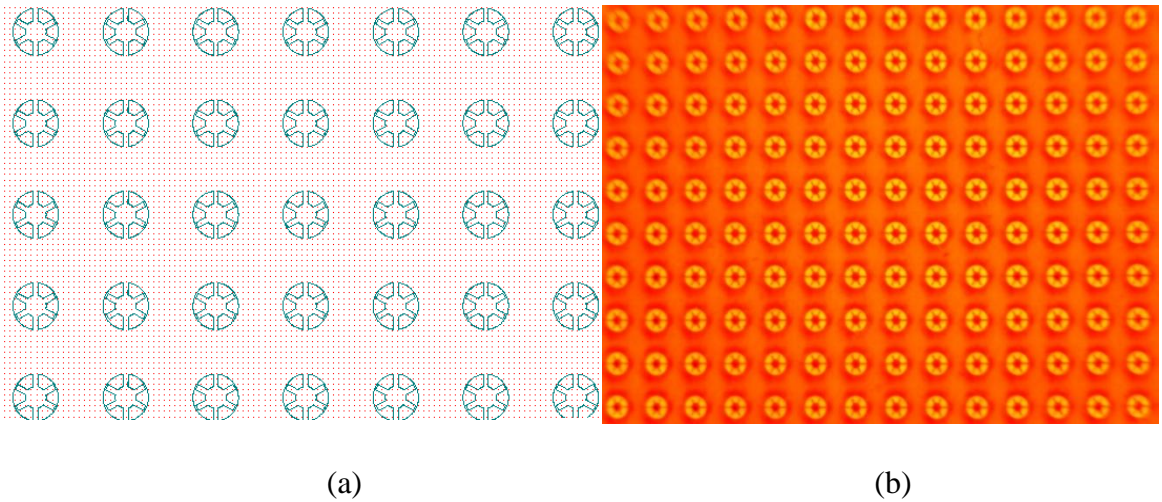
Figure 32: Laser fabricated polyimide cantilever on cycle (array) (a) The picture on the software. (b) The structure fabricated with laser.

Once the cantilever is created the laser micromachining is performed to obtain nearly 140 cantilevers on a 25µm thickness polyimide film at a speed of 50mm/s.
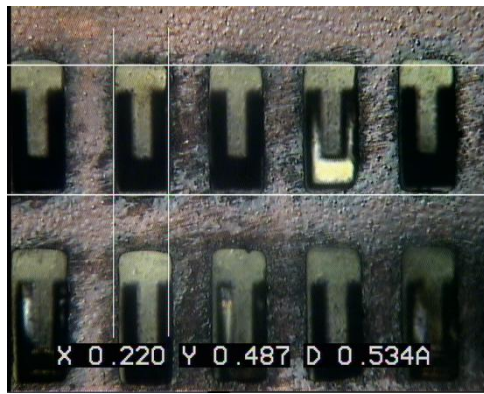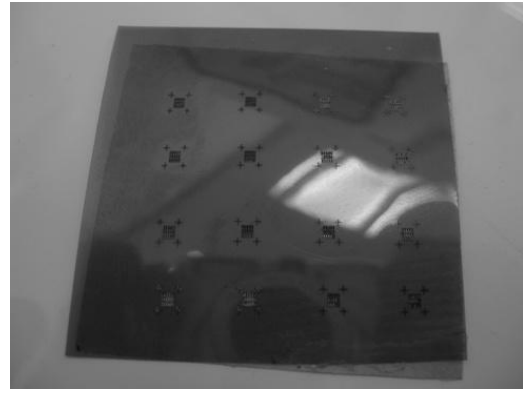
<center>(a)</center> <center>(b)</center>

Figure 33: Polyimide cantilever in rectangle the parameter of the cantilever is 50microns in width and 250microns in length. (a) The cantilevers under microscope. (b) The cantilevers under camera.

A more complex three dimension structure can be fabricated. It is a cantilever combined with rectangle. The rectangle is 220 microns in width and 487 microns in length. The cantilever is 50 microns in width and 250 microns in length. It is not difficult to fabricate the rectangle and cantilever, but it is difficult to align them together exactly. Even CCD has been used, it is still impossible to align them. In Figure 33, a method has been developed to fabricate it. A 75μm thickness polyimide with tape has been fabricated to rectangle array, and the rectangle array has not been moved away just be cleaned at situ. Subsequently, the tape has been peal out and the 7.6 micron thickness polyimide has been attached to it. And then, the focus of the laser has been changed and cantilevers have been fabricated. With this method, the three dimensional structure can be fabricated as shown in Figure 33. This structure has the potential to apply in cantilever array detection.

3.7 Investigation of Fluorescence labeled Microcantilever

Fluorescence labeled DNA has been test to confirm that laser fabricated cantilever after functionalization is suitable for DNA detection. Thiol modified DNA 5'-HS-TTA AGG TCT GGA CTG GCC TG-3' has been immobilized on the gold surface. The Rhodamine Green labeled 5'-Rhodamine Green-AAC AGG CGA GTC CAG ACC TT-3' has been hybridized to the Thiol modified DNA. Subsequently, the polyimide has

been fabricated to cantilevers. In Figure 34, it shows the Fluorescence labeled microcantilevers.

Fluorescence labeled DNA has been test to confirm that fabrication after fictionalization is suitable for DNA detection.   In Figure 34a ,thiol modified DNA 5'-HS-TTA AGG TCT GGA CTG GCC TG-3' has been imoblized on the gold surface. The Rhodamine Green labeled 5'-Rhodamine Green-AAC AGG CGA GTC CAG ACC TT-3' has been hybridized to the Thiol modified DNA. In area I, fluorescence labeled DNA has been coated, and in area II, it is not coated.   Subsequently, the polyimide has been fabricated to cantilevers in Figure 34b. In Figure 34c, it is a cantilever which is not coated fluorescence labeled DNA, which use to compare with Figure 34b to confirm the fluorescence has been coated. In Figure 34b, the edge of the cantilever are very narrow which means that laser ablating after DNA functionalization doesn't burn too much DNA.
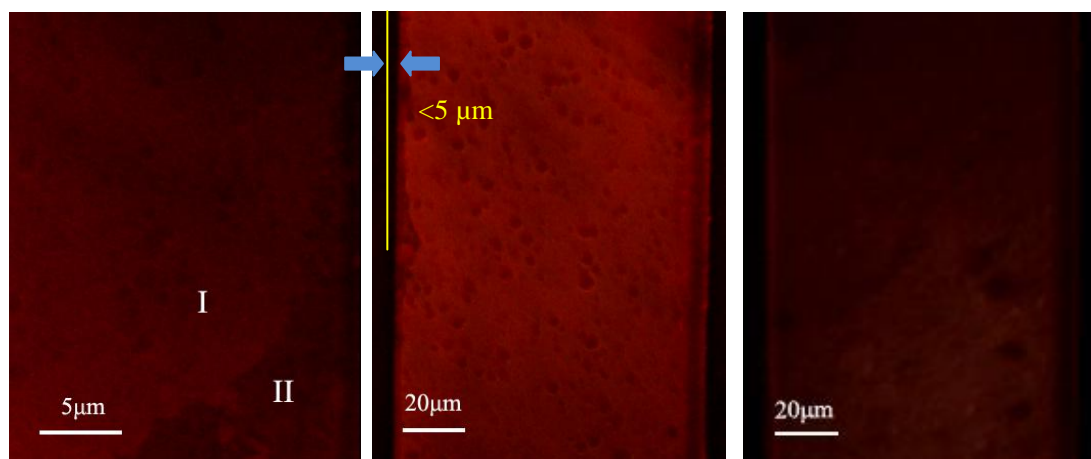
(a)   (b)   (c)

Figure 34: Fluorescence labeled mcirocantilever (a) I is with fluorescence and II is not. (b) The cantilever is labeled with fluorescence. (c) It is not labled with fluorescence.

3.8 DNA detection with the cantilever
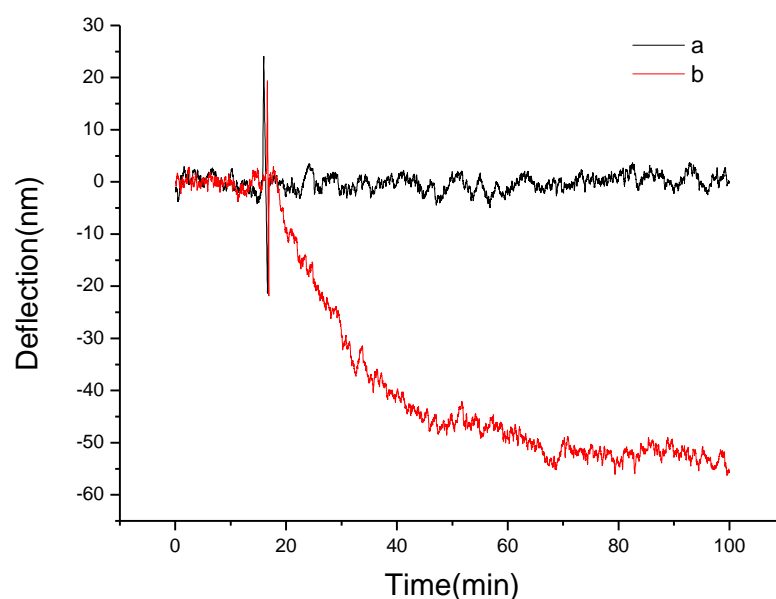
Figure 35: DNA detecting with polyimide based microcantilever. The black line is the reference and red line is the signal induced by DNA hybridization

DNA hybridization experiments have been demonstrated the applications of the polyimide based cantilevers. The probe DNA which is a 20 base oligonucleotide with the sequence of 5'-HS-TTA AGG TCT GGA CTG GCC TG-3', abbreviated as p-DNA is absorbed on the side of cantilevers coated with gold. The complementary DNA is used as target DNA, which sequence is 5' -AAC AGG CGA GTC CAG ACC TT-3', abbreviated as t-DNA. A noncomplementary DNA with the sequence of 5' -ATC ACG CCA GAC AAT TCT GT-3' is used as a reference, which is abbreviated as n-DNA. The oligonucleotides used in this experiment are synthesized by standard phosphoramidite chemistry and is purchased from IBA GmbH. Polyimide film is coated with 10μM probe DNA in 1M PBS buffer for 2h at room temperature. Subsequently, the film has been fabricated to cantilevers with laser and it is stored in a refrigerator at 4°C.The experiment has been repeated for more than 20 times and Figure 35shows one of the results.

DNA hybridization is performed in a saline sodium citrate hybridization buffer (5×SSC

buffer) at 25℃. The cantilever is set up inside the fluid cell and different buffers are introduced into the cell with the rotary valve and continues to flow for several hours till the signal does not drift. Target t-DNA (1μM) was then flown into the fluid cell, hybridizing with p-DNA, causing a signal increase, which means a downwards bending of the cantilever beam. When the liquid was injected into the chamber, the cantilever will be disturbed and cause a sharp peak of the signal. A reference experiment (non-complementary n-DNA) was carried out to confirm that the signal is indeed only caused by DNA hybridization. The experiment have been repeated more than 20 times, and Figure 35 shows one of the results.

3.9 Discussion

The driver for this work was to investigate the possibility of developing an alternative fabrication route for microcantlever devices which could be used for bio-MEMS applications. Currently, the established technology is the silicon cantilever which can cost in the region of £30 for an array of 10. The relatively high cost of these devices is due to material cost, laser cost (relatively high average power Excimer laser) processing via a multistep lithographic process and the requirement for a clean room environment. Consequently, this makes using these devices in large numbers or perhaps as a disposable bio-sensor unfeasible.

The direct laser writing of cantilevers in polyimide films is an attractive alternative to the silicon technology. We have demonstrated that the DPSS scanning technique is a simple, single step technique which can produce vast arrays of microcantilevers in a very short time (40 cantilevers per second). The DPSS system is a very robust turnkey laser and without the requirement for a clean room this presents a relatively straightforward fabrication facility. With the scanning method it is very simple to change the 2D configuration, size and shape of cantilever arrays making it a very flexible process. Naturally this therefore lends itself to a mass customizable process where one may require large numbers of sensors tailored to a specific application or biological system; without the need for a lithographic mask then the configuration can

be change very quickly. This is in contrast to an excimer-based mask projection fabrication route which is more naturally suited to producing many identical devices. Also, as we have demonstrated that an average power of only 0.56 W is required then the laser cost can be kept to a minimum as there is no need for a high average power DPSS laser. Also importantly, as it has been demonstrated the polyimide can be functionalised before laser processing which allows any 2D geometry to be made from the same bioactive starting material – again a very attractive prospect for potential bio-medical applications. The purpose of fluorescence labeled DNA test is to verify if DNA on cantilever surface will be burnt during the laser fabrication. The results show that DNA on the edge of the cantilever doesn't burn by the laser. Cantilevers fabrication after DNA functionalization is suitable for DNA detection.

3.10   Summary

- ❖ We have presented a viable low cost alternative to produce micro cantilevers compared to traditional established silicon technology.
- ❖ We have demonstrated that it is possible to fabricate large numbers of readily customizable biosensors using this relatively simple technique.
- ❖ A pre-functionalised polyimide sheet to be processed into active cantilever devices with a processing rate of 40 cantilevers per second has been demonstrated.

3.11　References for Chapter 3

1.　Arntz, Y., et al., *Label-free protein assay based on a nanomechanical cantilever array.* Nanotechnology, 2003. **14**: p. 86.

2.　Raiteri, R., et al., *Micromechanical cantilever-based biosensors.* Sensors and Actuators B: Chemical, 2001. **79**(2-3): p. 115-126.

3.　Lang, H., et al., *Nanomechanics from atomic resolution to molecular recognition based on atomic force microscopy technology.* Nanotechnology, 2002. **13**: p. R29.

4.　Jakeway, S.C., A.J. de Mello, and E.L. Russell, *Miniaturized total analysis systems for biological analysis.* Fresenius' journal of analytical chemistry, 2000. **366**(6): p. 525-539.

5.　Blankenstein, G. and U. Darling Larsen, *Modular concept of a laboratory on a chip for chemical and biochemical analysis.* Biosensors and Bioelectronics, 1998. **13**(3): p. 427-438.

6.　Martynova, L., et al., *Fabrication of plastic microfluid channels by imprinting methods.* Analytical Chemistry, 1997. **69**(23): p. 4783-4789.

7.　Becker, H. and U. Heim, *Hot embossing as a method for the fabrication of polymer high aspect ratio structures.* Sensors and Actuators A: Physical, 2000. **83**(1): p. 130-135.

8.　Dauer, S., A. Ehlert, and S. Büttgenbach, *Rapid prototyping of micromechanical devices using a Q-switched Nd: YAG laser with optional frequency doubling.* Sensors and Actuators A: Physical, 1999. **76**(1): p. 381-385.

9.　Rizvi, N.H., *Femtosecond laser micromachining: Current status and applications.* Riken review, 2003: p. 107-112.

10.　Hwang, D., T. Choi, and C. Grigoropoulos, *Liquid-assisted femtosecond laser drilling of straight and three-dimensional microchannels in glass.* Applied Physics A: Materials Science & Processing, 2004. **79**(3): p. 605-612.

11.　Sugioka, K., et al., *Three-dimensional microfluidic structure embedded in photostructurable glass by femtosecond laser for lab-on-chip applications.* Applied Physics A: Materials Science & Processing, 2004. **79**(4): p. 815-817.

12.　Giridhar, M.S., et al., *Femtosecond pulsed laser micromachining of glass substrates with application to microfluidic devices.* Applied optics, 2004. **43**(23):

p. 4584-4589.

13.	Klank, H., J.P. Kutter, and O. Geschke, *CO2-laser micromachining and back-end processing for rapid production of PMMA-based microfluidic systems.* Lab on a Chip, 2002. **2**(4): p. 242-246.

14.	Srinivasan, R., B. Braren, and R. Dreyfus, *Ultraviolet laser ablation of polyimide films.* Journal of Applied Physics, 1987. **61**(1): p. 372-376.

15.	Brannon, J.H., et al., *Excimer laser etching of polyimide.* Journal of Applied Physics, 1985. **58**(5): p. 2036-2043.

16.	Brannon, J. and J. Lankard, *Pulsed CO2 laser etching of polyimide.* Applied physics letters, 1986. **48**(18): p. 1226-1228.

17.	Lavrik, N.V., M.J. Sepaniak, and P.G. Datskos, *Cantilever transducers as a platform for chemical and biological sensors.* Review of scientific instruments, 2004. **75**(7): p. 2229-2253.

18.	Raimondi, F., et al., *Quantification of polyimide carbonization after laser ablation.* Journal of Applied Physics, 2000. **88**(6): p. 3659-3666.

19.	Bietsch, A., et al., *Rapid functionalization of cantilever array sensors by inkjet printing.* Nanotechnology, 2004. **15**(8): p. 873.

20.	McKendry, R., et al., *Multiple label-free biodetection and quantitative DNA-binding assays on a nanomechanical cantilever array.* Proceedings of the National Academy of Sciences, 2002. **99**(15): p. 9783.

21.	Bietsch, A., et al., *Inkjet deposition of alkanethiolate monolayers and DNA oligonucleotides on gold: evaluation of spot uniformity by wet etching.* Langmuir, 2004. **20**(12): p. 5119-5122.

22.	Zhou, F., et al., *Highly reversible and multi-stage cantilever actuation driven by polyelectrolyte brushes.* Journal of the American Chemical Society, 2006. **128**(16): p. 5326-5327.

23.	Herne, T.M. and M.J. Tarlov, *Characterization of DNA probes immobilized on gold surfaces.* Journal of the American Chemical Society, 1997. **119**(38): p. 8916-8920.

24.	Steel, A., et al., *Immobilization of nucleic acids at solid surfaces: effect of oligonucleotide length on layer assembly.* Biophysical Journal, 2000. **79**(2): p. 975-981.

Chapter 4   Internally referenced Microcantilever Biosensors

4.1 Introduction

Biosensor research is a promising and rapidly progressing field, with a wide range of applications such as disease diagnostics, environmental monitoring, and process control in industry. Most biosensors are based on electrochemical transducers, optical, piezoelectric and thermal effects [1]. Microcantilevers in particular possess advantages such as being label free, sensitive, real time, and massive parallelization have attracted considerable interest in the last few years, especially in single-nucleotide polymorphisms (SNPs) detection which is a major focus of genomics research.[2-4]

Single mismatch oligonucleotides detection has been carried out with cantilever arrays, and which has been further studied with high background of unspecific sequences [5, 6]. More detailed experiments have demonstrated the relationship between cantilever bending and the length, place of mismatch and quantity of mismatch of DNA oligonucleotides on surfaces. [7]

However, all of the experiments need to solve some problems, such as unwanted bimetallic effects and cross contamination of receptors on each side[8]. Generally, one side is with inert coating and the other side is functionalised with receptors layers to cope with cross contamination and temperature control system used to meet bimetallic effects, which can bend the silicon-gold structure with slight changes in temperature.[9] An internally referenced cantilever sensor has been developed with a double-sided gold coated surface, which can dramatically reduce the bimetallic effects[10]. But the thickness and quality of the gold film is still not identical, because the speed and time for gold evaporation cannot be controlled under   the same condition, if the double sides cannot be coated at the same time. A method has been discussed in this thesis to solve this problem.

This study describes a label-free detection method for sequence-specific detection of DNA by using an internally referenced polyimide based microcantilever sensor. The unique feature of this microcantilever sensor design is the use of reference coatings on the backside of the same chip. The effect of thermal drift can be substantially reduced by coating both top and bottom surfaces of the cantilever with identical gold thin films. To ensure that the gold coating on each side of the microcantilever is identical, a rotary motor was used to thermally coat the both sides of the cantilever simultaneously. The efficiency of functionalization on double sided cantilevers has been improved in this thesis, as thousands of double sided functionalised cantilevers can be fabricated in a few minutes, without cross contamination of receptors on each side. The reference receptors on one side is used as a control to adjust the difference between each cantilever, therefore the system errors among cantilevers can be cancelled. By coating a different DNA sequence monolayer on each side of the cantilever sensor, a highly accurate DNA biosensor using microcantilevers has been demonstrated with sufficient precision to reliably discriminate a single mismatch.

4.2 Internally referenced microcantilever system

4.2.1 Double sided gold evaporation and DNA functionalization

As shown in Figure 36a, a rotary motor has been used to rotate the polyimide film (Kapton), allowing gold to be evaporated with identical thicknesses on both sides. (50 nm of Au with a 5 nm chromium adhesion layer, BOC Edwards Auto 500, U.K.; base pressure, 1×10^{-7} mbar; a thermal evaporation rate, 0.4 nm/s).
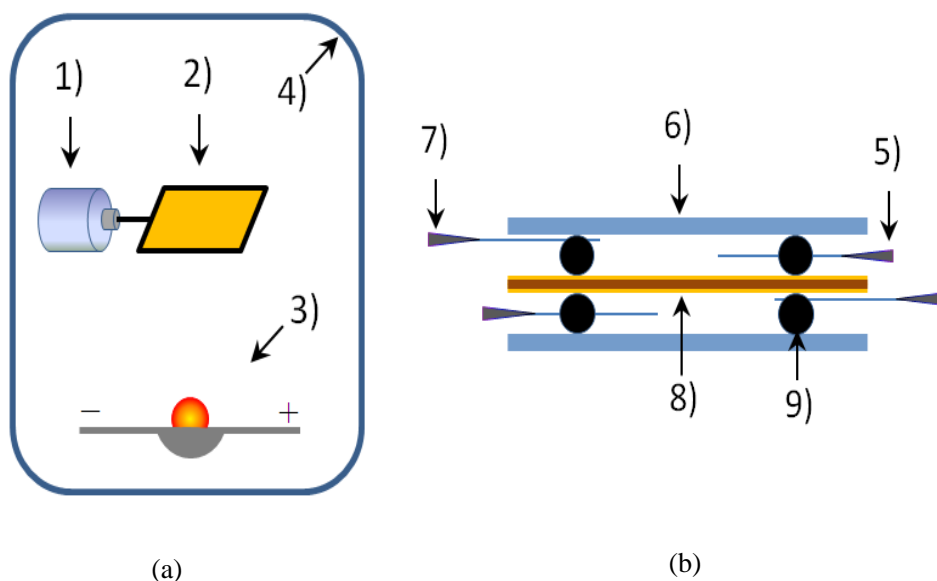
(a)

(b)

Figure 36: Schematic drawing of double sided gold evaporation (a) Gold coating sysem (1) rotary motor,(2) polyimide, (3)boat and gold or chromium, (4) vacuous chamber. (b) Schematic drawing of polyimide functionalization on double sides (5)needles for solution inputting, (6) glass wafer, (7) needles for air outputting, (8) polyimide (double sided coated gold) , and (9) O-rings.

DNA hybridization experiments have been performed in this paper to demonstrate the applications of the internally referenced cantilever. In Fig. 1b, gold-coated polyimide was attached with two O-rings on both sides, and then two pieces of glass wafer was used to cover the two O-rings. Then the receptor and reference receptor (10 M DNA in a buffer containing 1.0M potassium phosphate) was injected into the chamber with a syringe and allowed to rest for 2 hrs, at room temperature. The polyimide was subsequently immersed in 1mM 2-mercaptoethanol (Sigma Aldrich) for 1 hr., to remove non-specifically adsorbed DNA.[11, 12] The polyimide films were then rinsed by water (18.2 M Ohms, Elga Maxima), and dried with a stream of nitrogen.
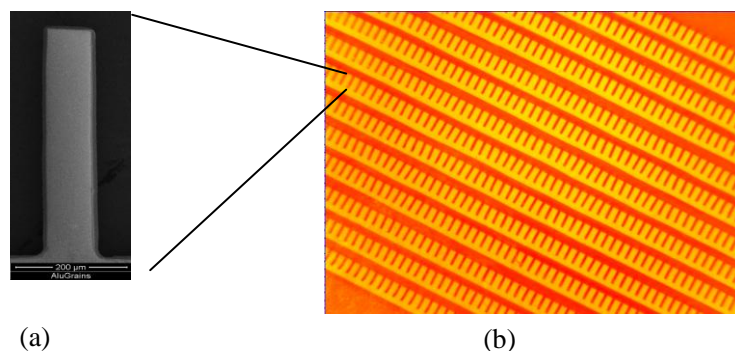
4.2.2   Cantilever Fabrication with laser

<div align="center">(a)   (b)</div>

Figure 37: (a) A polyimide based microcantilever fabricated with nanosecond laser. (The dimension of the cantilever: width 100µm× length 500µm× thickness7.6µm) (b) image of cantilever array.

The polyimide films were fabricated to cantilevers through laser micromachining immediately after DNA functionalization and stored at 4℃. Figure 37a shows the SEM image of a laser-fabricated cantilever, which are 500µm in length and 100µm in width. Polyimide can be rapidly machined with UV laser ablation technique, with optimized parameters. Nanosecond processing was carried out using a Nd:YAG system (JK705, GSI Group, Rugby, U.K.). This laser provides an average power of up to 350 W, pulse energies of between 0.1 and 50 J, at a wavelength of 355 nm. Pulse length can be varied between 0.5 and 5 ms, with repetition rates between 0.2 and 500 kHz. The sample is moved underneath the beam using a x–y–z-translation stage with an accuracy of 0.1 mm. Light from this laser was coupled to a galvanometer scan head (XLR8-10, Nutfield Technology, Windham, NH). The conditions for the polyimide are frequency (15 kHz), speed (45mm/s), and power (500mW).
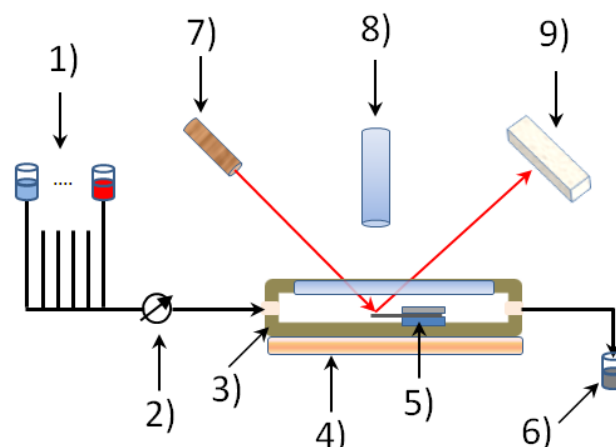
4.2.3   Cantilever system

Figure 38: Caption Schematic drawing of microcantilever detection system: (1) buffer solutions, (2) rotary valve, (3) fluid cell, (4) temperature control system and temperature sensor, (5) microcantilever sensor, (6) waste, (7) laser diode, (8) video microscope, and (9) position sensitive diode (PSD)

The cantilever optical readout system developed in this thesis includes a rotary valve, microcantilever chip mounted inside a fluid cell, laser diode, position-sensitive detector (PSD), and microscope with a digital CCD camera (Figure 38). The cantilever system is set up on an optical table (Newport Laminar Flow isolator) to reduce vibrations. The system is mounted in a non-transparent box made of PMMA (5mm thickness), with thermal insulated materials(10mm thickness), which reduces the external disturbance from air flow, background light, and temperature variations in the lab. The rotary valve switch device communicates via RS-232 and is used to flow different liquids into the fluid cell. With the use of the rotary valve, in addition to gravity pumping of the liquid (2mL/h), the spike of the curve in the results can be significantly reduced. The fluid cell is fabricated from PEEK, and sealed with a sapphire cover due to them both being inert to all chemicals involved in this experiment. Probe DNA-coated cantilevers were mounted in the fluid cell.   The optical resolution of the microscope is 5 m, which is used to confirm that the laser beam is on the tip of the cantilever. The laser beam reflected by the cantilever is aligned on to a position-sensitive detector (PSD) and an amplifier was used to amplify the current signal from the PSD and convert into voltage

signals. A National Instrument data acquisition card was then used to record data in LabView.

4.3 DNA detection

4.3.1 Concentration dependent

Concentration dependent

Name	DNA Sequences
probe: A	5'-thiol-TT AAG GTC TGG ACT GGC CTG-3'
target:Ac	3'- C TGA CCG GAC-5'
target:Ac1	3'- C TCA CCG GAC-5'
probe: B	5'-thiol-TT AAG GTC TGG ACT CGC CTG-3'
target:Bc	3'-C TG A GCG GAC-5'
probe: MF	5'-thiol-TT AAG GTC TGT AGT GCA GCG-3'
target:MFc	3'-A TCA CGT CGC-5'
target:noncomp1	3'-A AAT GTT CCC -5'
target:noncomp2	3'-G CAA TTA ATT -5'

Table 5 DNA sequence for concentration dependent and one mismatch DNA detection experiment.

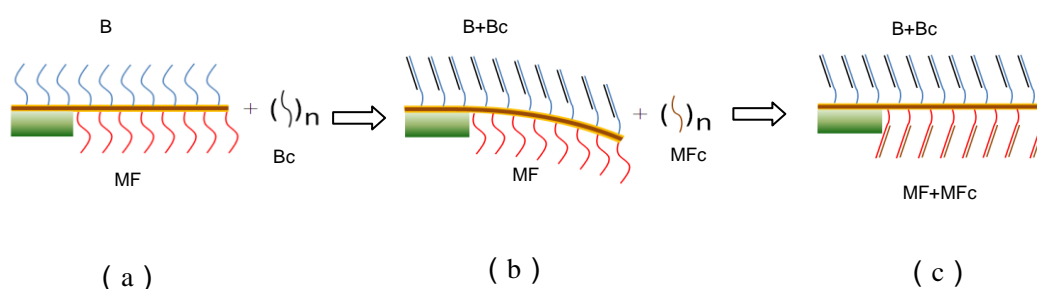(a)   (b)   (c)

Figure 39: scheme of double coated cantilever detection (a)Cantilever coated with probe DNA-B and probe DNA-MF. (b)DNA-Bc which is complementary to DNA-B introduced into the cell to cause the cantilever bending toward one side. (c) DNA-MFc which is complementary to DNA-MF introduced into the cell to cause that the cantilever bending back

Two experiments were performed in this thesis to demonstrate the applications of the internally referenced microcantilever sensor. The oligonucleotides used in these experiments are listed in Table 5. The oligonucleotides used in this experiment are synthesized by standard phosphoramidite chemistry and is purchased from IBA GmbH.

In the first experiment the device is used as a DNA concentration sensor. As shown in

Figure 39, the probe DNA-MF and DNA-B is thiolated single-strand DNA immobilized on each side of the cantilevers. The 20 base oligonucleotide with the sequence of 5'-thiol-TT AAG GTC TGG ACT CGC CTG-3' abbreviated as DNA-B, is coated on one side of the polyimide film. Another 20 base oligonucleotide with the sequence of 5'-thiol-TT AAG GTC TGT AGT GCA GCG-3' abbreviated as DNA-MF, which is noncomplementary to DNA-B, is coated on the other side of the polyimide film. The thiolated modification enables covalent binding to the gold coated surface. DNA-B and DNA-MF are reference to each other. The 10 bases oligonucleotide DNA-Bc and DNA-MFc are used as the target DNA which is complementary to DNA-B and DNA-MF.
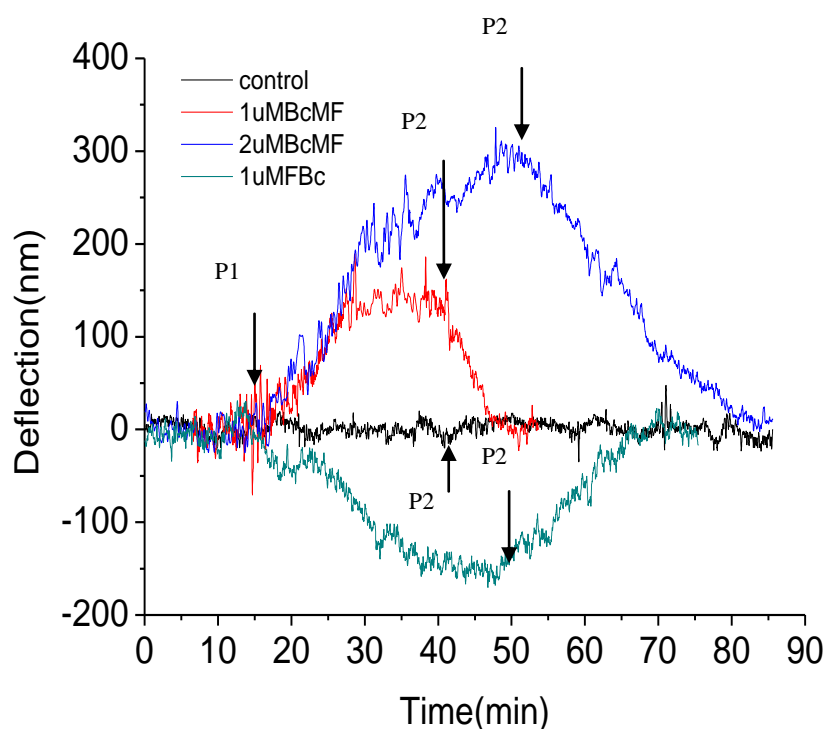

Figure 40: results of double coated cantilever detection Introduce 2μM DNA-noncomp1 at P1, introduce 2μM DNA-noncomp2 at P2.1uMBcMFc(red): Introduce 1μMBc at P1,and introduce 1μM MFc at P2. 2uMBcMFc(blue): Introduce 2μM Bc at P1, introduce 2μM MFc at P2. 1uMMFcBc(green): Introduce 1μMMFc at P1, introduce 1μM Bc at P2. Each cantilever is 500 μm in length, 100 μm in width and 7.6μm thickness. 25℃. The red line shows

DNA hybridization is performed in a saline sodium citrate hybridization buffer(5×SSC buffer) at 25℃. The cantilever is set up inside the fluid cell and different buffers are introduced into the cell with the rotary valve and continue to flow for several hours till the signal does not drift. Target DNA-Bc (2μM) was then flown into the fluid cell, hybridizing with DNA-B, causing a signal increase, which means a downwards bending of the cantilever beam. After the introduction of the target DNA-MFc, the signal decreased back to baseline.

Figure 40 also shows the results when the experiments are repeated for 1μM DNA-MFc concentration to demonstrate that the device can differentiate between varying concentrations. A reference experiment (non-complementary DNA-nomcomp) was carried out to confirm that the signal is indeed only caused by DNA hybridization. The red line is that target DNA-Bc was injected to the system to cause a positive signal and the target DNA-MF was introduced to the system to cause a negative signal. The green line was operated in the reverse way, and we can find that the negative signal firstly and then the positive signal. It can be explained that DNA-Bc which is complementary to DNA-B which always cause the cantilever bends to one side, and DNA-MF cause the cantilever bends to the other side.

4.3.2　Single mismatch detection

In the second experiment, the device was used to detect a single mismatch DNA sequence. The experiment is similar to
Figure 39, except that the probe DNA-MF has been replaced with DNA-A, and target DNA-MFc has been replaced with DNA-Ac. DNA-B is one base different from DNA-A, and they are coated on the two sides of each cantilever.   As shown in
Figure 39b, target DNA-Bc was introduced into the fluid cell to hybridize with probe DNA-B, which caused the cantilever to bend toward downwards. In Fig. 4c, target DNA-Ac was introduced into the cell to hybridize with probe DNA-A, which causes the cantilever to bend upwards. Before the experiment, DNA was tested with Native

polyacrylamide gel electrophoresis and ultraviolet spectrum (UV) to confirm that it will be suitable for the experiment.
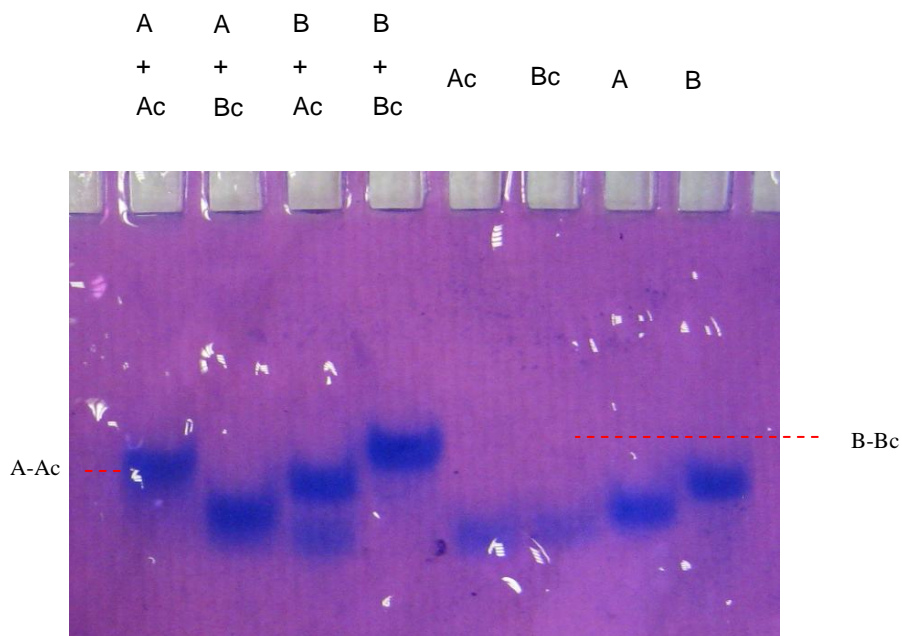

Figure 41: Native gel electrophoretic analysis of DNA duplex formation in Tris-HCl buffer

DNA-A and DNA-Ac, DNA-B and DNA-Bc are complementary strands respectively. Strands A and B have one base mismatch. As shown in Figure 41, native polyacrylamide gel electrophoresis was used to verify if A+Ac, A+Bc, B+Ac, and B+Bc can form duplex DNA. The DNA samples were made by mixing equal molar amounts of their component strands in Tris-HCl buffer solution (Tris-HCl 50mM, NaCl 100mM, pH7.5) at 25℃. The results showed that strand A was able to associate with strand Ac to form an A-Ac duplex (lane A + Ac). Similarly, strands B and Bc formed a B-Bc duplex (lane B + Bc). However, both A+Bc and B+Ac could not form duplex (lanes A + Bc and B+Ac). This indicated that the mismatch base pair we chose could determine the formation of duplex DNA at 25℃.
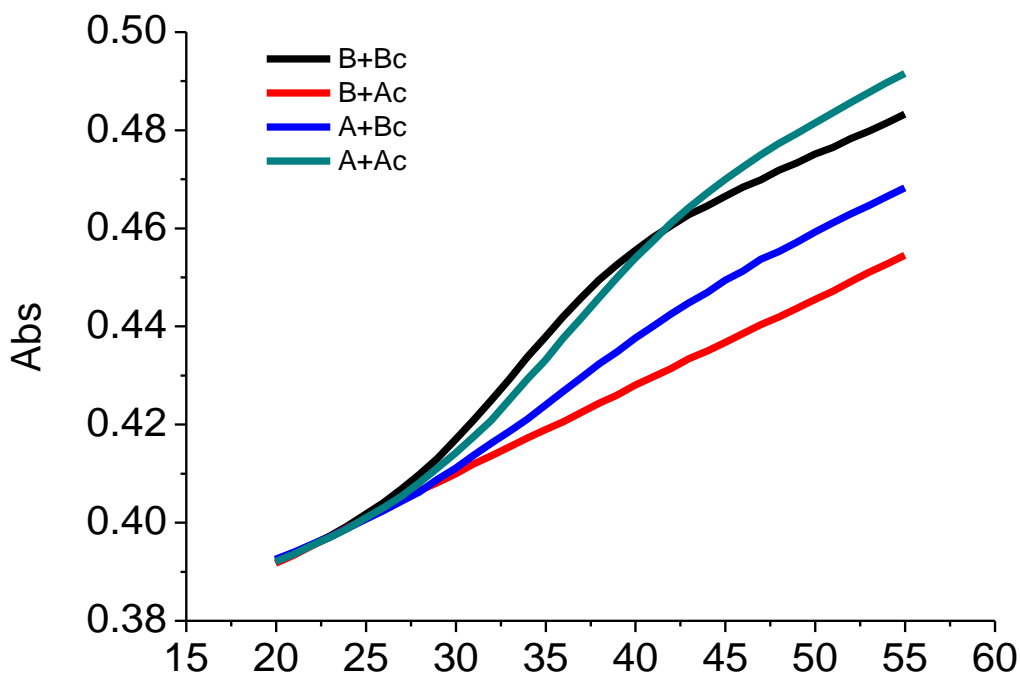
Figure 42: The UV results for DNA hybridization test.

As shown in Figure 42 UV(Ultraviolet spectrum) was also taken to confirm the results. DNA (5μM) was dissolved in 1xTris buffer with a pH of 7.5. The variation of UV absorption in the DNA solution was recorded from the temperature ranges of 20 to 55℃, using a scan rate of 1℃/min with a constant UV wavelength of 260nm. Figure 42 shows B+Bc and A+Ac have melting points of ~31℃ and 33.5℃ respectively, and B+Ac and A+Bc do not have melting points. This signifies that B+Bc and A+Ac can form duplex DNA at 25℃ but B+Ac and A+Bc can not.

The results of Native polyacrylamide gel electrophoresis and UV demonstrate that the DNA sequences are suitable for the experiments. In Figure 42 (line-BcAc), target

DNA-Bc(1uM) was introduced into the fluid cell at P1, which caused an increased signal (downwards cantilever bending), and when target DNA-Ac was switched into the cell at P2, there was a decreased signal (upwards cantilever bending). It can be explained that the cantilever deflects towards one side and bends back. In Fig. 8(line-BcAc1), there is one mismatch between target DNA-Ac1 and probe DNA-A. There are two mismatches between target DNA-Ac1 and probe DNA-B. Target DNA-Bc introduced into the fluid cell to cause an increased signal, and when Target DNA Ac1 was introduced into the cell at P2, the curve decreased slightly.

The results of curve BcAc and BcAc1 demonstrates that the cantilever sensors are able to distinguish a single mismatch between Bc and Ac. The device can distinguish one mismatch (Ac-B) and two mismatches (Ac1-B). In Fig. 8(line-control), a reference experiment was performed to ensure that non-complementary DNA cannot cause any signal.
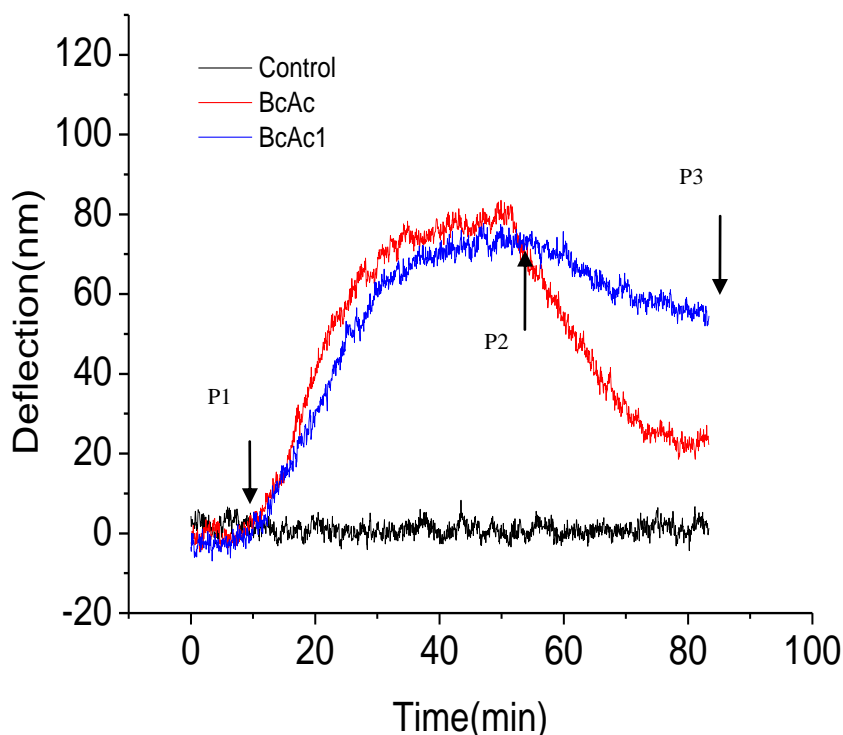

Figure 43: results of cantilever detection. The black line is control, the

In Figure 43, it is a scheme to detect one single mismatch DNA. A and B were one base different. Ac and Bc are complementary strands to A and B respectively. BcAc: The

functionalised microcantilever sensor was exposed to a solution of Bc at P1, then Ac was introduced to the system at P2. BcAc1: The functionalised microcantilever sensor was exposed to a solution of Bc at P1, then Ac1 was introduced to the system at P2. Control1: The functionalised microcantilever sensor was exposed to a solution of noncomp1 at P1, and then noncomp2 was introduced to the system at P2.

4.4 Discussion

Internally referenced sensors signify that the receptor and reference receptor are coated on both sides of a single cantilever uniformly. It is difficult to coat similar receptors on both the top and bottom sides of a micro-size cantilever due to the difficulty in handling such small sizes and the possibility for cross contamination. A method has been developed to solve this problem in this work. First of all, the thickness of the gold and chromium film evaporated on the top and bottom sides needs to be exactly the same. In the traditional method, one side was coated gold; the cantilever was removed, flipped over, and coated again. With this method, the gold evaporation speed, the condition for evaporation will affect the thickness of gold layer and the quality of the surface to cause the gold film on both sides to differ. Due to this differing gold film on each side of the cantilever, and if the temperature changes, the cantilever will bend unevenly toward one side. Therefore, a rotary motor to evenly rotate the polyimide film has been used in Fig 1(a), to provide the same condition for each side of the polyimide surface.

In traditional methods, one side of the cantilever with inert coating and the other side with receptors has been used to cope with the cross contamination from receptors on each side. In this paper, the process of fabrication cantilevers has been modified to solve this problem. The polyimide film has been coated with gold, functionalised with receptors on each side, rinsed with DI water, and lastly fabricated into cantilevers. With this method, the contamination problem has been perfectly solved and the condition for functionalization can be controlled to be completely the same. The more important advantage of this method is that the character of receptors on each side can be similar. In this paper the top and bottom of the cantilevers can be coated DNA-A and DNA-B

which is only one base different.　This ensures that the characters of double sides of each cantilever after functionalization are quite similar, which completely removes temperature disturbances.

Cantilevers are inevitably different due to factors of fabrication. Therefore no two cantilevers are completely identical. The internally referenced microcantilever system has the advantage to cancel the difference between each cantilever. In Fig. 8(BcAc, BcAc1), from P1 to P2, Target DNA-B was introduced to the system, which caused the cantilevers to bend towards one side. The concentration of target DNA-B, buffer, and temperature are the same, therefore the difference between the two curves are caused by the difference of the two cantilevers. From P2 to P3, the two cantilevers are used to detect target DNA Ac and Ac1. With the mathematical method, the curve from P1 to P2 can be used to cancel the difference between two cantilevers to obtain more precise results for target DNA Ac and Ac1. This means that one side of the cantilever can be used to compensate for the system errors among different microcantilevers, and the other side can be used to detect target analytes. With this method, the difference among each cantilever can be cancelled.

Another advantage of this method is that thousands of internally referenced microcantilevers can be fabricated in a few minutes. Traditional methods functionalise the cantilevers after fabrication. It is difficult to coat different receptors on each side of one cantilever, and it is more difficult to fabricate thousands of internally referenced microcantilevers at one time. Polyimide based cantilevers are sensitive, low cost, fast fabricating, which succeed the advantages of polymer.[14]

4.5 Summary

❖ Internally referenced polyimide based microcantilever system has been developed. Thousands of this kind of cantilevers can be fabricated with laser in a few seconds.

❖ The quality of the top and bottom surface of the cantilevers is similar, and this method can confirm that the receptors on each side will not contaminate each other.

❖ DNA concentration detection experiment has been designed to find the system has the potential to be a DNA concentration sensor.

❖ Mismatch DNA detection experiment shows that the system can be used to detect one base mismatch DNA.

4.6 References for Chapter 4

1. Eggins, B.R., *Biosensors: an introduction*. Vol. 212. 1996: Wiley-Teubner New York.

2. Raiteri, R., et al., *Micromechanical cantilever-based biosensors*. Sensors and Actuators B: Chemical, 2001. **79**(2-3): p. 115-126.

3. Lang, H., et al., *Nanomechanics from atomic resolution to molecular recognition based on atomic force microscopy technology*. Nanotechnology, 2002. **13**: p. R29.

4. Schafer, A.J. and J.R. Hawkins, *DNA variation and the future of human genetics*. Nature biotechnology, 1998. **16**(1): p. 33-39.

5. Fritz, J., et al., *Translating biomolecular recognition into nanomechanics*. Science, 2000. **288**(5464): p. 316-318.

6. McKendry, R., et al., *Multiple label-free biodetection and quantitative DNA-binding assays on a nanomechanical cantilever array*. Proceedings of the National Academy of Sciences, 2002. **99**(15): p. 9783.

7. Hansen, K.M., et al., *Cantilever-based optical deflection assay for discrimination of DNA single-nucleotide mismatches*. Analytical Chemistry, 2001. **73**(7): p. 1567-1571.

8. Fritz, J., *Cantilever biosensors*. Analyst, 2008. **133**(7): p. 855-863.

9. Love, J.C., et al., *Self-assembled monolayers of thiolates on metals as a form of nanotechnology*. Chemical Reviews-Columbus, 2005. **105**(4): p. 1103-1170.

10. Shu, W., et al., *Highly specific label-free protein detection from lysed cells using internally referenced microcantilever sensors*. Biosensors and Bioelectronics, 2008. **24**.

11. Herne, T.M. and M.J. Tarlov, *Characterization of DNA probes immobilized on gold surfaces*. Journal of the American Chemical Society, 1997. **119**(38): p. 8916-8920.

12. Steel, A., et al., *Immobilization of nucleic acids at solid surfaces: effect of*

oligonucleotide length on layer assembly. Biophysical Journal, 2000. **79**(2): p. 975-981.

13.   Zhang, X.R. and X. Xu, *Development of a biosensor based on laser-fabricated polymer microcantilevers.* Applied physics letters, 2004. **85**(12): p. 2423-2425.

Chapter 5   Microfluidic Channel based Cantilever Biosensors for Enhanced Pathengen Detection

5.1 Introduction

Cantilever biosensors have demonstrated impressive sensitivity for the detection of nucleic acids, proteins and cells [1-4]. However, in solution, when operated in the resonance mode, viscous damping severely degrades the resolution of detection [5]. Alternatively, cantilevers can be operated in static mode, with surface stress and mass determining the degree of cantilever bending. While this eliminates the problem of viscous damping for measurements in liquid, the challenge then becomes effective delivery of the sample to the cantilever surface, especially in applications where the analyte sample is not small [6]. In order to address this dilemma, Manalis and his college developed a novel strategy whereby microfluidic channel is directly integrated onto a silicon based microcantilever, which employed in the resonance mode [5, 7, 8]. The analyte can be transported through the microfluidic channel to sensor surface in liquid environment, but the cantilever channel will not be damped as the liquid is embedded inside the cantilever device. This highly successful strategy has bead to the weighting of single cells in fluid [5].

However, the silicon based device has to be operated in vacuum [9-11]. In order to achieve the sensitivity required. Additionally, the fabrication of the channel embedded microcantilevers is highly challenging and require sophisticated instrument for readout high frequencies [12].

Therefore, we here aim to develop a new approach to fabricate a polymer based microcantilever sensor with embedded microfluidic channel. Instead of operating in

dynamic mode, the polymer cantilever is expected to be soft enough to operate in static mode. The main advantage of the system presented here is that since the device is made entirely of polyimide it is both cheaper and easier to manufacture.

The application of polyimide microfluidic microcantilevers to the detection of waterborne pathogens, in particular Cryptosporidium, is reported here. Cryptosporidium is a protozoan pathogen, which is highly problematic for the water industry due to a low infectious dose [13] and high degree of robustness which enables long survival times in water along with resistance to standard disinfection by chlorination [14]. The UK disease burden is estimated at around 60,000 cases annually with the most common cause of infection being waterborne oocysts [15], while worldwide it is estimated that 250-500 million cases occur every year in developing countries, making a significant contribution to childhood mortality [16].

Several biosensor technologies have been applied to the detection of Cryptosporidium as reported in a recent review article. Both quartz crystal microbalance (QCM) and piezoelectric microcantilever (PEMC) approaches utilised relatively large flow cells and delivery of the sample to the sensor surface was not characterised. The approach reported here has the advantage of ensuring effective sample delivery to the surface of the sensor, enabling high capture efficiency, which is useful in the situation of detecting rare pathogens. Miniaturisation of sample delivery in this way limits the throughput of devices, although there is potential to negate this problem through parallelization or effective sample pre-processing. Previous work using microcantilevers without microfluidic channels presented low sensitivity to Cryptosporidium oocysts whereas use of the microfluidic channel has enabled a detection limit of oocysts/mL.

5.2 Fabrication Scheme:
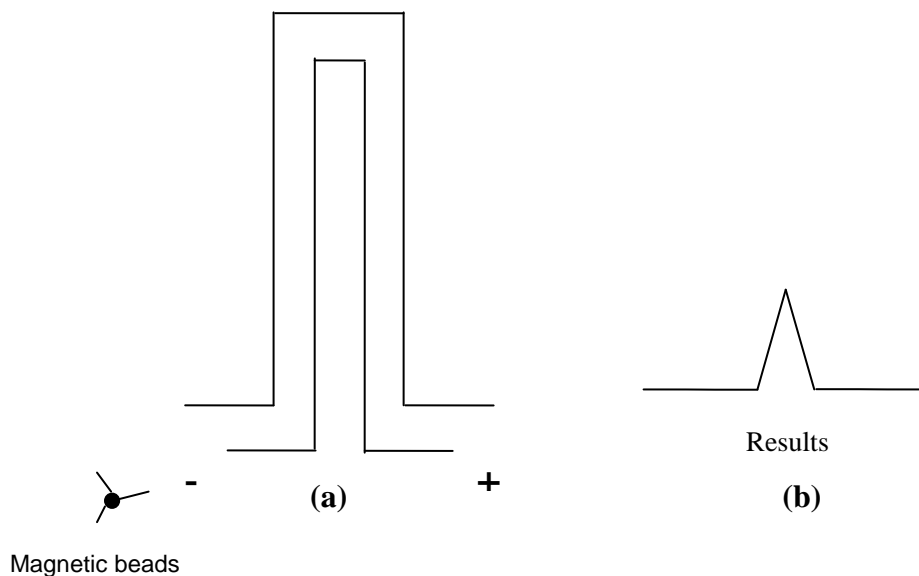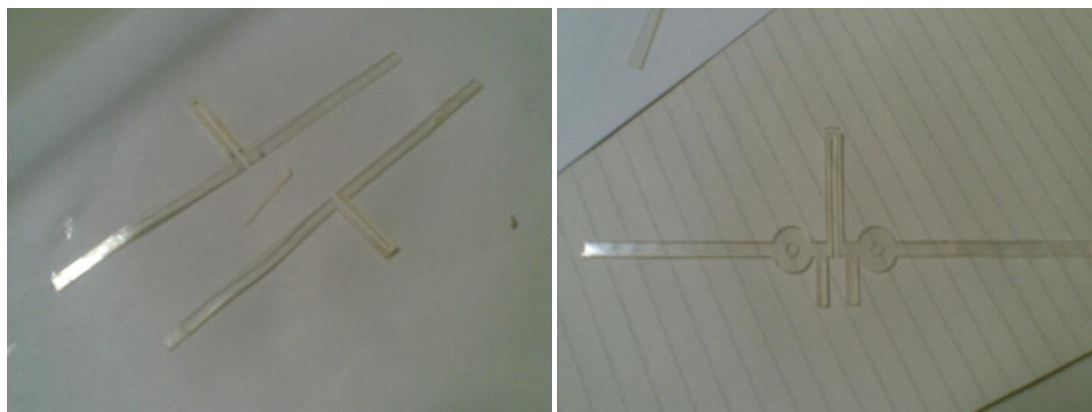

Magnetic beads

Results

(a)   **(b)**

Figure 44: scheme for microfludic-microcantilever device

It is the general idea of the microfludic-microcantilever device. As shown in Figure 44a, the microfluidic is in the microcantilever and the device is under a magnetic field. Then the labeled magnetic beads come through the cantilever, it will cause the cantilever beading. This will generate a signal as shown in Figure 44b. The magnetic beads may be pumped by electrophoresis or others.

5.3 PAGE- Microfludic-Microcantilever system

A   B

Figure 45: PAGE- Microfludic-Microcantilever. A) version I of PAGE -cantilever. B) version II of PAGE-cantilever.

Polyacrylamide gel electrophoresis (PAGE)-cantilever has been tried to detect magnetic beads with analyte. Figure 45a shows the first version of PAGE-cantilever. The gel has been made and packed with plastic film. It has been fabricated to cantilever with nanosecond laser. The disadvantage of this version is that the channel on the left and right is too long, and it takes too much time for the magnetic beads to go through from the end to the cantilever. Therefore, version 2 has been designed which is shown in Figure 45b. There are two cycle pads with holes on the right and left which is near the cantilever beam. The holes are used for sample to dip in the cantilever, and two holders are designed to fix the cantilevers.

(a)   (b)
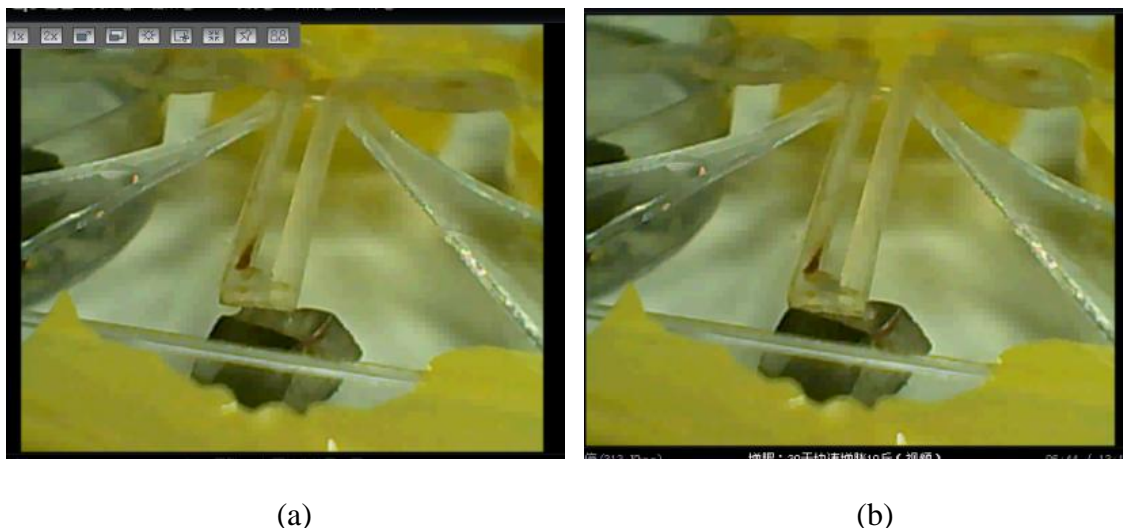
Figure 46: PAGE- Microfludic-Microcantilever under magnetic field (a) The cantilever with magnetic beads. (b) The cantilever bend with magnetic beads come through the tip.

Figure 46, shows a PAGE-cantilever of the new design. The current is much higher than paper-chromatography-cantilever with the same voltage. Therefore, the magnetic beads run much faster than that in the paper channel. The magnetic field was set under the cantilever. When magnetic beads run through the tip of the cantilever, it bend with huge deflection as shown in Figure 46. The advantage of the system is that the PAGE is popular used, the parameters are easy to control. The resistance is much lower than paper, and the magnetic beads can run much faster. The disadvantage of the system is that it is a little difficult to fabricate as small as the paper cantilever.

5.4 microfludics-electrophoresis system

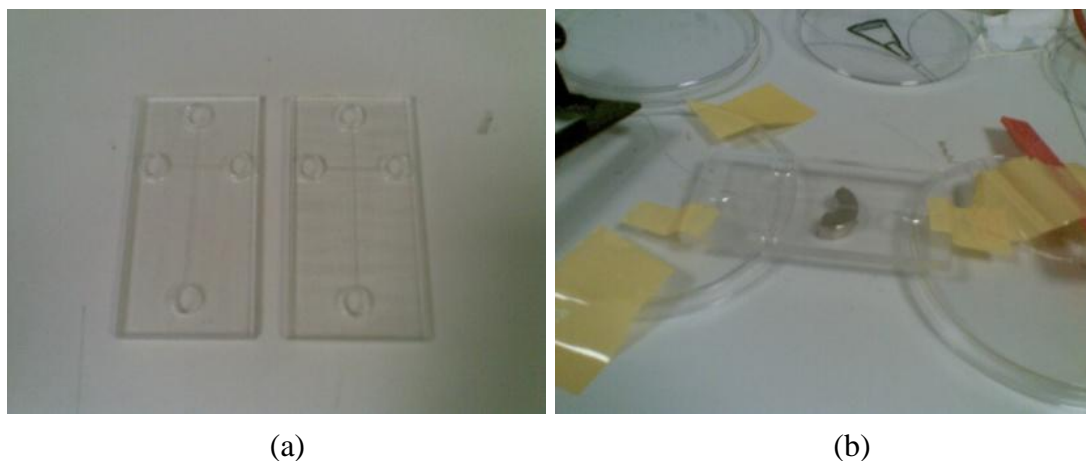(a)   (b)

Figure 47: microfluidics electrophoresis

Figure 47a shows a microfluidics electrophoresis system made of PMMA. It is a sandwich structure, the PMMA on the top and the bottom are 5mm, and the middle one is 0.125mm. The width of the channel is 1mm and 0.5mm. The hole in the end of the channel have been used as electrophoresis baths to hold buffer. As shown in Figure 47b, TBE buffer has been injected to the electrophoresis baths, and platinum electrode has been put in the baths, as well. With a power supply, a simple eletrophoresis system has been built.

(a)   (b)
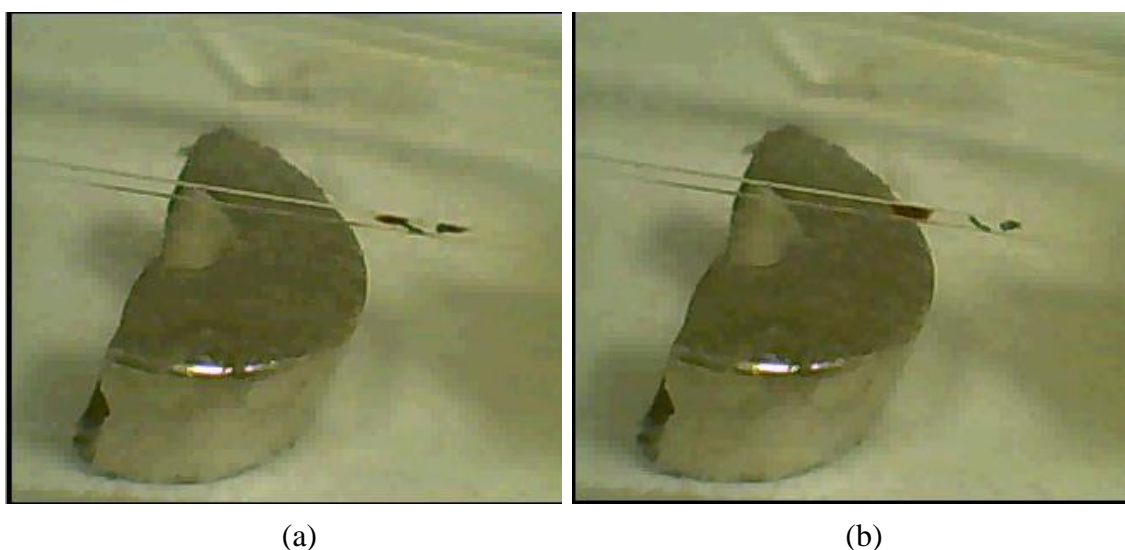
Figure 48: Microfluidics electrophoresis under magnetic field. The magnetic beads

moved from (a) to (b), it still cannot pass over the magnetic field.

To find if the magnetic beads can go through the channel with magnetic field under it, 2.5μL 100μm magnetic beads has been injected into the electrophoresis baths. Figure 48 shows that the magnetic beads move under the force of the electrophoresis field.
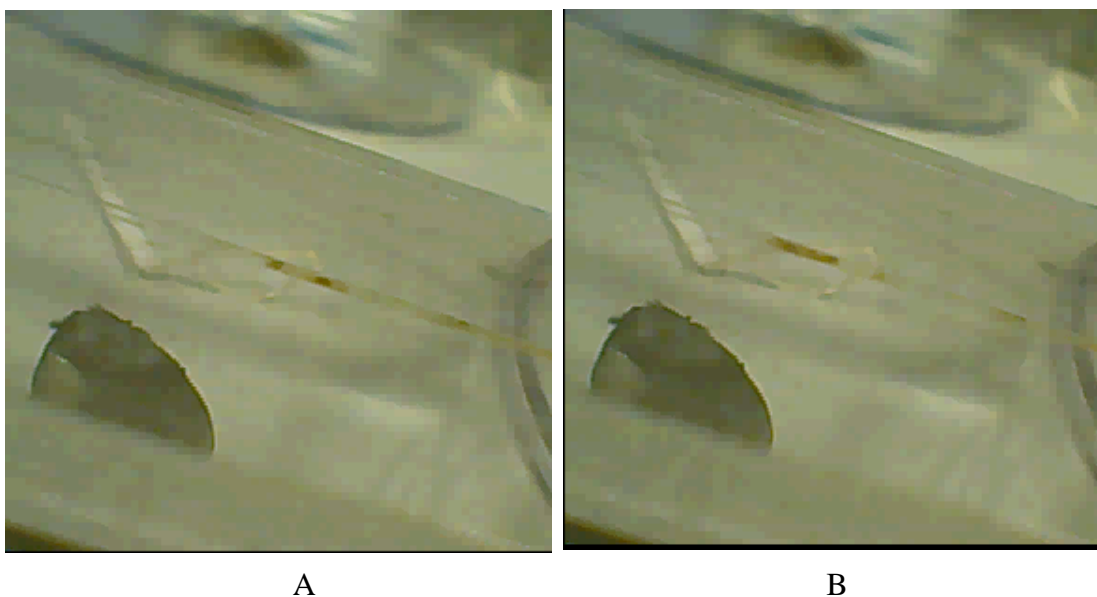

A   B

Figure 49: microfluidics electrophoresis under weak magnetic field. Magnetic beads moved from A) to B), it still cannot pass over the magnetic field.

However, with the magnetic field, the magnetic beads can't go through the channel.
As shown in Figure 49, to reduce the strength of the magnetic field, the chip was moved a little farther from the magnet. However, it maybe still not far enough from the chip, the magnetic beads cannot go through the channel, neither. There may be a distance, where the magnetic beads can go through the channel and the force is strong enough to bend a cantilever.

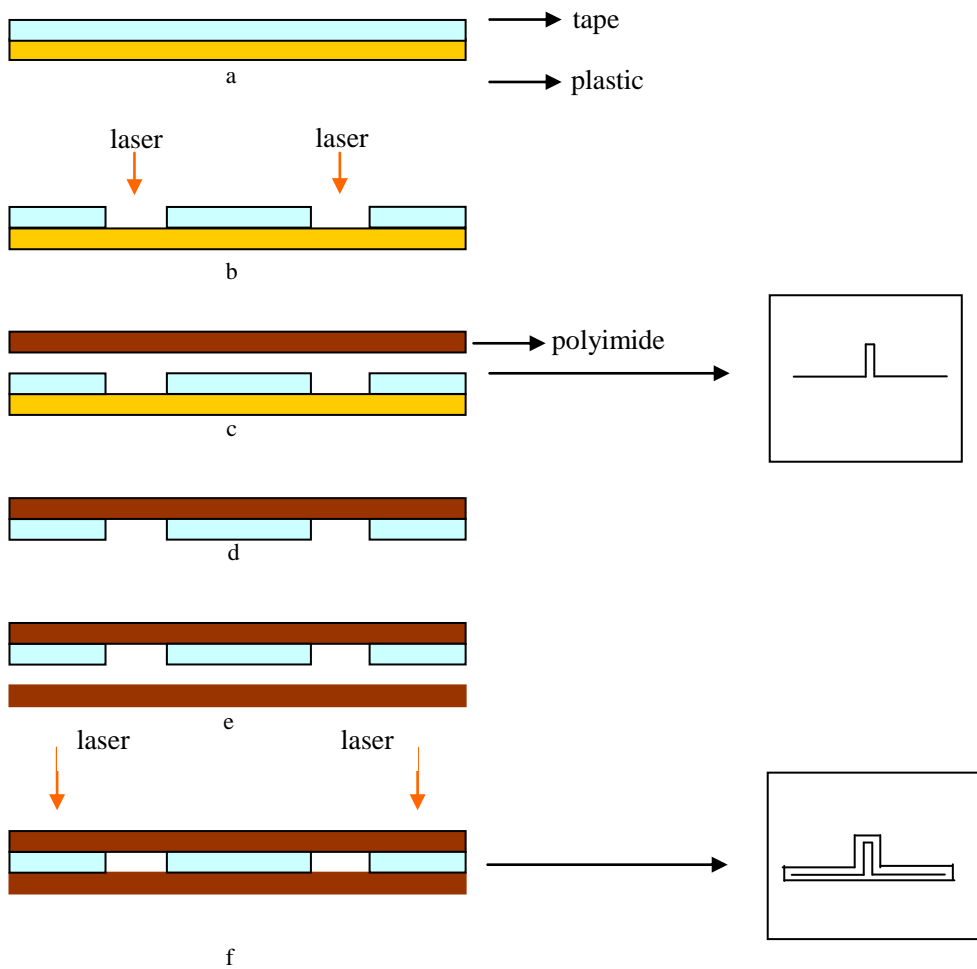## 5.5 Microfludics-Microcantilever System

Figure 50: The scheme to fabricate microfluidics-microcantilever system(version I)

Figure 50 illustrate the scheme to fabricate microfluidics-microcantilever system. In Figure 50ab, channel has been fabricated on tape, and then 25μm thick polyimide has been attached to it. On the other side, the plastic has been peeled out, and attach to a 25μm polyimide as well in Figure 50c,d,e. At last, as shown in Figure 50f, the sandwich structure has been fabricated to cantilever with laser.

However, it is very difficult to fabricate, because the cantilever is very small, and it is a little tough to fabricate in situ. What is worse, it is not easy to cut though the tape with 532nm wavelength laser. Therefore, another method has been developed.
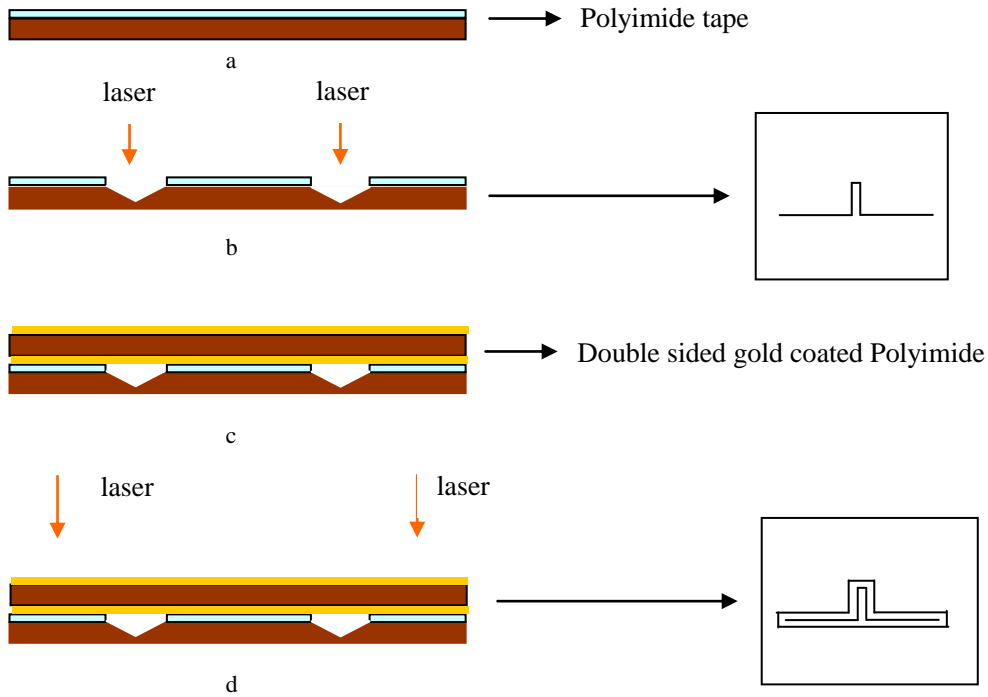
Figure 51: a scheme to fabricate microfluidics-microcantilever system(versionII)

In Figure 51, polyimide tape has been chosen to fabricate the microfluidics cantilever.

In Figure 51a, it is a polyimide tape which is purchased from RS Components International. The thickness of the polyimide is about 25um. In Figure 51b, channel has been fabricated on polyimide tape with laser. The parameter of the laser should be selected to cut a channel on the polyimide and cut through the tape and not cut through the polyimide. Double sided gold coated polyimide has been attached to the polyimide tape, and the tape has been fabricated to cantilever with laser(Figure 51cd).
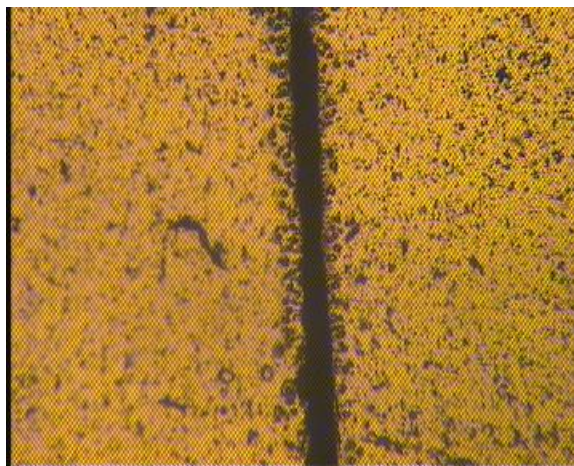
Figure 52: laser fabricated polyimide channel

Figure 52 shows microfluidic channel which has been fabricated with the parameter: current 75, frequency 15 kHz, speed 40mm/s. To confirm that the laser beam can cut a channel on the polyimide but not cut through the polyimide, a array of parameters can be arranged. The current and frequency can be fixed, and the speed can be arranged like 20mm/s, 25mm/s, 30mm/s, 35mm/s,40mm/s……100mm/s to find which parameter is suitable for the fabrication.
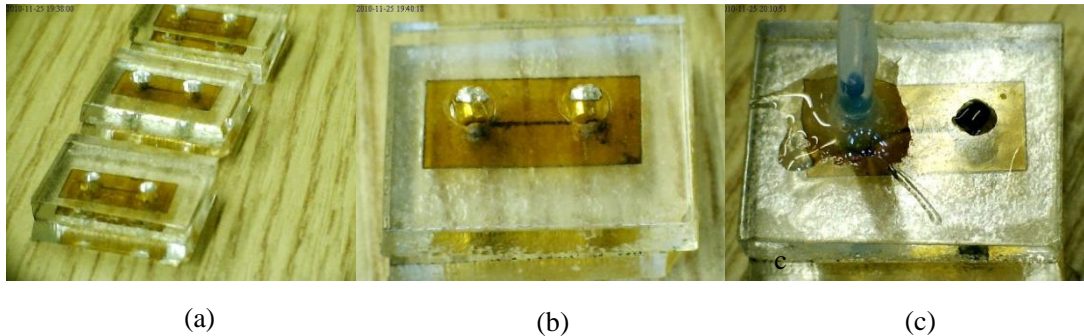

<div align="center">(a)   (b)   (c)</div>

Figure 53: Polyimide channel devices. (a) Three devices. (b) One device under camera. (c) Food color can pumped through the microfluidic channel.

Figure 53 shows device, which is used to find which parameter is suitable to fabricate microfluidics, and test if the channel works. There are one line and two holes were fabricated in the polyimide without a cantilever structure. The simple structure is easy to find a condition that the food color can come through the channel.

At last a parameter was found to fabricate microfluidics with polyimide. With this parameter, the food color can go through the channel easily, and the polyimide has not been cut through. The parameter is 532nm wavelength, current 74, speed 15mm/s, 15k Hz and cut twice. In Figure 53ab, the chip has been set on a PMMA holder which attached with double sided tape. The top PMMA holder has been drilled two holes which one used to insert a tubing to input the food color. In Figure 53c, one tubing was insert into the hole, and the food color has been dipped on the other hole. The tubing has been pumped with a syringe to find that the food color can come through the microfludics. It means that the microfludics channel doesn't blocked in the middle and it works.
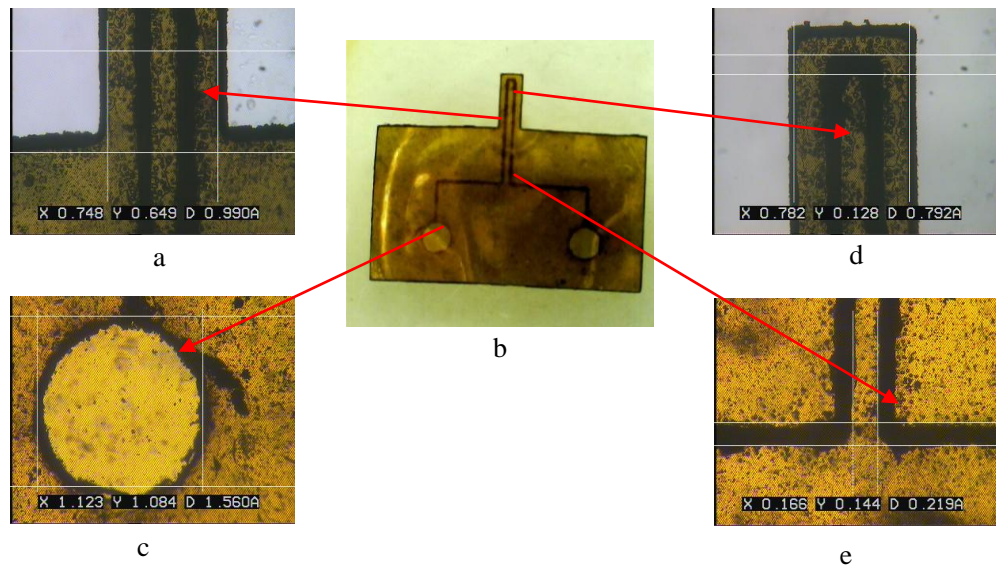
Figure 54: polyimided based microfluidics cantilever. (a) The whole picture of microcantilever. (b),(c),(d),(e) are part of the cantilevers.

Figure 54a shows the microfluidics cantilever fabricated by the procedure in Figure 51, and the parameter has been optimized by the last step. It is a two layers structure, which is combined with a polyimide tape and a double sided gold coated polyimide. Figure 54c shows the hole for sample to input, the diameter of the hole is 1.123mm. Figure 54bd shows the cantilever beam, whose width is about 0.74mm. Figure 54e shows the channel of the microfluidic cantilever. The channel is about 0.144mm.
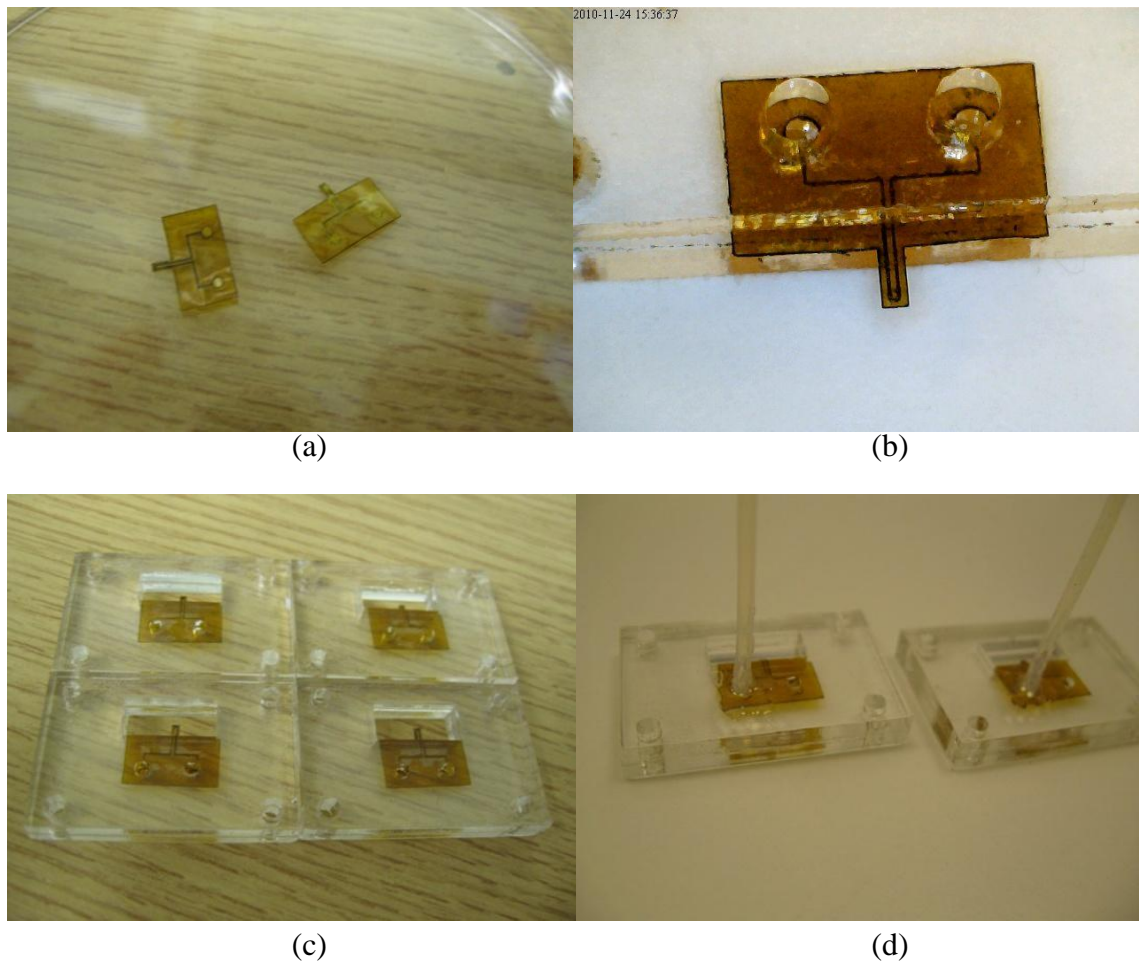
Figure 55: microfluidics cantilever device. (a) Polyimide based cantilever. (b) Cantilever assembled between PMMA chip. (c) Four chips of cantilever. (d) The chips jointed with microfluidic tubing.

As shown in Figure 55a, PMMA was used to assemble the polyimide chip to make a microfluidics cantilever device. A tape was attached to the PMMA and fabricated with laser. There are two holes on the top side of the chip which are used for inputting and outputting sample. Figure 55b shows a piece of tubing was inserted into the hole, which was sealed with glue. In the other hole, blue food color was injected. One syringe was used to suck through the tubing.

5.6 Integrated microfluidic microcantilever sensor

A new sensor has been developed, which is capable of detecting biological species such as cells, proteins, toxins, and DNA at low concentrations. Microcantilever sensors,

magnetic beads, and microfluidic technology have been combined to create a polymer based biosensor. The advantage of this sensor is sensitive, easy fabricated, and cheaper than silicon cantilever.

In Figure 56, the sensor is packaged in a sandwich structure; the top and bottom are gold coated with 7.6μm thick polyimide, 20μm thick photoresist has been sandwiched in the middle. The sensor was precision fabricated by laser machining and lithography.

Antibody has been chosen as an example to show how the sensor works. Antibody has been functionalised on the inside surface of the micro-channel and magnetic beads; therefore, the detected analyte will bend the cantilever when it is flowed through the channel (a magnetic field is applied under the cantilever). The signal will be read out with an optical system and into a computer.

The signal changed with the concentration of the magnetic beads. The signal is caused by the magnetic beads, when they flow through the cantilever. An array of more cantilevers will provide greater sensitivity and the capability to detect multiple species simultaneously.
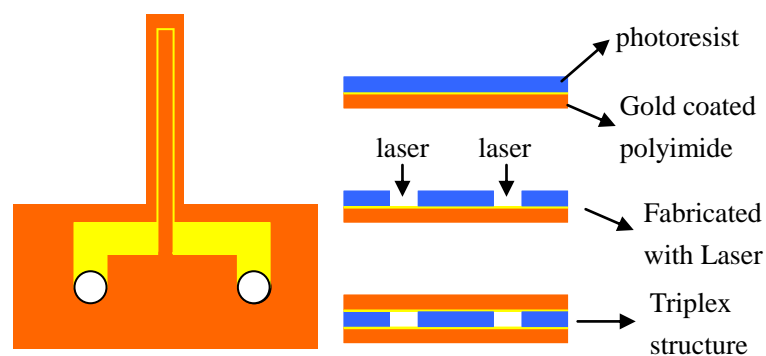
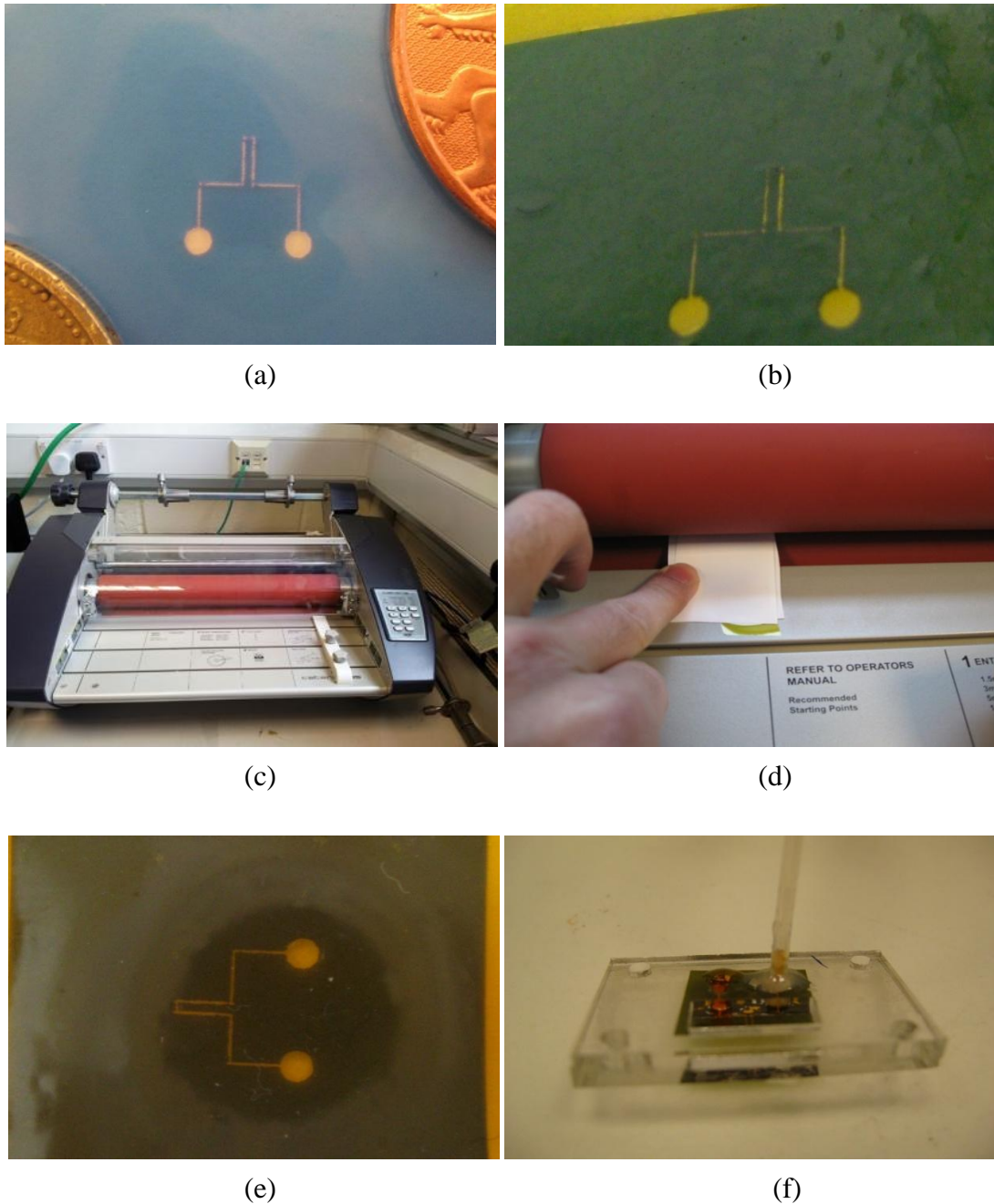Figure 56: Scheme of integrated microfluidic microcantilever sensor

Figure 57: cantilever fabricated process. (a) and (b) are cantilevers fabricated on photoresist. (c) and (d) show the process of laminating. (e) the cantilever after laminating. (f) cantilever with microfluidic.

Figure 57a shows the photoresist which has been fabricated to cantilever channel by nanosecond laser. The parameters are scanning speed 60mm/s, current 70, frequency is 15000Hz. It needs to cut 3-5times to cut through. In Figure 57b, the photoresist has been attached to a polyimide film, whose thickness is 7.6 micron which is purchased from VHG labs. In Figure 57cd, the Thermal film laminator is purchased from GBC

Company, the temperature for laminating the photoresist and polyimide is 100degree. In Figure 57e, the polyimide with photoresist has been attached with polyimide tape to seal the channel. To test if the microfluidic channel work, the chip has been attached with PMMA with double sided tape. There are two holes on the PMMA to reservoir the liquid. It can be seen from the Figure 57f that the liquid can be pumped from the channel. It means the microfluidics channel works.
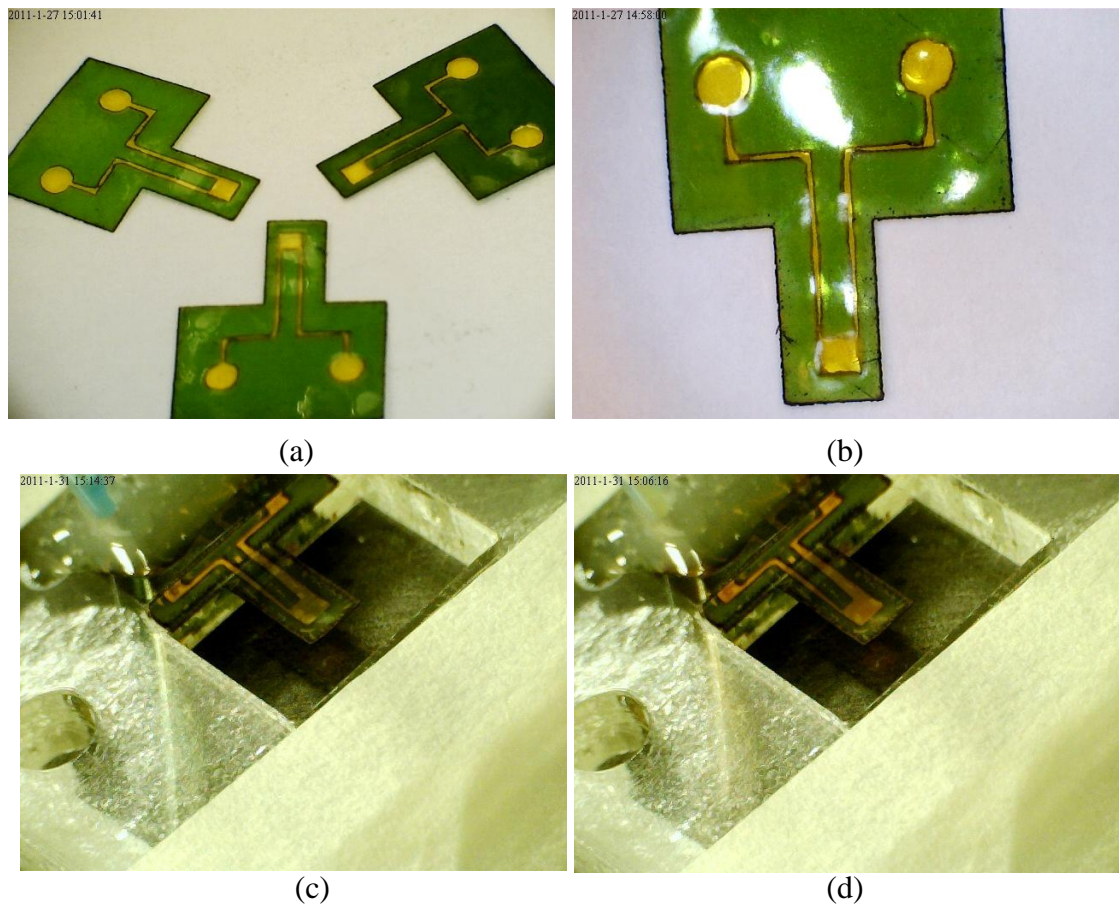

| (a) | (b) |
| (c) | (d) |

Figure 58: Microfluidic microcantilever (a) and (b) Polyimide and photoresist based cantilever. (c) Cantilever connected to microfluidic channel. (d) Cantilever microfluidic with magnetic beads.

Figure 58a and b show some cantilevers which are fabricated by following the step shown in Figure 57. There is a square at the end of the cantilever, which is used to hold more magnetic beads to increased the signal. There are two circular pads, which are used to input the liquid in the channel. The width of the channel is about 200μm, which is enough for the magnetic beads to run through it. The height of the channel is 40μm.

As shown in Figure 58c the cantilever is set on the holder, which is used to input liquid into the cantilever. When high concentration magnetic beads input into the cantilever, it can be seen from Figure 58d that the color has changed.
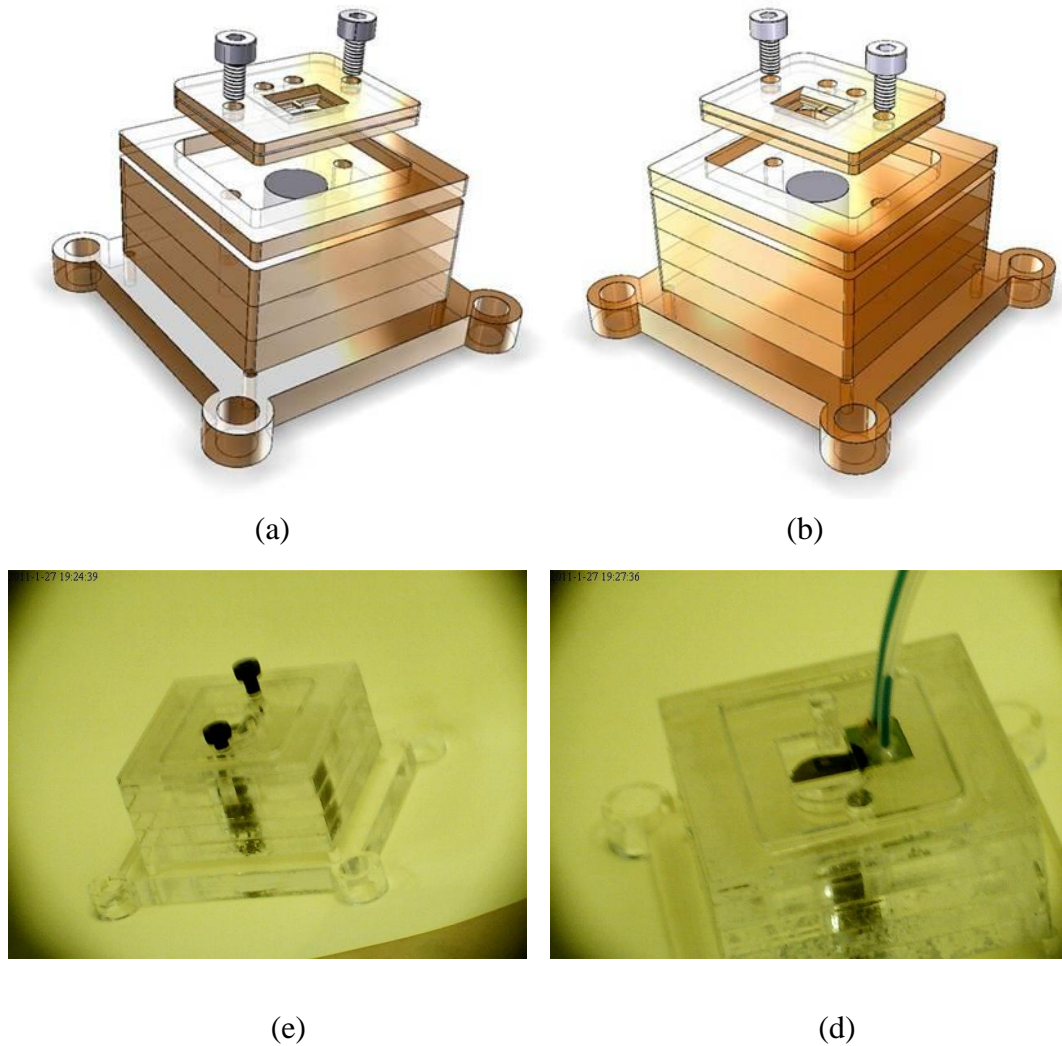

(a)   (b)

(e)   (d)

Figure 59: The holder of microfluidic microcantilever system (a) and (b) are designed with autoCAD. (c) and (d) are the real holder (PMMA) fabricated with laser.

Figure 59ab show the design holder of the system. It can divided into two parts. The part on the top is used to hold the cantilever and connect the tubing on the system. The holder on the bottom is used to hold the magnetic and set the holder on the cantilever system.

Figure 59c shows the holder fabricated with. Double sided tape is used to bind each PMMA. The magnet was set in the middle of the holder, which is under the cantilever.

Four holes have been drilled on the bottom of the holder, which used to mount the holder on the cantilever system. Figure 59d shows that the liquid can run through the cantilever.
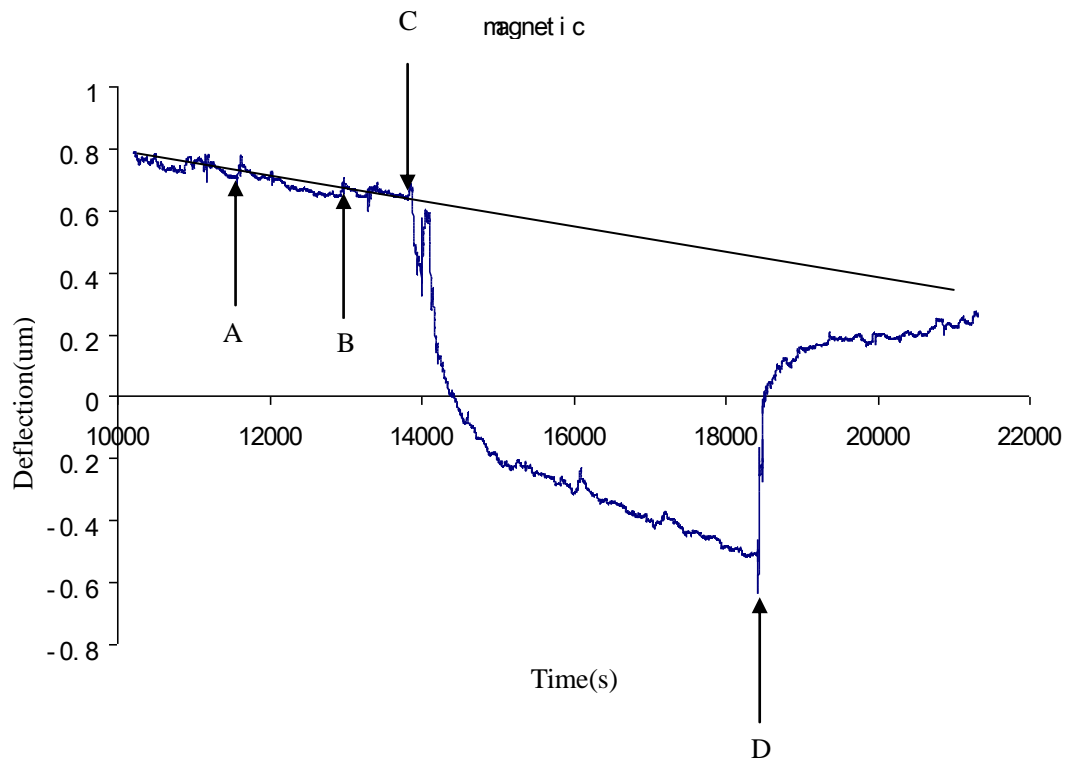

Figure 60: Results of magnetic beads detection

Figure 60 shows the results of the magnetic beads detection in order to find if the cantilever are sensitive enough. At point A and B, the buffer was sucked in by syringe. At point C, magnetic beads were input into the microfluidics cantilever. A sharp signal was got and it increased slower later. At point D, magnetic beads were pumped out to find the signal bending back.
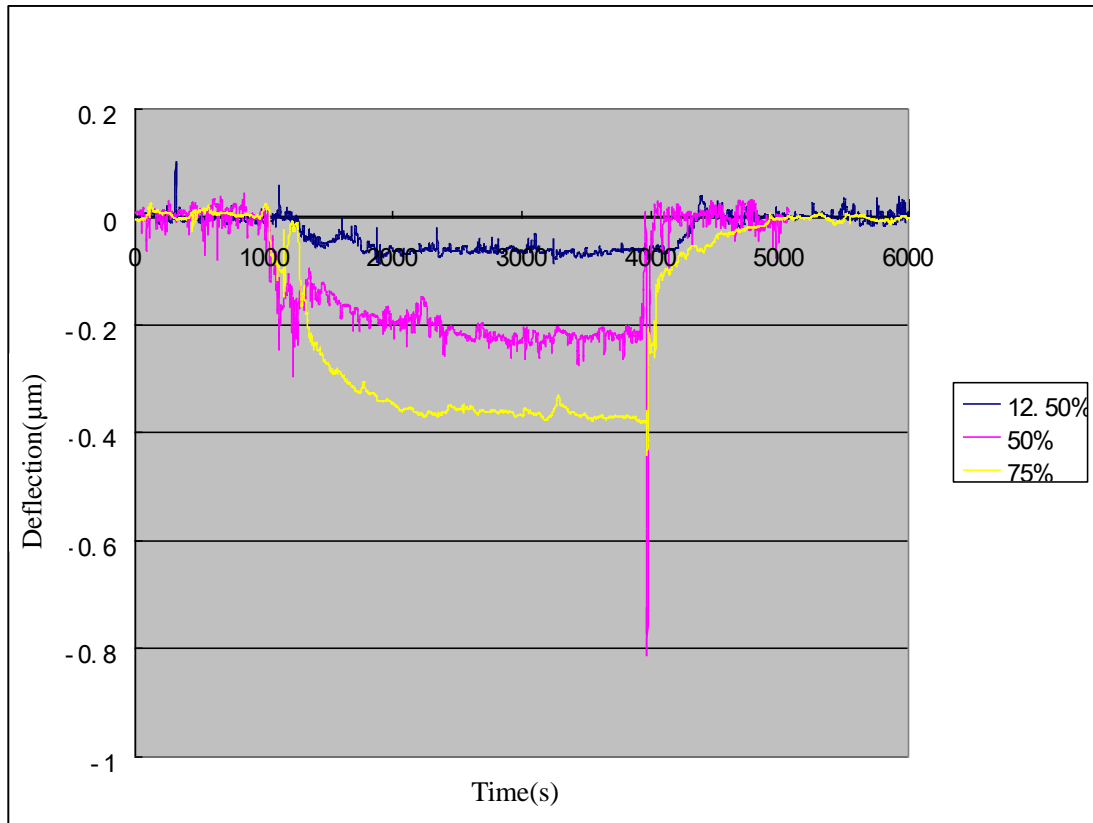
Figure 61: Results of detecting different concentration of the magnetic beads.

The results of detecting different concentration of the magnetic beads by the device are shown in   Figure 61. The concentration is 12.5%, 50%, 75% of the origin magnetic beads solutions, and the volume is 25uL. The size of the cantilever is 1.25x6.25mm. When the magnetic beads introduced into the cantilever, the cantilever beams bends sharply shown in Figure 61 to cause the signal decreased sharply. The deflection of the cantilever increased with the concentration of the magnetic beads. When the magnetic beads pumped out, the cantilever bending back to cause the signal reverse to baseline. The cantilever with gold coated surface has the potential to be used as biosensor. The disadvantage of this method is that it is difficult to fabricate smaller device. The channel is not very smooth, the sample may attached to the wall of the channel.
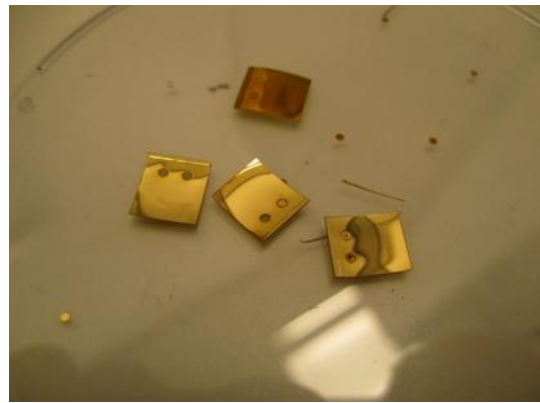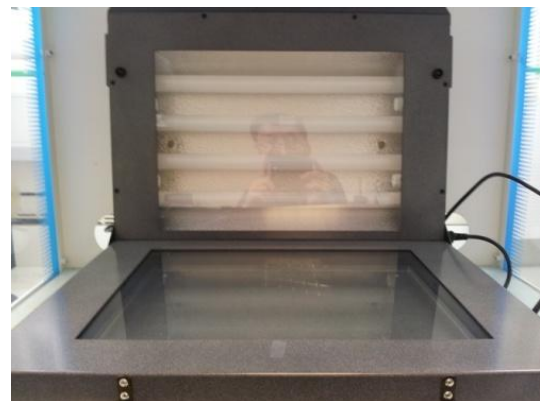
(a)   (b)
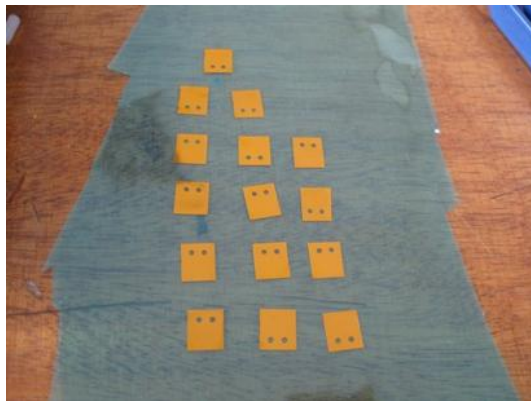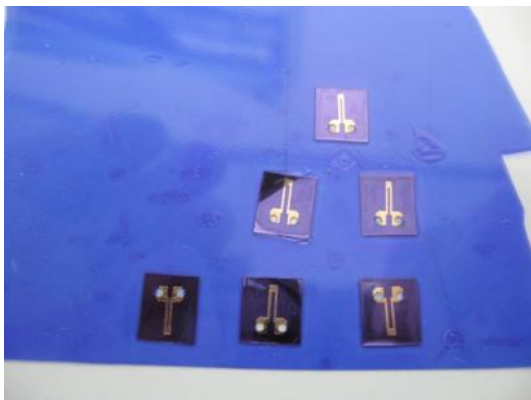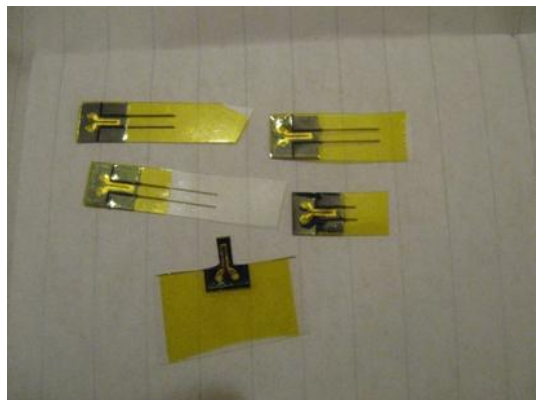
(c)   (d)

(e)   (f)

Figure 62: Device fabricated by lithography. (a) and (b) are gold coated polyimide rectangle with two holes fabricated with laser. From (c) to (d) , The gold rectangle has been laminated and exposed under UV light with mask. From (e) to (f), it has been developed to cantilever channel and fabricated to cantilever with laser.

The sensor is also fabricated by lithography. Firstly, a sheet of 25μm polyimide (purchased from RS) was sputter-coated with an adhesive layer of chromium (5 nm)

followed by a layer of gold thickness of 20 nm. The gold coated polyimide has been fabricated to square shape with two holes on it (Figure 62ab). Secondly, this gold-coated polyimide was attached to a sheet of 40µm thick positive photoresist as shown in Figure 62c (Dry Film ALPHA920, purchased from ORDYL), and the two sheets were bonded together using pressure applied at 100ºC with a laminator. The temperature to laminate the photoresist and polyimide is 100degree. Thirdly, a mask (purchased from Fabricated Micro Lithography Services Ltd) was employed to control the UV exposure creating patterns of microchannels. The UV exposure was performed by using UV light with an exposure time of 30 seconds in Figure 62d. Fourthly, the UV exposed sheet was developed (in developer for 2mins) removing the positive photoresist in the exposed areas. These areas define the microfluidic channels in Figure 62e. fifthly; the microchannels were sealed using 25µm polyimide tape as a top layer. This process is summarized in Figure 62. Finally, a 532nm laser was used to cut the structures into individual microcantilever microfluidic chips in Figure 62f, with cantilever dimensions of 1mm in width and 5mm in length and microfluidic channel sizes of 100µm in width and 40µm in length.

5.7 A new holder for cantilever system

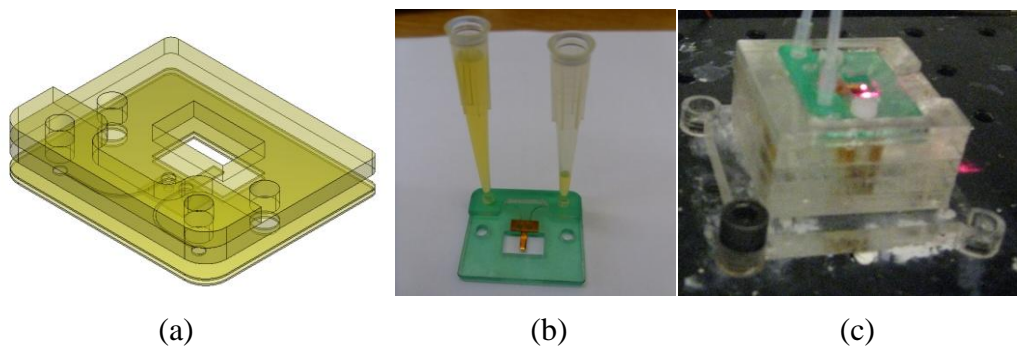| (a) | (b) | (c) |

Figure 63: A new holder for microfluidic microcantilever. (a) The holder for cantilever and microfluidic was designed with autoCAD. (b) The real holder made of PMMA. (c) The hold set above magnetic field.

Figure 63a shows a new holder which is designed with autoCAD. The holder is combined with four layers, which sealed a channel for the liquid. Figure 63b shows the device which has been fabricated with polyimide and transparent plastic. The first and

last layers are 2mm thickness PMMA. Pipette tip can be set up in the holder easier than the last version. It will cost hours to connect with the tubing to the holder in the last version. In Figure 63c, it shows the holder connect with tubing, the holder can connect with tubing and pipette tip in a few second. If the reagent is very little, the tip will be chosen. If the reagent need to be added continuous, the tubing can be selected.
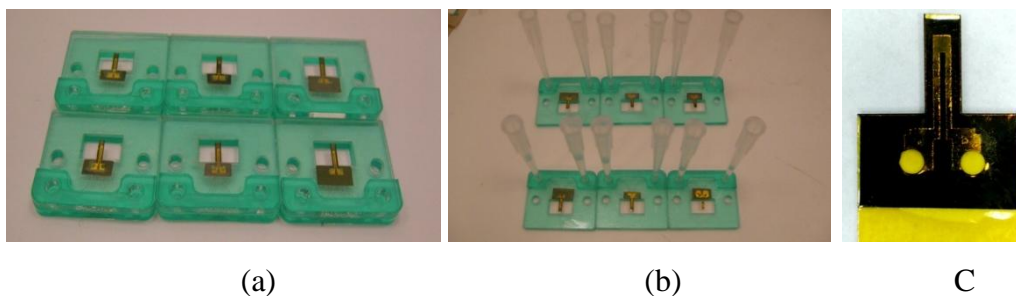

(a) (b) C

Figure 64: Microfluidic microcantilever holders. (a) and (b) six microfluidic microcantilever with holder. (c) Microfluidic microcantilver under microscope.

With this method, many holders can be fabricated at the same time quickly. Figure 64 show a batch of holders with cantilevers. The PMMA and cantilevers can be fabricated with laser and combine together. The four cantilevers on the left are fabricated with 25μm thickness polyimide and the cantilevers on the right are fabricated with 7.8μm thickness polyimide. Before the functionalization, the cantilevers have been test with buffer to find if it lacked or blocked. If it works, the cantilevers will be functionalised at the same time.
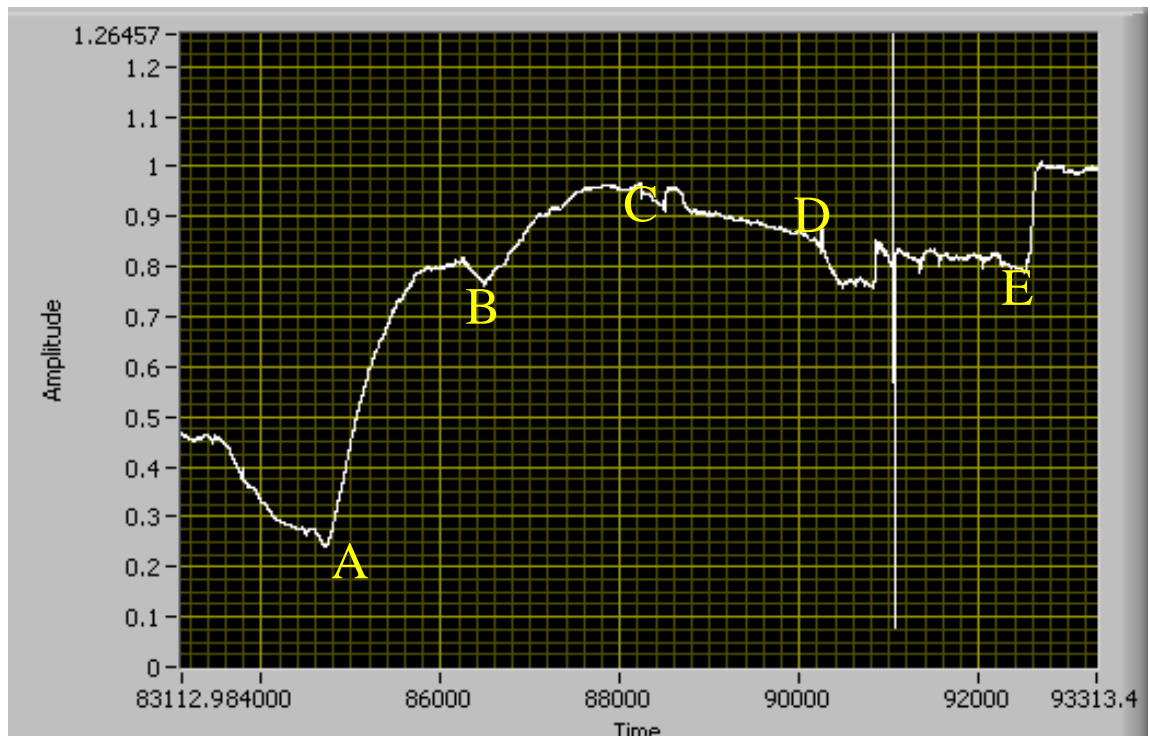
Figure 65: Microfluidic microcantilever for density detection (Application 1 Density detection)

Tris-HCl (100mM, pH=7.4) was injected at point A.

Tris-HCl (25mM, pH=7.4) was injected at point B.

Tris-HCl (75mM, pH=7.4) was injected at point C.

Tris-HCl (50mM, pH=7.4) was injected at point D.

Each step is 33mins.

Point C is higher than Point B, and Point D is lower than point C are right, but Point E should be a little higher than Point D.

We observed that when water was injected at E, the signal increased. 100mM Tris-HCl was injected at point F to cause a decreased signal which is opposed to AB. (Figure 66) There is a big peak between D and E. Many reasons can disturb the cantilever and cause the peak, for example, there may be a particle in the solution which hit the cantilever, and if someone slam the door, the sound will affect the experiment.
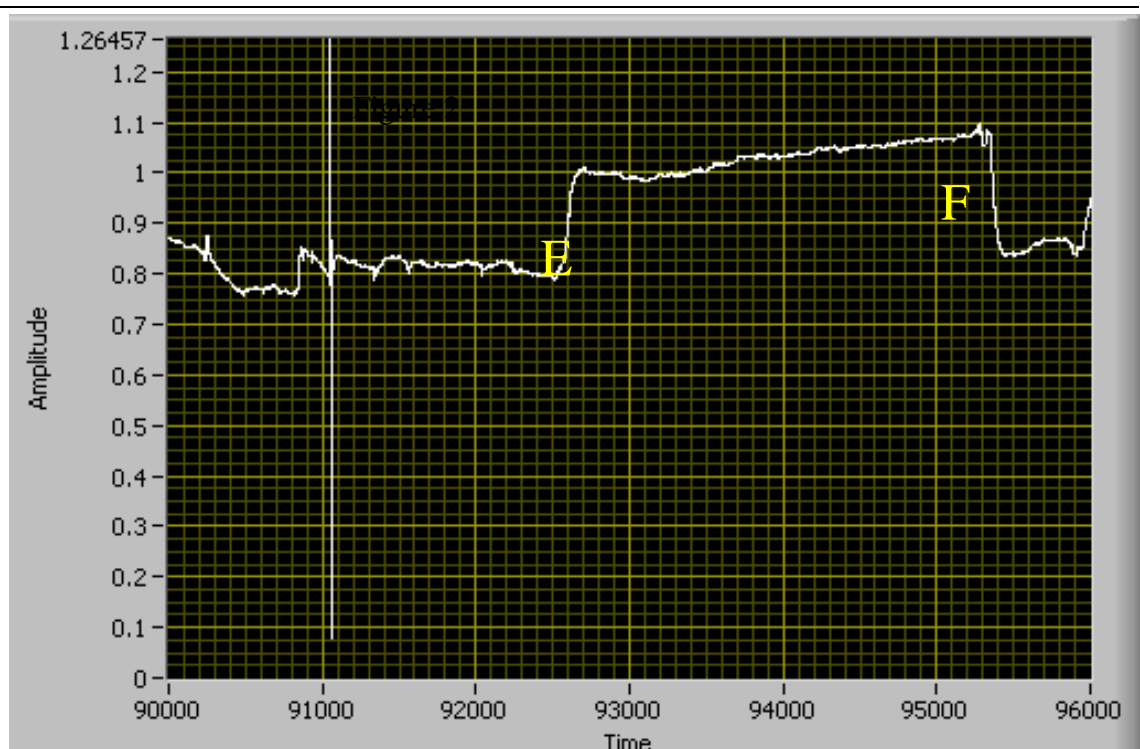
Figure 66: Microfluidic microcantilever detect Tris-HCl

The reason for these results can be explained that when the Tris-HCl injected in the device for the first time, there may be some chemical reactions which caused the increase of signal. When the reactions come to a balance, the device can detect mass, the water is lighter than 100mM tris buffer, so when the tris buffer injected again, it will cause a decreased signal.
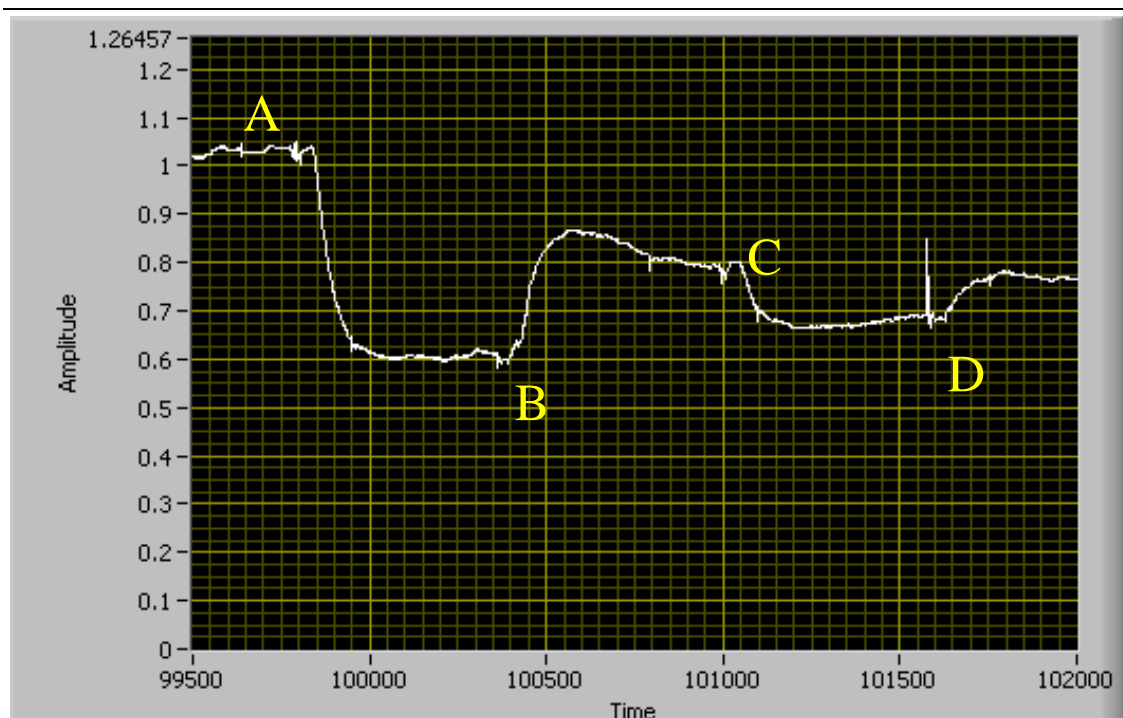
Figure 67: Microfluidic microcantilever detect different concentration of Tris-HCl

The experiment has been repeated:

Tris-HCl (100mM, pH=7.4) was injected at point A.

Tris-HCl (25mM, pH=7.4) was injected at point B.

Tris-HCl (75mM, pH=7.4) was injected at point C.

Tris-HCl (50mM, pH=7.4) was injected at point D.

Each step is 10mins.

The results seems reasonable. But, some other reasons may cause this results instead of mass. For example, if 100mM Tris-HCl pH=7.4 has been diluted to 25mM Tris-HCl the pH will change a little. The difference of the pH may cause the signal.   A control experiment has been carried out: KCl has been diluted in 100mM Tris-HCl to obtain KCl saturated solution (3.4M). When it is injected to the device, it caused a sharply decreased signal at point A.   1.7M KCl, 100mM Tris-HCl was injected at point B which caused the cantilever bending back. 100mM Tris-HCl without KCl was injected at point C to find that the cantilever can bend back a lot but not completely. It takes a long time for the cantilever bending back completely.

It can prove that the device can be used as a mass sensor. But our device has a disadvantage that it can't bend back completely at once, if it bends toward one side too much.
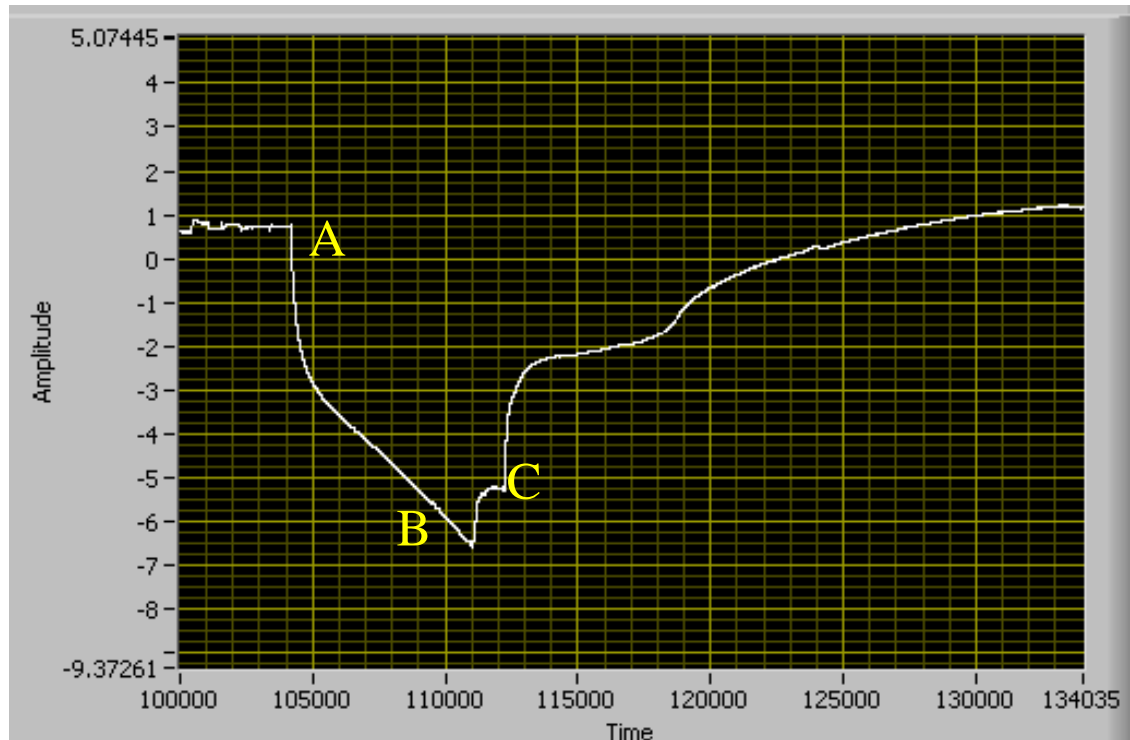
Figure 68: Microfluidic microcantilever detect KCl

5.8 Detection of *Cryptosporidium*

5.8.1 *Details of the set-up and operation of the system*

Viable *C. parvum* oocysts were purchased from Creative Science Company, Moredun Research Institute. Magnetic beads and goat polyclonal antibody immunoglobulin G (IgG) specific to *C. parvum* were purchased from Waterborne Inc. Lectin concavalin A (conA), 11-mercaptoundecanoic acid (11-MUA), protein G, 1-ethyl-3(dimethylaminopropyl)-carbodiimide (EDC), sulfo-N-hydroxysuccinimide (sulfo-NHS) and phosphate-buffered saline (PBS) were obtained from Sigma-Aldrich. Functionalization of cantilever microfluidic biosensor is with protein G, antibody IgG and immobilization with *C. parvum* solution

The sensor was functionalised with protein G solution (20mg/ml) for 2 hours, IgG solution (20μg/ml) for another 2 hours and finally incubated with *C. parvum* solution (1×10^6 oocysts/ml, 5×10^6 oocysts/ml, 10^7 oocysts/ml) for 1 hour causing the oocysts' immobilization on the surface of the sensor. After each step was complete, the sensor was rinsed with PBS solution (10mM, pH 7,4). After immobilization of oocysts,

91

biosensor was left to stabilize and afterwards it was incubated with magnetic beads solution (5mg/ml) for approximately 30 minutes. Finally the sensor was rinsed with PBS solution. Every rinsing was performed in order to remove the unbound reagents. The protocol was performed in room temperature. The flow rate was 1ml/hr.

Functionalization of cantilever microfluidic biosensor with 11-MUA, EDC, NHS and immobilization are with *C. parvum* solution. Microfluidic biosensor was incubated with 11-MUA solution (1mM) under dark conditions for 24 hours, EDC-sulfo-NHS solution (volume ratio 1:1) for 1 hour and finally with conA (1mg/ml) for 1 hour. After functionalization was finished, the sensor was covered with C. *parvum* solution (1×10^6oocysts/ml) for 1 hour, causing the oocysts' immobilization on the sensor surface. After each step was performed, the sensor was rinsed with PBS solution (10mM, pH 7,4). After immobilization of oocysts, biosensor was left to stabilize and afterwards incubated with a magnetic beads solution (5mg/ml) for approximately 30 minutes. Finally the sensor was rinsed with PBS solution. Every rinsing was performed in order to remove the unbound reagents. The protocol was performed in the room temperature. The flow rate was 1ml/hr.

5.8.2 Results and Discussion

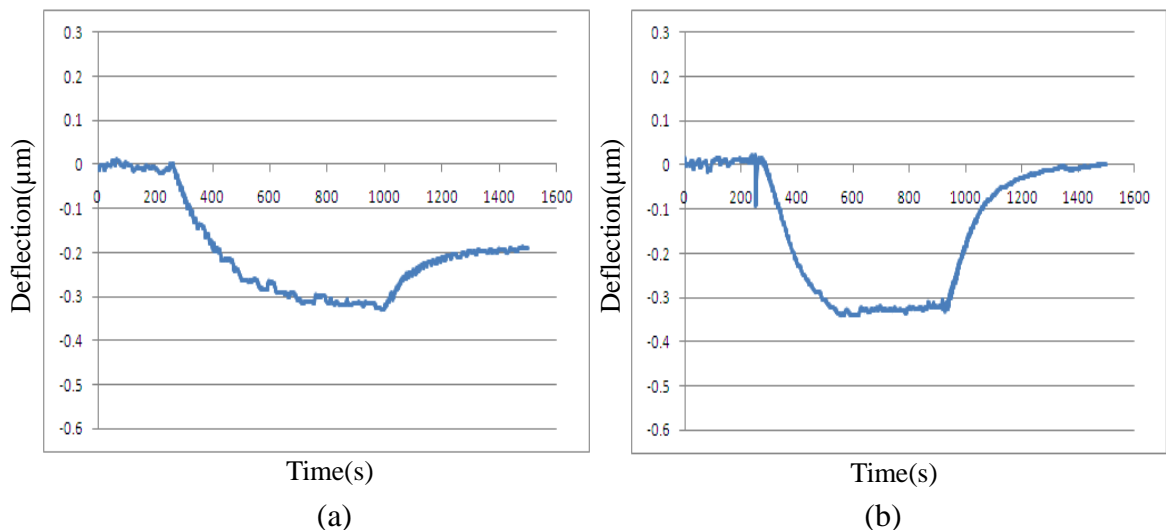(a)   (b)

Figure 69: 10^7 Cryptosporidium/ml magnetic beads has been reduced. A) the positive results B) the reference results.

In Figure 69a, 10^7 Cryptosporidium/ml has been pumped into the cantilever,

subsequently, 25µL magnetic beads has been introduced into the microfluidic cantilever to cause a decrease signal, which can be explained that the cantilever bends toward one side. When the magnetic beads has been pumped away to cause the signal bend back partly, which can be explained that part of the magnetic beads has been grappled by the cryptosporidium on the surface of the microfluidics and the cantilever can't completely bend back. In Figure 121b, it is a reference experiment for the crypto detection. In the reference experiment, the crypto didn't introduce to the cantilever.

When the magnetic beads introduced in to the cantilever, which caused a sharp decreased signal and when the magnetic beads pumped out, the signal completely comes back. It can be explained that the cantilever bent and completely bent back. It can distinguish if there is crypto in the cantilever.
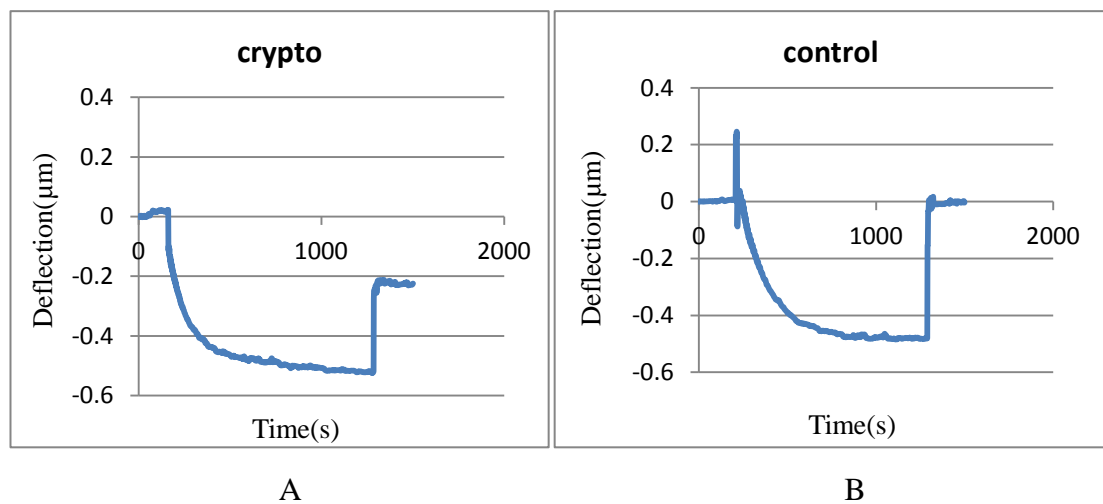

A   B

Figure 70: 10^7 Cryptosporidium/ml magnetic field has been increased. A) is the positive result, B) is the reference result.

The quantity of the magnetic beads has been increased to test if the result is affected.

Figure 70a shows that when more magnetic beads introduced into the cantilever, the signal is higher, and when the magnetic beads are pumped out the signal can bend back at the same level. It can be explained that the signal is dependent on the quantity of the crypto, not the magnetic beads. The control experiment has been test to verify if the cantilever can completely bend back without crypto in Figure 70b. It can be seen that the signal can completely come back, when the magnetic beads pumped out.
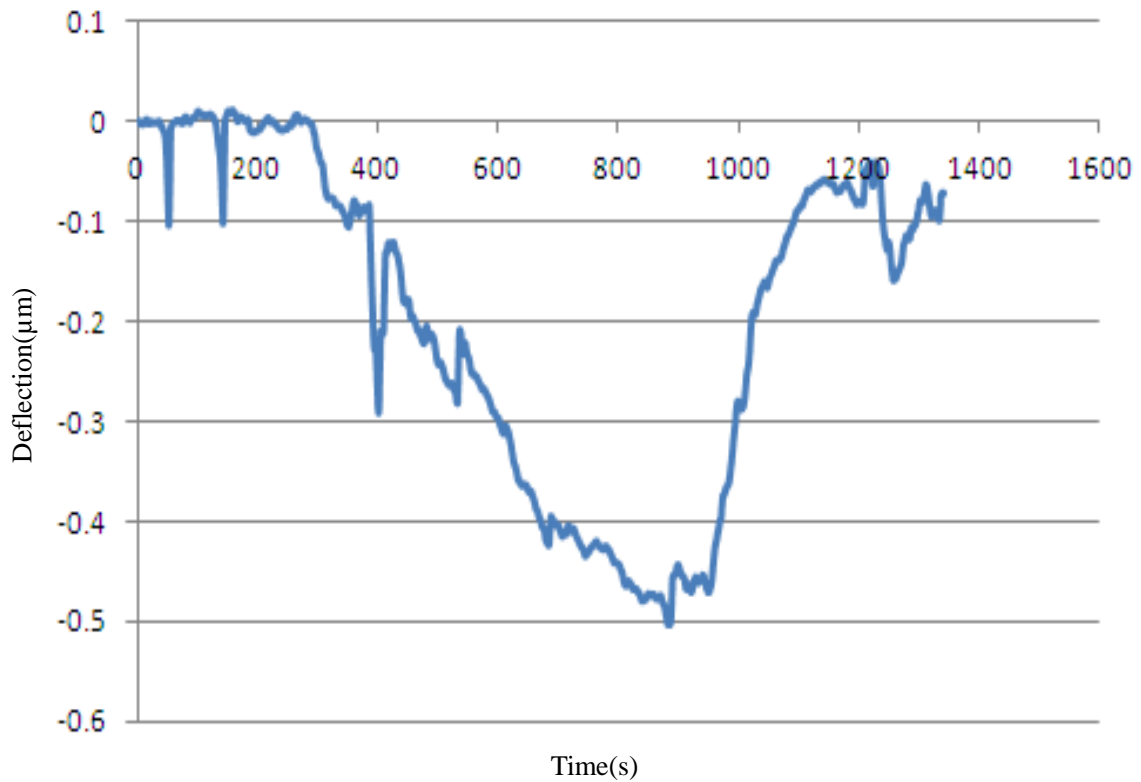
Figure 71: the results of 5×10^6 Cryptosporidium

To find the limited of the device, deferent concentration of Cryptosporidium has been tested. Figure 71a shows the results when 5×10^6 Cryptosporidium is introduced into the cantilever after the cantilever has been prepared with IgG and protein G. When magnetic beads are introduced into the cantilever they will cause a decreased signal and when the magnetic beads pumped out, the signal increased but not come back. It means that the cantilever can detect the concentration as low as 5×10^6. The same experiment has been carried out to detect Cryptosporidium whose concentration is 10^5, but there is no signal for this concentration. It maybe the limitation of detection of this device.
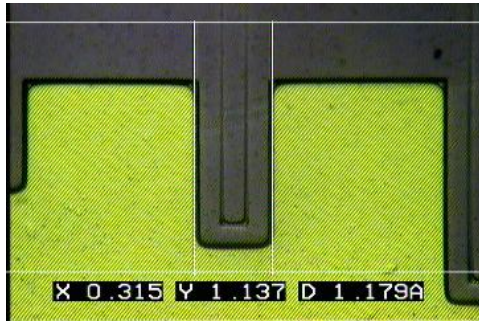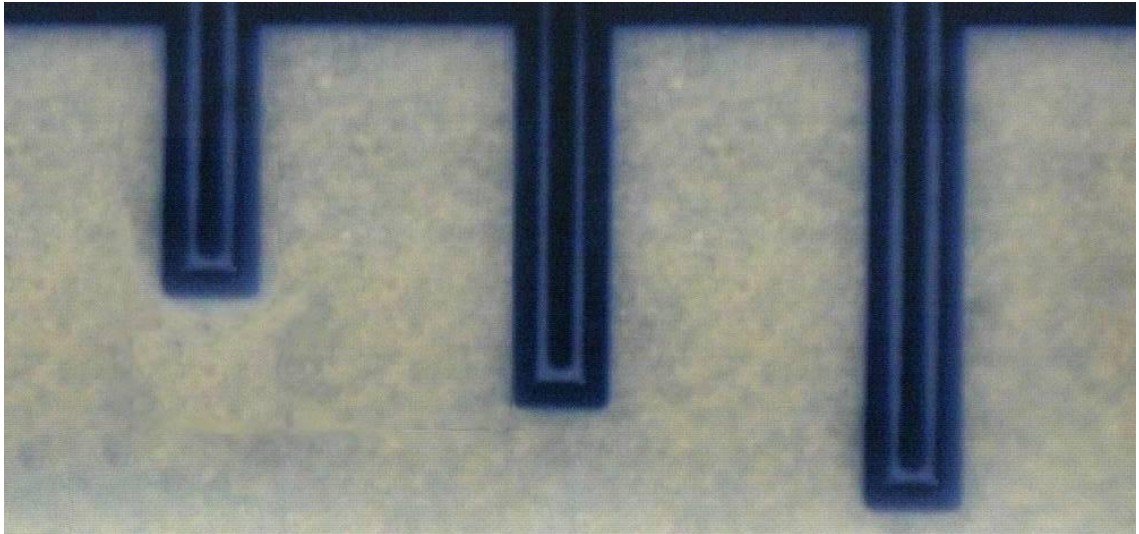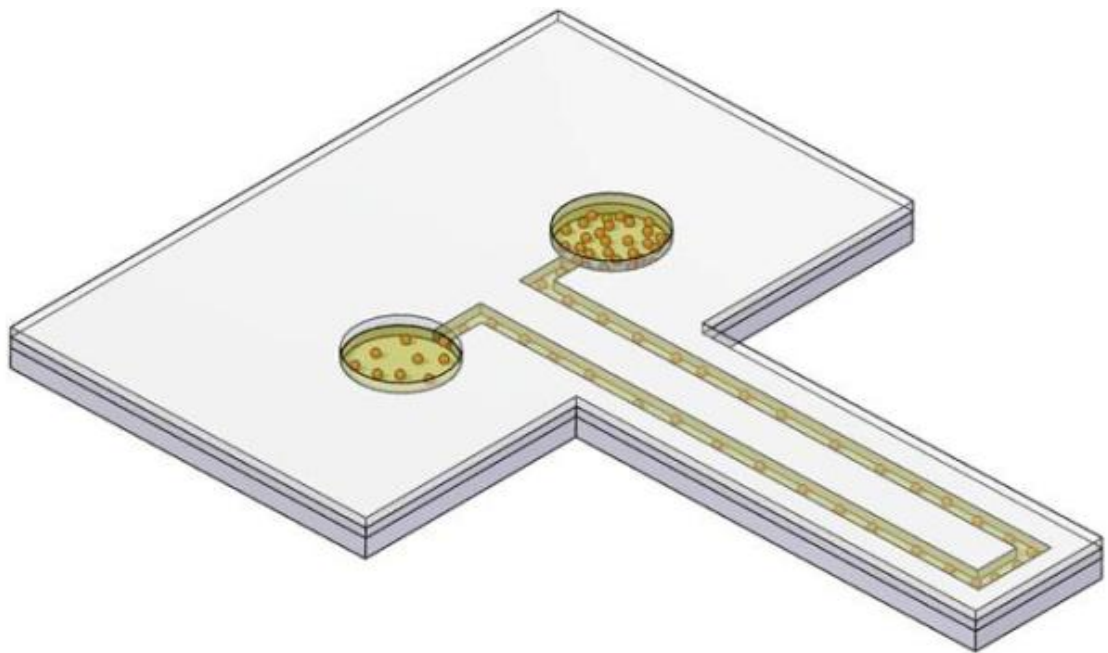
(a)
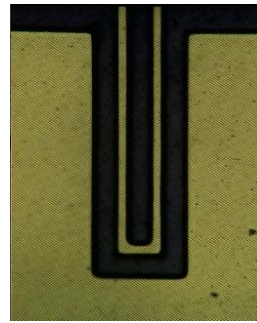
(b)

(c)

(d)

(e)

Figure72 (a),(b),(c),(d) Microfluidic microcantilever under microscope, (e) The 3D structure of the device.

To overcome the limitation for detection, the magnetic field has been increased and the width of the cantilever has been decreased to 315µm. Figure72a and b show the cantilever array with polyimide. Figure72c shows the cantilever with gold coated polyimide after laser fabrication. A strong magnetic field has been used in the system at the same time.

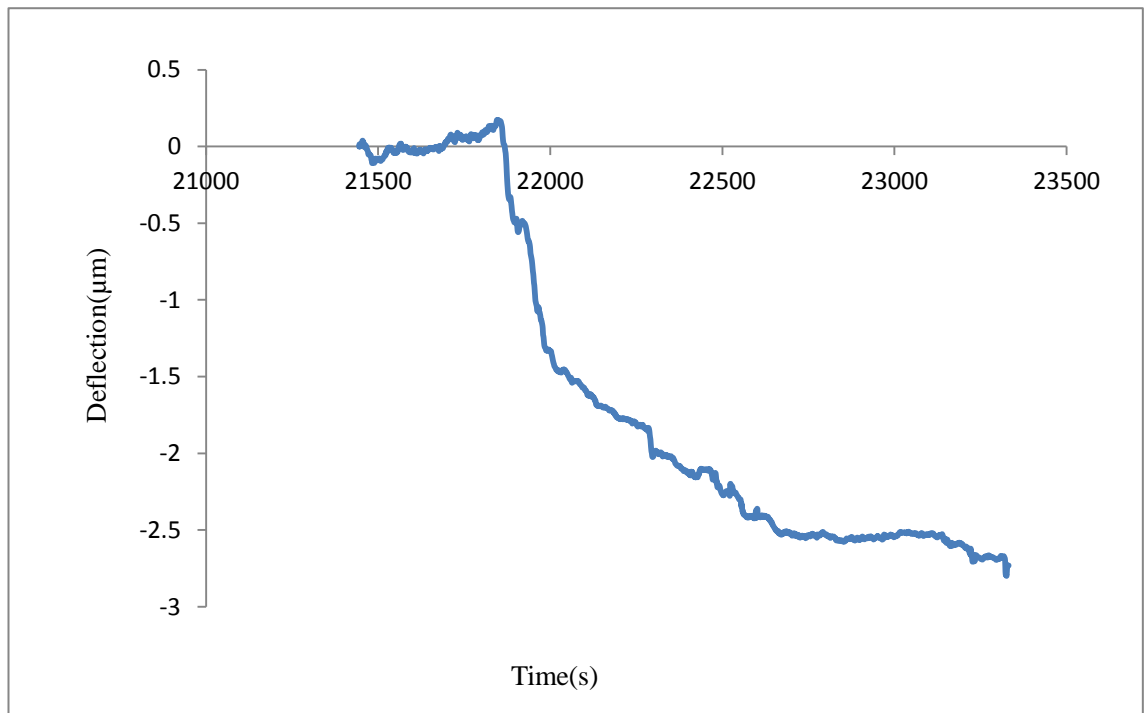Figure 73: results of microfluidic microcantilever detection

The smaller cantilever and the stronger magnetic field has been used to detect crypto. As shown in Figure 73, introduction of the magnetic beads in the cantilever result in the decrease of signal. However, when it cannot be pumped out, because the magnetic field is too strong. To solve the problem, a new holder has been designed in Figure 74b.

(a)   (b)   (c)
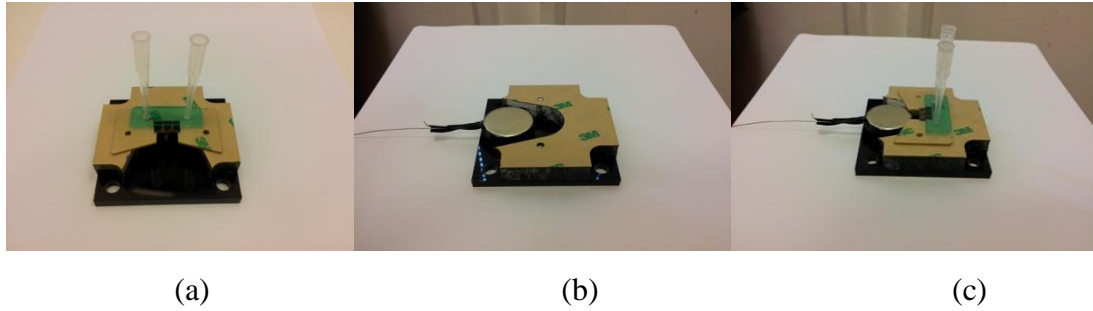
Figure 74: Microfluidic microcantilever holder. (a) The holder made of PMMA and fabricated with laser. (b) The holder with magnetic. (c) The holder with magnetic and cantilever microfluidic.

Figure 74a shows the first version of holder, the magnetic is fixed in the middle of the holder, and it can't be changed to other magnet with different size. In Figure 74bcd shows the second version for the magnetic and cantilever. The advantage of the version is that different magnet can be set in the holder and the magnet can be moved away when it is testing. It means that even the magnet is very strong, which can be moved away, and then, the magnetic beads have been pumped out. The magnet has been ground which is used to prevent the static.

Figure 75: results of cantilever detection

Figure 75 shows the results of the cantilever used to detect crypto with the new holder,

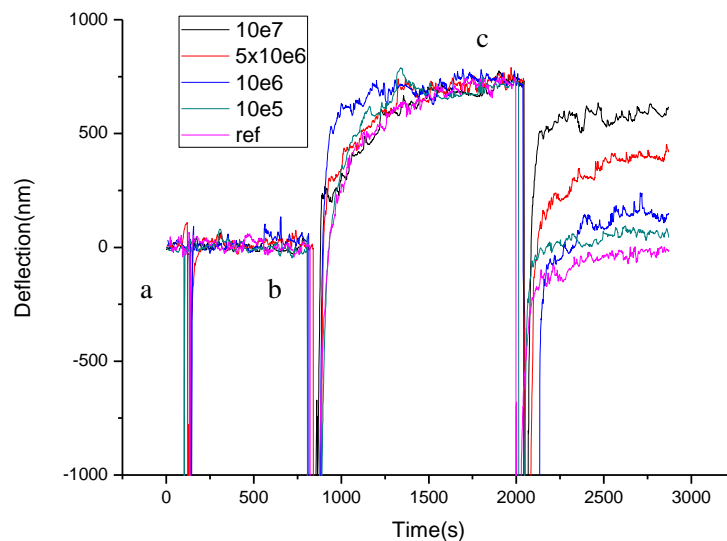and more powerful magnetic field. At point A, the liquid has been pumped to test if the cantilever can bend back. The magnetic beads have been introduced to the cantilever at point B to find that the cantilever bent to one side and caused increase of signal. The magnet has been move away at point C and the magnetic beads have been pumped out at the same time to find that the cantilever can bend back.

Five groups of experiments have been carried out, the ref is the reference. The concentration of crypto of line 10e5 is 10^5; The concentration of crypto of line 10e6 is 10^6; The concentration of crypto of line 5x10e6 is $5x10^6$; The concentration of crypto of line 10e7 is 10^7. With the new holder and the powerful magnetic field, even the concentration of the crypto is as low as 10^5, it can still be detected by the system.
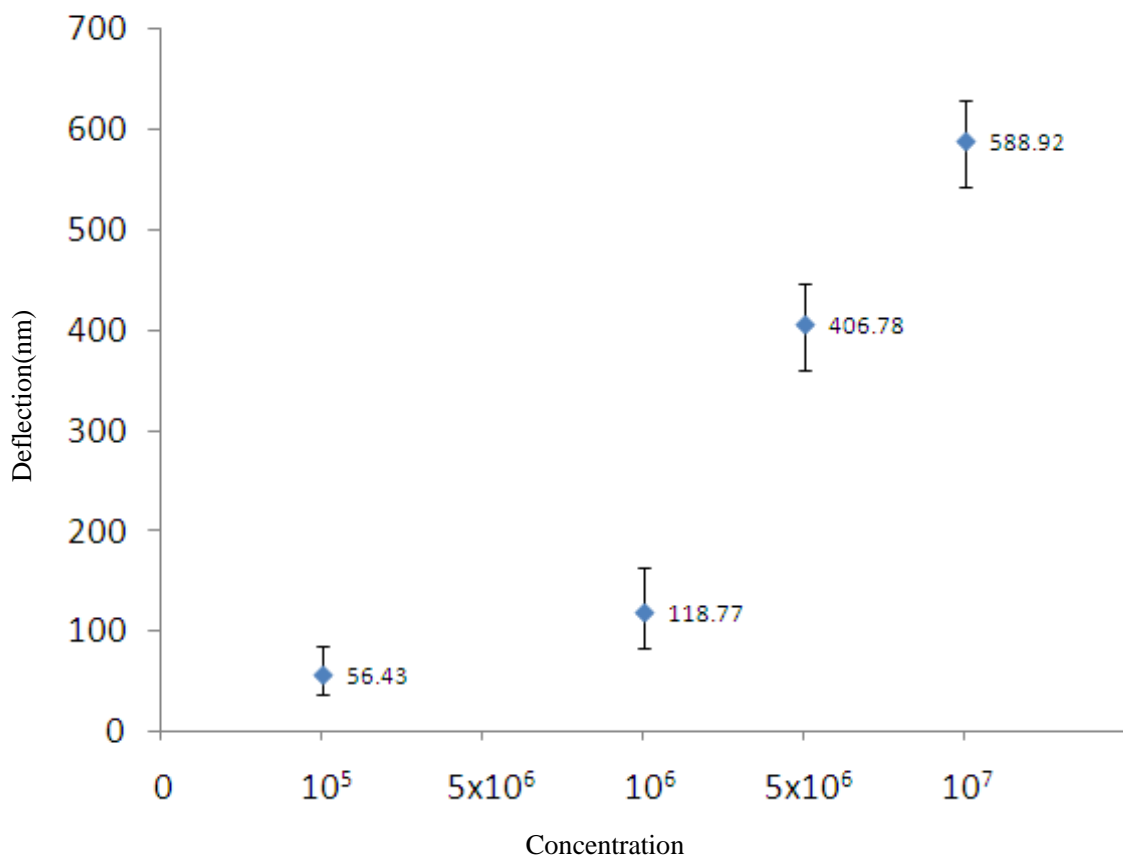

Figure 76: The results of cantilever deflection increased with concentration increased

Figure **76** shows the data has been summarized to fund that it is nearly linear. The device has the potential to be more sensitive. If the magnet can be change to be a more

powerful one, the limited detection should be improved.

5.9 Thrombin detection
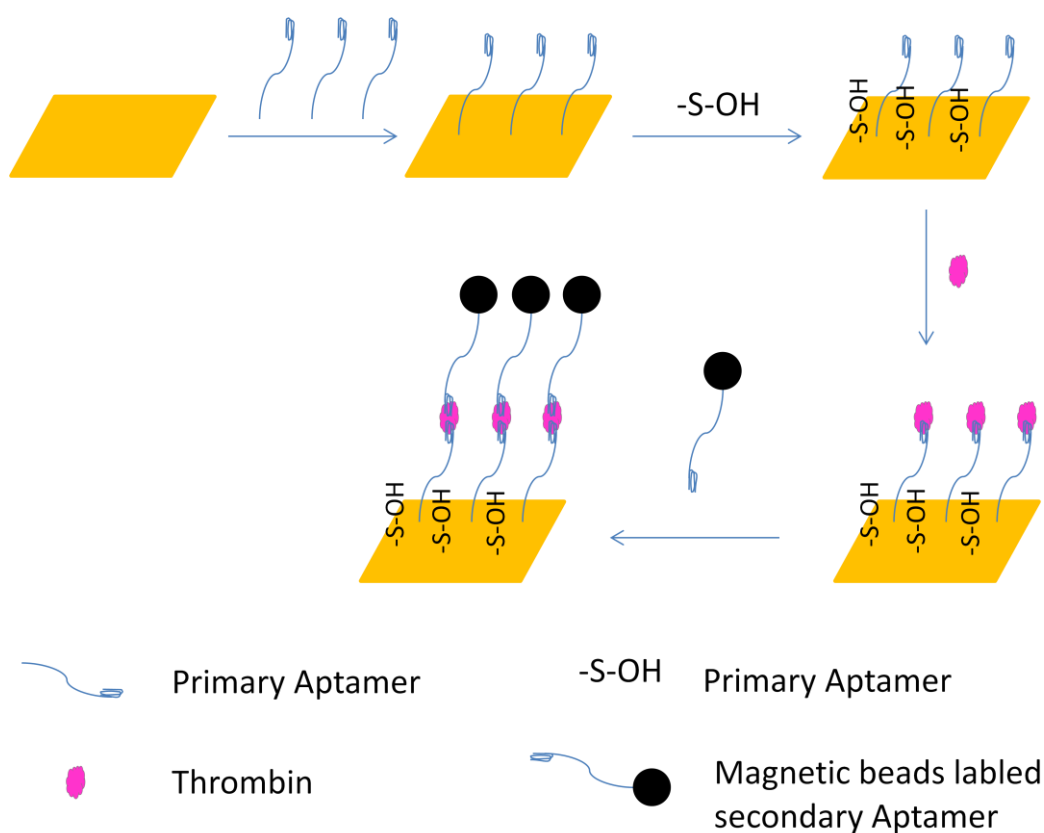
Figure 77: scheme for thrombin detection

Figure 77 shows a schematic of this experiment protocol. Firstly, immobilization of the primary anti-thrombin aptamer to the Au coated cantilever surface; secondly, addition of human thrombin to the system; thirdly, secondary binding with Magnetic beads-labeled aptamer,

5.9.1   Materials

Thrombin (human a-Thrombin) was purchased from Sigma Aldrich (UK). DNA was purchased from IBA lifesciences (Germany). Their sequences are as follows: The primary aptamer 5'-SH-(CH2)6-TT TTT TTT TTG GTT GGT GTG GTT GG-3' and the secondary aptamer 5'-biotin-TT TTT TTT TTG GTT GGT GTG GT T GG-3'. Magnetic beads coated with Streptavidin were purchased from Sigma (USA). 2-Mercaptoethanol was purchased from Sigma Aldrich (UK). All chemicals were of analytical grade and were used without further purification. All solutions were prepared with bi-distilled

water.

5.9.2   Results and discussion

The mirofluidic cantilever are fabricated with polyimide and photoresist. The surface of polyimide are coated 5nm Chromium followed by 20nm Gold. 1μM thiol labeled DNA was injected into the cantilever for 2hours. Subsequently it was washed with buffer (20 mM Tris–HCl,140 mM NaCl, 5 mM KCl, and 1 mM MgCl2, pH 7.4) to remove the DNA which didn't attach to the gold surface. 2-Mercaptoethanol (1mM) was pumped into the cantilever for 1hr which used to remove nonspecifically adsorbed DNA. Thrombin with different concentration was introduced into the cantilever to be detected for about 20mins. The cantilever was washed with buffer to removed the thrombin which didn't attached to the G-quadruplex. The reference experiment without thrombin was carried out to confirm the signal. The magnetic beads with labeled secondary aptamer were introduced to the cantilever. If there is thrombin in the cantilever, the magnetic beads will be attached in the cantilever. The powerful magnetic field is under the cantilever, which will bend the cantilever if there are magnetic beads in the cantilever.
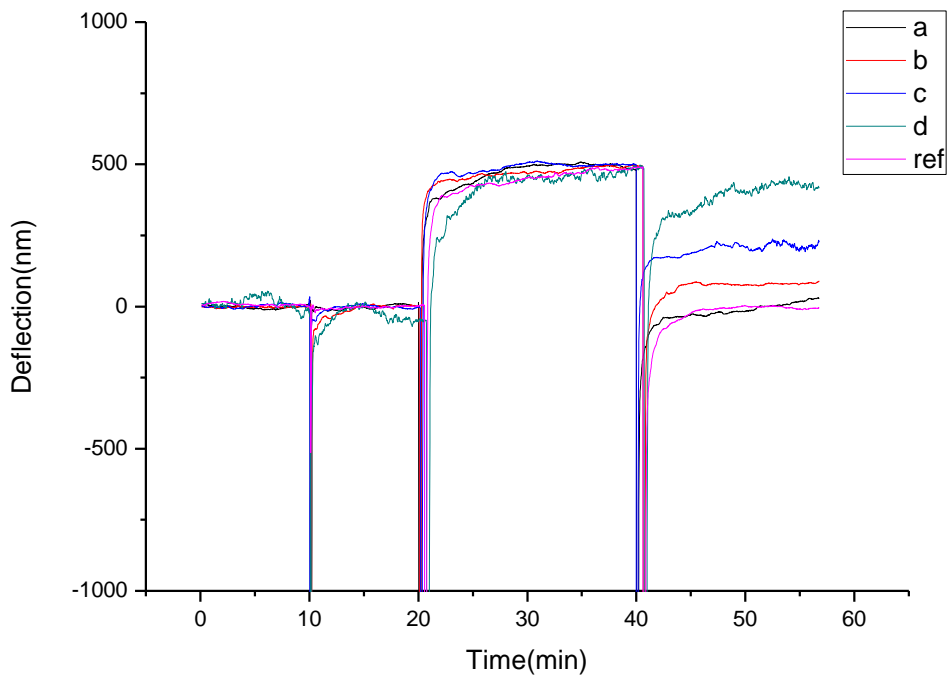
Figure 78 Results of detection of deferent concentration of Thrombin
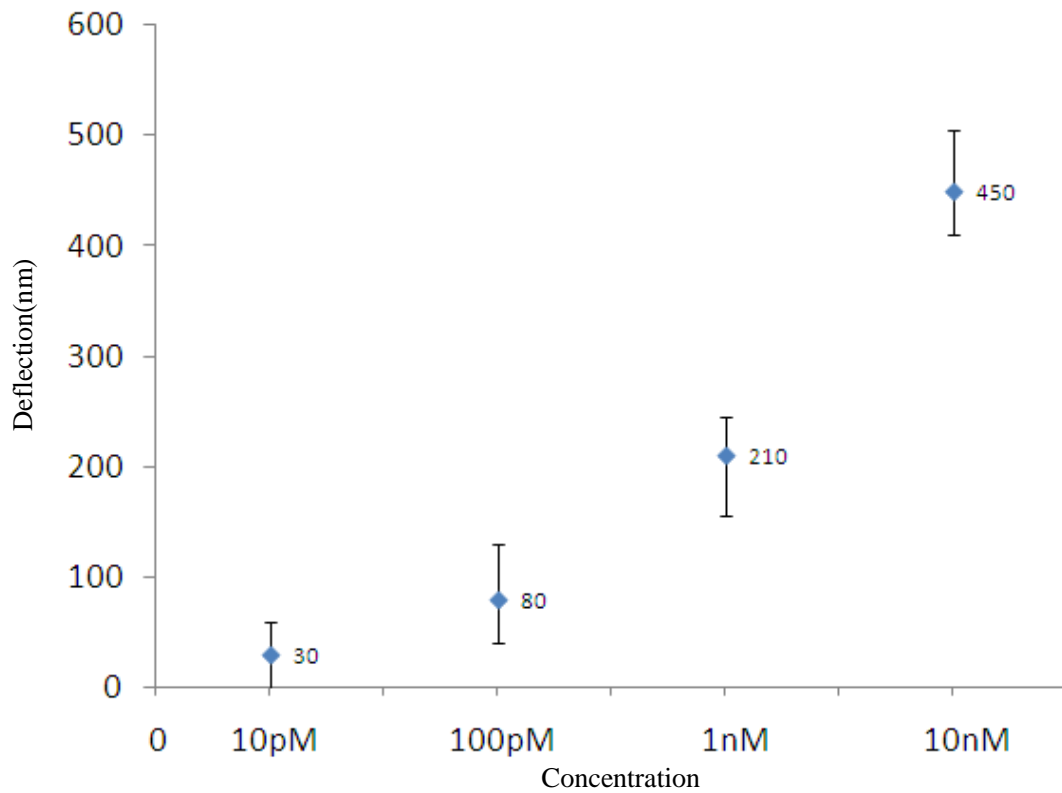(a:10pM, b:100pM, c:1nM, d:10nM. Ref is reference experiment without thrombin.)

Figure 79: Relationship between the cantilever deflection and the concentration of crypto

.

Figure 78 shows the results of the detection. Four group of experiment with different concentrations and reference experiment has been carried out to test if the device can distinguish them. The concentration of Line a (black) is 10pM; the concentration of Line b(red) is 100pM; the concentration of Line c(blue) is 1nM; The concentration of Line d(green) is 10nM. The line ref (pink) is the reference experiment. At about 10minites, the buffer has been pumped to test if the cantilever can completely bend back. Subsequently, at about 20 minutes, the magnetic beads with secondary aptamer have been introduced into the cantilever to find that a sharp signal has been caused. When the signal is stable, it is about 500nm over the baseline. It can be explained that the cantilever has been bent by the force between the magnetic beads and magnetic field. At about 40 minutes, the magnet field has been moved away and the magnetic beads have been pumped out at the same time to find how much the cantilever bends at last. The signal of the reference experiment can completely bend back. When the concentration of the thrombin is 10pM, the signal is nearly the same as the reference experiment. If the concentration of the thrombin increased, the signal will increase. The 10pM is found to be the limited detection of the device.

Figure 79 shows results at 56minutes with error bar. When the concentration of thrombin is 10pM the deflection is about 30nm; when the concentration of thrombin is 100pM the deflection is about 80nm; when the concentration of thrombin is 1nM the deflection is about 210nm; when the concentration of thrombin is 10nM the deflection is about 450nm. The experiments have been repeated for three times to build the graph with the errors bar.

5.9.3   Summary

❖ A new static mode polyimide based microfluidic microcantilever sensor has been demonstrated.

❖ Advantages of this are low-cost materials, easy and fast to fabricated, sensitivity.

- ❖ It has been demonstrated the potential of this system for the detection of thrombin.
- ❖ Waterborne pathogen Cryptosporidium has been detected with the system, which sensitivities is comparable to existing literature reports, particularly showing greater sensitivity than QCM.

5.10   References for Chapter 5

1. Su, M., S. Li, and V.P. Dravid, *Microcantilever resonance-based DNA detection with nanoparticle probes.* Applied Physics Letters, 2003. **82**(20): p. 3562-3564.

2. Marie, R., et al., *Adsorption kinetics and mechanical properties of thiol-modified DNA-oligos on gold investigated by microcantilever sensors.* Ultramicroscopy, 2002. **91**(1): p. 29-36.

3. Biswal, S.L., et al., *Nanomechanical detection of DNA melting on microcantilever surfaces.* Analytical chemistry, 2006. **78**(20): p. 7104-7109.

4. Liu, F., Y. Zhang, and Z.-c. Ou-Yang, *Flexoelectric origin of nanomechanic deflection in DNA-microcantilever system.* Biosensors and Bioelectronics, 2003. **18**(5): p. 655-660.

5. Burg, T.P., et al., *Weighing of biomolecules, single cells and single nanoparticles in fluid.* Nature, 2007. **446**(7139): p. 1066-1069.

6. Squires, T.M., R.J. Messinger, and S.R. Manalis, *Making it stick: convection, reaction and diffusion in surface-based biosensors.* Nat Biotechnol, 2008. **26**(4): p. 417-426.

7. Datar, R., et al., *Cantilever sensors: nanomechanical tools for diagnostics.* Mrs Bulletin, 2009. **34**(06): p. 449-454.

8. Savran, C., et al., *Microfabricated mechanical biosensor with inherently differential readout.* Applied physics letters, 2003. **83**(8): p. 1659-1661.

9. Lee, J., et al., *Electrical, thermal, and mechanical characterization of silicon microcantilever heaters.* Microelectromechanical Systems, Journal of, 2006. **15**(6): p. 1644-1655.

10. Wilson, C., A. Ormeggi, and M. Narbutovskih, *Fracture testing of silicon microcantilever beams.* Journal of applied physics, 1996. **79**(5): p. 2386-2393.

11. Wilson, C.J. and P.A. Beck, *Fracture testing of bulk silicon microcantilever beams subjected to a side load.* Microelectromechanical Systems, Journal of, 1996. **5**(3): p. 142-150.

12. Liju, Y., *Dielectrophoresis assisted immuno-capture and detection of foodborne pathogenic bacteria in biochips.* Talanta, 2009. **80**(2): p. 551-558.

13. Okhuysen, P.C., et al., *Virulence of three distinct Cryptosporidium parvum*

isolates for healthy adults. The Journal Of Infectious Diseases, 1999. **180**(4): p. 1275-1281.

14.   King, B.J. and P.T. Monis, *Critical processes affecting Cryptosporidium oocyst survival in the environment.* Parasitology, 2007. **134**: p. 309-323.

15.   Bridge, J.W., et al., *Engaging with the water sector for public health benefits: waterborne pathogens and diseases in developed countries.* Bulletin of the World Health Organisation, 2010. **88**: p. 873-875.

16.   Snelling, W.J., et al., *Cryptosporidiosis in developing countries.* J Infect Dev Ctries, 2007. **1**(3): p. 242-56.

Chapter 6　Paper based Microcantilever Sensors and Device for autonomous Detection

6.1 Introduction

In previous chapters, the rapid laser micromachining of polymer based microcantilever array and internally referenced microcantilever biosensors are discussed. However these systems require external pump or force to drive the liquid though the sensor system. In this chapter, we intend to fabricate an autonomous microcantilever and timer device with paper based microfluidic. Paper based microfluidic as a new class of microfluidic has significant potential in devices for use in drug development, environment monitoring [1-5]. The advantage of paper microfluidic is low cost and simplicity of fabrication[6-8]. There are many diagnostic assays are time-based, for example, some of the point-of-care (POC) diagnostic devices [9-12] [13]. Many reactions are also time dependent, for example, biochemical reaction kinetic assay [14, 15]. This paper describes a method for time control reaction, which is able to control time from minutes to months. The devices are paper based, the advantage of the devices are: 1) it is easy to fabricate. 2) The price of the device is not expensive. 3) It is easy to expand to array, even for hundreds of gradient 4) Time period is from minutes to months. 5) Simulation can be used to predict results exactly, which is important for long time reaction. A device, which can control concentration and time for biochemical reaction kinetic assay has been demonstrated in this chapter.

6.2　Material and experimental design

Filter paper is Fisherbrand FB59025 which diameter is 125mm and the thickness is 110μm.The brand of the Food color is Dr.Oetker.　Trotec laser Speedy 300TM is used to cut paper. In this chapter, we try to use paper to build a timer with paper microfluidics technology. The advantage of paper timer is that it is precise, light and cheap; paper is one of the best materials to make one-off timer. In this chapter, a new method to control time with paper microfluidic device has been presented. The advantage of this method is

that time period can be controlled from seconds to months. Shape of the paper, capillary, diffusion has been considered. A device which can control concentration and time for biochemical reaction kinetic assay has been demonstrated. The filter paper has been designed in different structure to control the speed. Simulation has been applied to optimize the parameter, which also can use to predict the results.

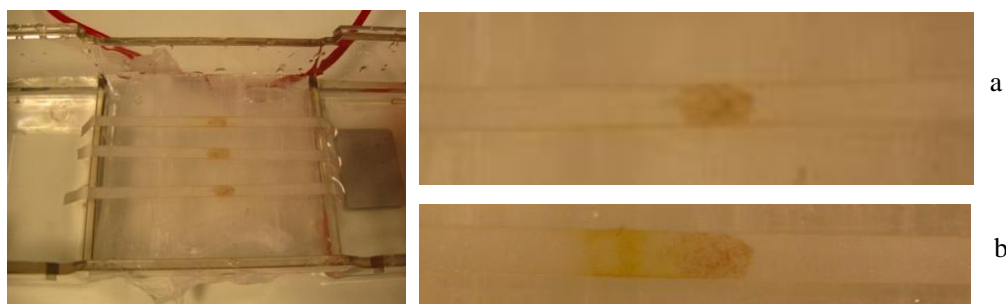## 6.3 Paper microfludic-microcantilever-electrophresis system

Figure 80: filter paper has been tested for the experiment to confirm it is suitable for the microfludic-microcantilever system

The filter paper has been dipped in Formic (1mole/L) for 24 hours. The paper has been washed with DI water to make sure the pH is higher than 3. Subsequently, the paper has been baked at 60 degree centigrade until it is dried. The filter paper has been set in the electrophoresis system. The voltage is 250V and it has been tested for one hour. Figure 80a shows the magnetic beads with streptavidin which has been dipped on the filter paper. It can be seen from Figure 80b, there is two bands on the filter paper in one hour. The band on the right hand is the magnetic beads which attached on the paper, and the band on the right is the magnetic beads which have been moved by the electric field. From this experiment we can conclude that the filter paper should be suitable for the microfluidic-microcantilever system.
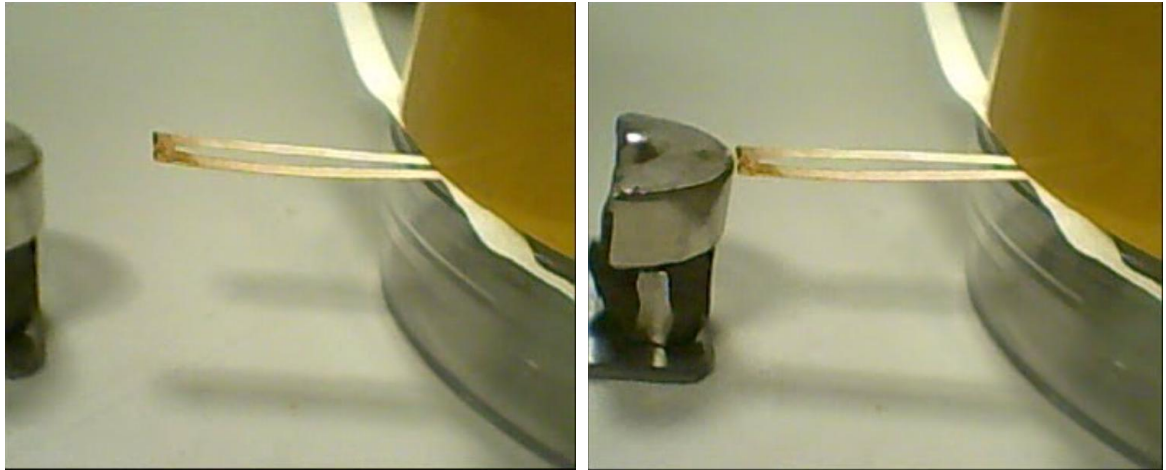
<div align="center">(a)   (b)</div>

Figure 81: paper cantilever with magnetic beads. (a) The paper cantilever with magnetic beads. (b) The paper cantilever with magnetic bends bent when the magnetic field is near it.

It should be tested if the magnetic field is strong enough to bend the paper cantilever with magnetic beads. The filter paper has been pretreated with Formic (1mole/L) for 24 hours, and fabricated with laser to cantilever, which is a nanosecond laser the speed is 20mm/s, the frequency is 15kHz, and the current is 85%. In Figure 86a, the magnetic beads with streptavidin dipped on the paper cantilever. When the magnetic field is near the paper cantilever the cantilever will bend down, and when the magnetic field move away the cantilever will bend back. It means that the magnetic field is strong enough for the experiment and the paper is suitable for fabricating cantilever, which can bend back when the magnetic field has been move away. Then experiment has been repeated for many times and the paper cantilever are found to be able to bend back to the same position.

(a)   (b)

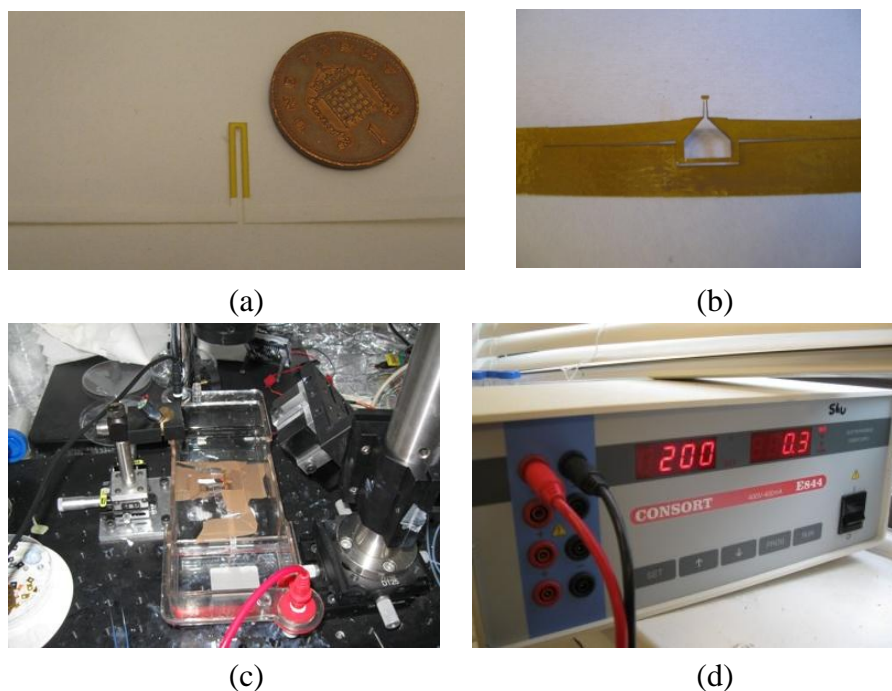(c)   (d)

Figure 82: Paper cantilever fabrication. (a) and (b) are paper cantilever with polyimide. (c) and (d) The cantilevers set on electrophoresis system.

The filter paper has been taped with 25μm thickness Polyimide tape on double side, after it has been pretreated. The filter paper with polyimide has been fabricated to cantilever with nanosecond laser (current 85, frequency15kHz, speed 40mm/s, three times). In Figure 82a (the left one), the width of the channel is 2mm, and the width of the channel on the right shown in Figure 82b is 0.1mm. The cantilever has been mounted on the electrophoresis system. The buffer is 50mM Citric acid-Na buffer, and pH is 7.5. When the Voltage is 200V, the current is 0.3mA.

The polyimide on the top of the filter paper is used to reflect the laser beam. If it coated a layer of gold film the effect will be much better. The polyimide tape can make the cantilever more flexible. The current of electrophoresis system come through the cantilever will heat the cantilever and the buffer on the cantilever will evaporate away and cause crystallization. The polyimide tape can reduce the evaporation and the crystallization. However, the advantage of the polyimide tape is that it can slow down the speed of the sample coming through the cantilever.

If the channel is wider, the magnetic beads will flow through the channel more quickly. However it will waste more sample, and increase the size of the cantilever which will reduce the sensitive of the system. If the channel is narrow, the speed of the magnetic beads flow through the channel will slow down. If it is too narrow, the current of the system need to turn down, otherwise it will burn the cantilever.

Different width of the paper has been tried to make sure there are stable current at acceptable voltage. To increase the current, the length of the paper should be shorter. A new cantilever hold can make the length of the paper short enough and the two culture dishes use as electrophoresis baths. A simple paper cantilever electrophoresis system has been built.

For the paper electrophoresis, the current is still too low to drive the magnetic beads cross the cantilever. Generally, the voltage of paper electrophoresis is 500～10 000V, because the resistance of paper is very high. Therefore, high voltage power supply will be needed to overcome the problem.

6.4 Paper microfluidic-microcantilever-chromatography system

(a)   (b)

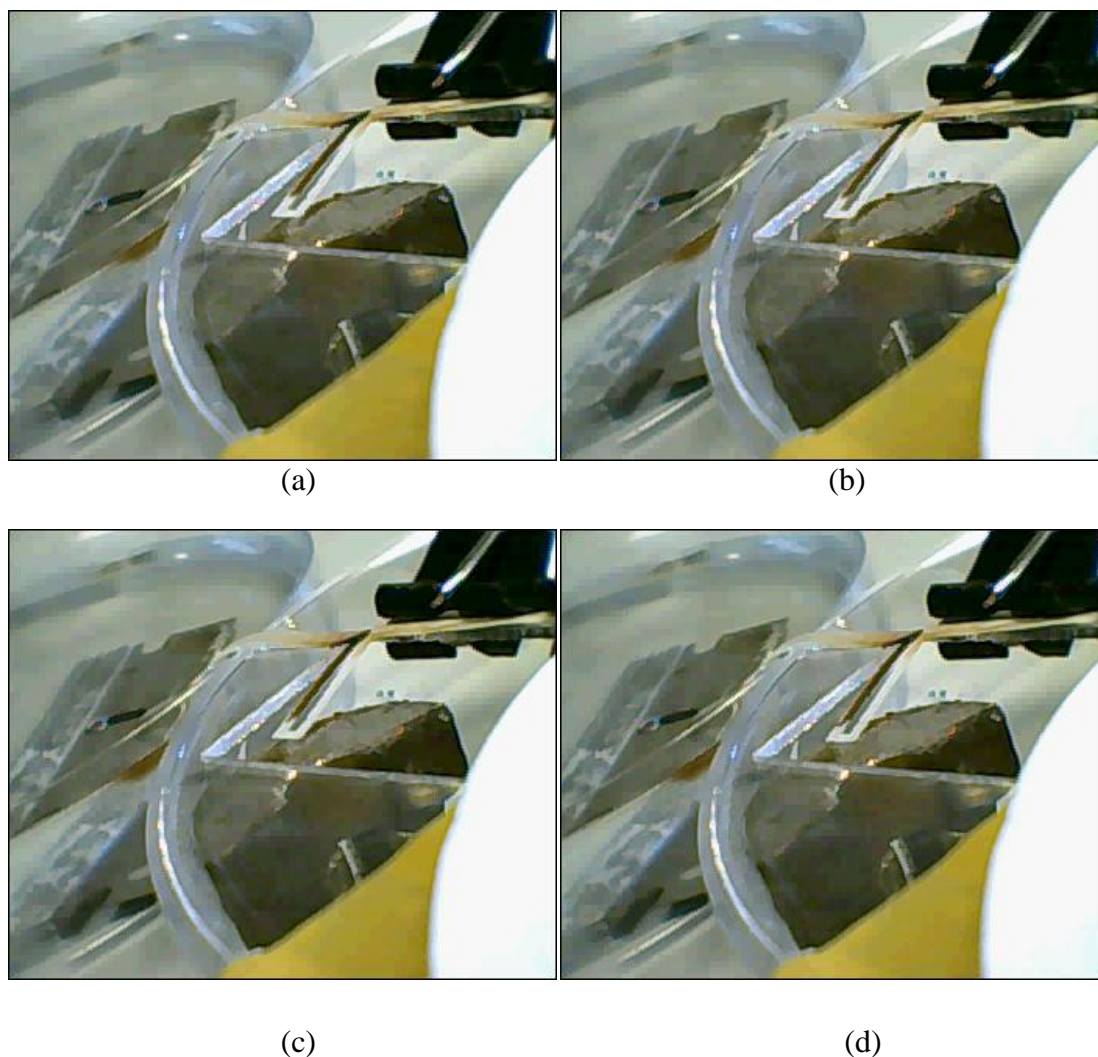
(c)   (d)

Figure 83: microfluidic-microcantilever-chromatography. From (a) to (d) the cantilever bend with the magnetic beads go through the cantilever.

Figure 83 shows Chromatography was combined with paper cantilever. Filter paper has been pretreated and cut into cantilever with laser. One end of the paper cantilever was dipped in DI water, and there is a magnetic field under the cantilever. 1.5µL magnetic beads were induced to the paper cantilever. It is a simple paper chromatography system. The cantilever bent sharply, with the magnetic beads flowing in the paper channel.

The advantage of chromatography is that it does not need the electrophoresis system. It means that it has potential to build portable cantilever system. Another advantage of the system is that it doesn't heat the cantilever. The cantilever is sensitive to temperature; it is helpful to improve the sensitive of the cantilever system. If it is needed to set under

the optical system, it need to tape with polyimide tape as well. It has potential to combine to piezoelectricity system, which is used to build portable cantilever system.

6.5 Paper based microcantilever portable device
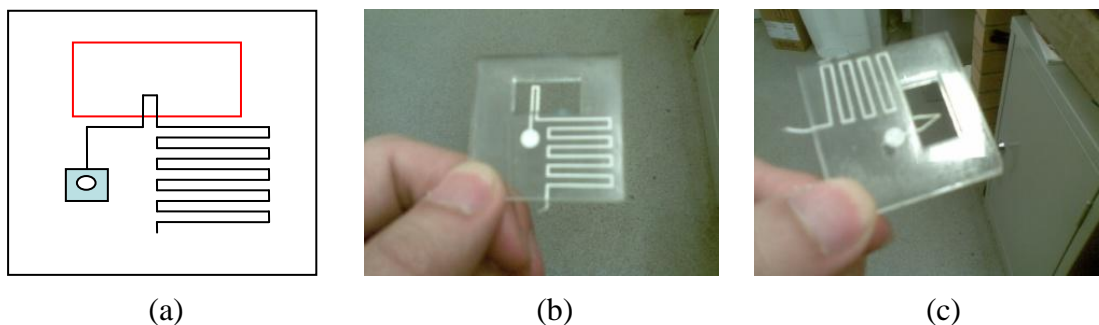

| (a) | (b) | (c) |

Figure 84: Chromatography cantilever portable device. (a) the sketch of the cantilever device. (b) and (c) are different version of the device.

Figure 84a illustrates the paper chromatography cantilever. The blue box with a hole on it is use to inject sample and buffer. The red box with a cantilever is used to detect sample. There is a long channel on the right side, the liquid will go through this channel to bring the sample come through the cantilever.

In Figure 84bc, the cantilever chromatography was packed into a chip. The holder was made by PMMA (thickness is 5mm), which was fabricated by laser. One side of the PMMA chip was attached to a double sides tape. Then the paper cantilever was sandwiched in the middle. There is a hole on one side of the PMMA holder, which is used to dip sample into the chip.
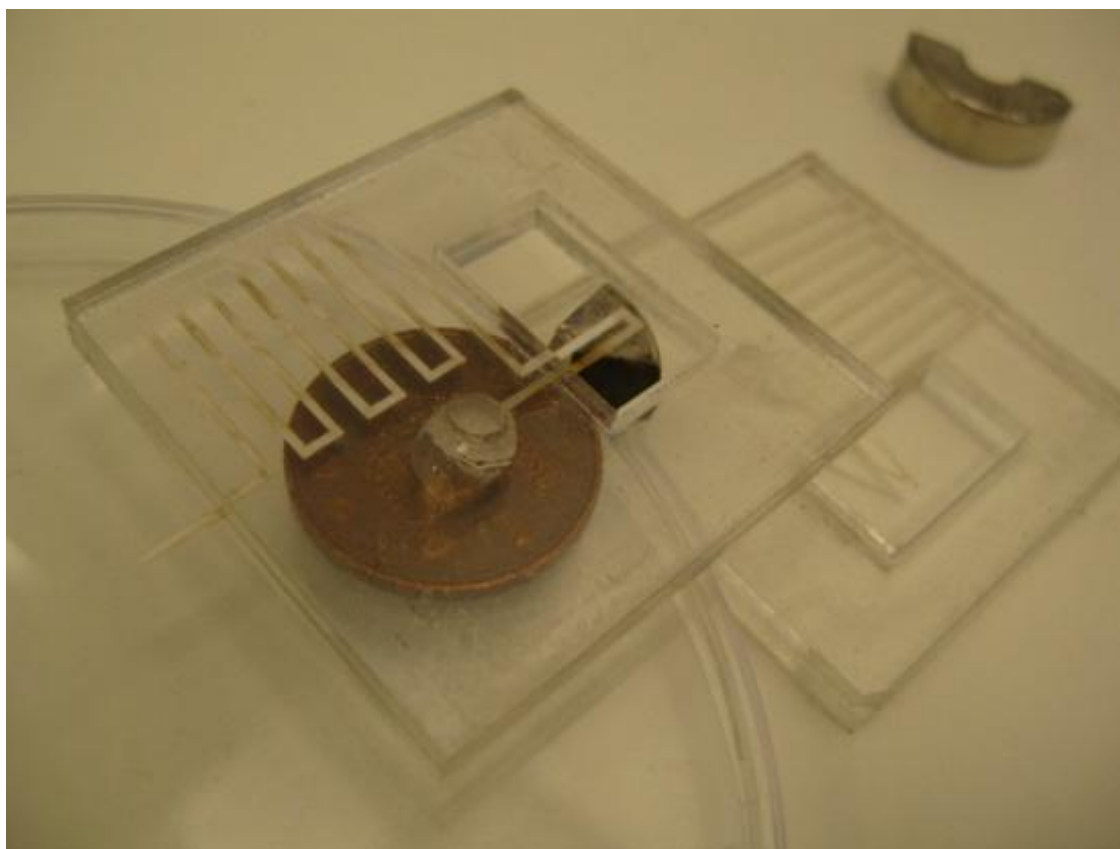
Figure 85: chromatography cantilever portable device above magnetic field

Figure 85 shows the cantilever chromatography system. A magnetic field is needed to put under the chip, and it needs to set under a optical system. A drop of magnetic beads (diameter 100um) was added to the hole, and then water used as mobile phase was introduced into the hole. The magnetic beads come through the paper cantilever channel and cause the cantilever bend down. When all the magnetic beads go through the paper cantilever channel, the cantilever bends back.
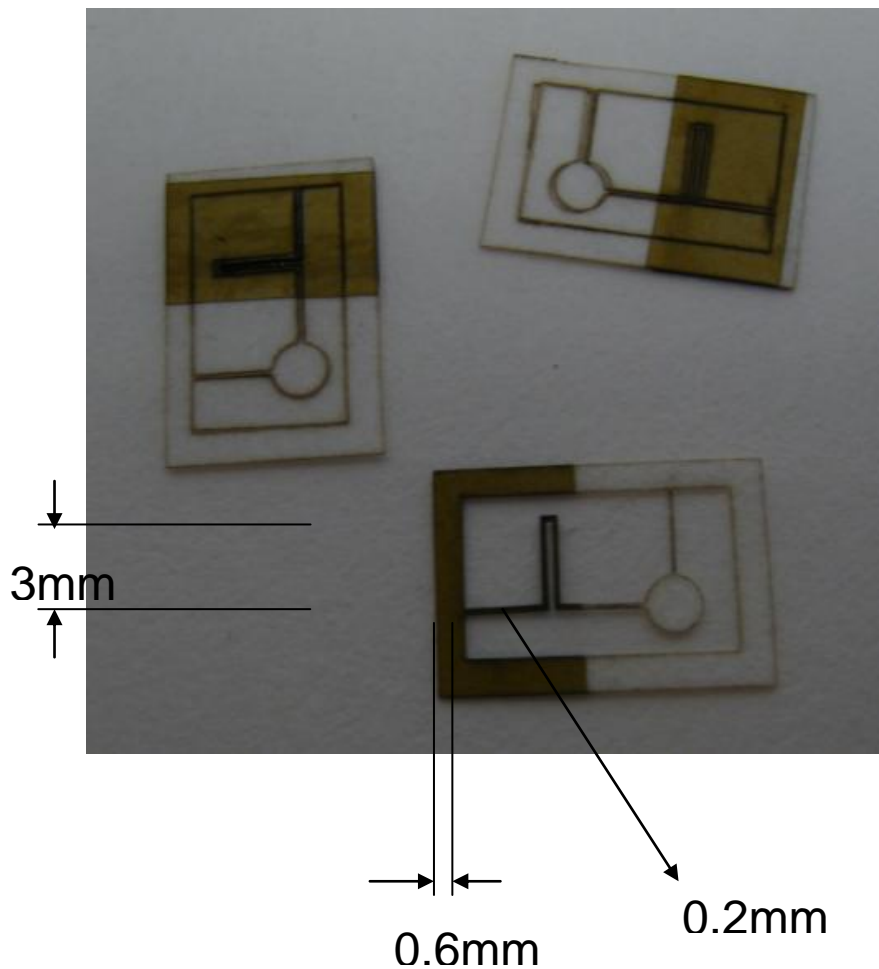
Figure 86: smaller chromatography cantilever device

If the device needs to detect sample under optical system, a polyimide tape need to cover it to reflect the laser beam. In Figure 86, the device can be fabricated much smaller. The width of the channel is 0.2mm, and the width, and height of the cantilever is 0.6mm and 3mm. There is a cycle pad on the right hand side of the cantilever. When the sample dipped on the pad it will run through the cantilever to the left hand side. The disadvantage of the system is that it is not very fast, sometimes, it will cause hours time to flow all the beads through the channel. This will limit the application of this technology.

6.6 Paper microfluidic timer
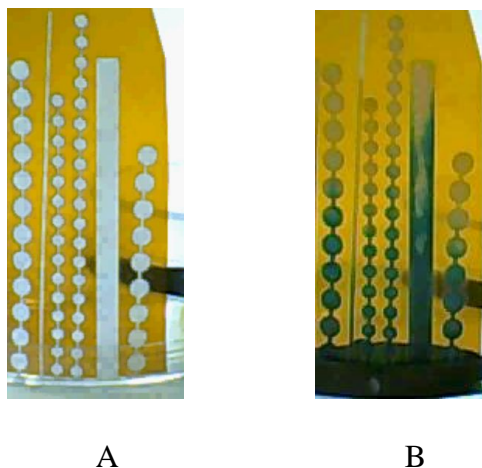

A   B

Figure 87: comparison of paper channel. A) different kind of paper channel.   B)   the channel dipped in food color.

Channel 1 and 6: diameter of the pads is 4 mm. channels 2: width of the line is 0.74mm. Channel 3 and 4: The diameter of the pads is 3mm. Channel 5: the width of the line is 4mm.

To find which shape of the Paper Microfluidic device is suitable for the timer; different versions of the channels have been designed which are shown in Figure 87. The channel 1 is combined with pads and line. The diameter of the pad is 4mm and the width of the line is 0.74mm. To make a control for the channel 1, channel 2 and channel 5 were designed. The width of Channel 2 and 5 are 0.74mm and 4mm. In this design, we try to find which one will be slower. In Figure 2, the paper pads have been dipped in the food color for 30mins. To compare Channel 1 and Channel 6, the shape of them are the same, and only difference is the length. Figure 87B shows that Channel 1 is faster than channel 6. The same situation happened between channel 3 and channel 4, as well. In Figure 87B, the channel 2 is the slowest one, and the channel 5 is the fastest one.

It seems difficult to find a rule for these results. The food color in channel 4 is faster than that in channel 3. The food color in channel 1 is faster than that in channel 6. It seems that the longer the channel is , the faster the food color run. Comparing channel 2 and 5, it seems that the thinner the channel is the slower the food color runs. A precise

hours timer has been fabricated.

6.7 Application hours timer (capillary)

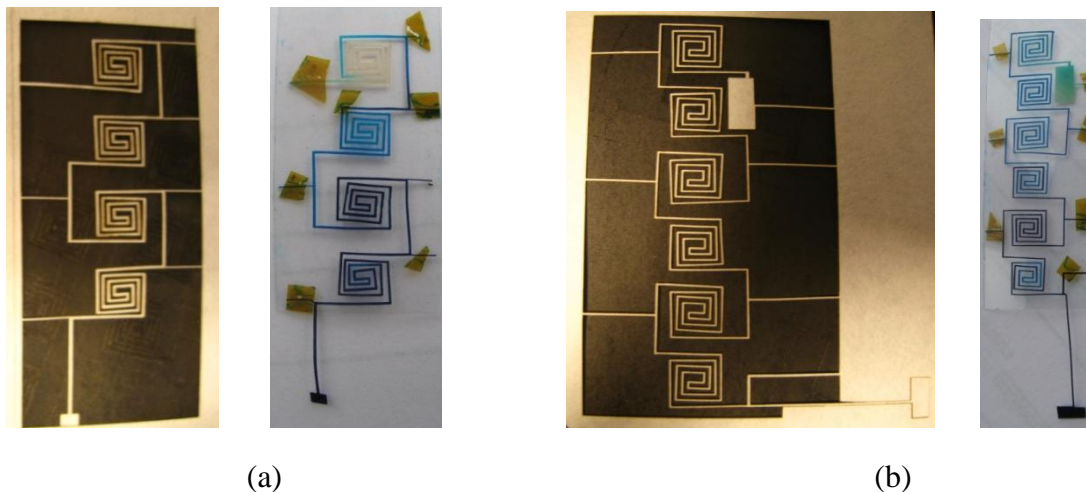(a)   (b)

Figure 88: paper based hours paper timer. (a) 4 pads hours timer. (b) 6 pads hours timer

With the capillary force, hours timer has been made which is shown in Figure 88a. To make the timer precise, the width of the channel is 400um. It took four hours and 34mins that the food color ran from one end to the other end. In Figure 88b the width of the channel is 0.3mm, and the width of the square is 5mm.

To extend the length of the timer, two changes had been made. Firstly, the channel of the filter paper had been fabricated thinner (from 0.4mm to 0.3mm). Secondly, the cycle had been increased from four to six. Third, a square pad has been added to the end to make sure the liquid can stop after the cycle. In the end, 11 hours timer had been made.

If the length and width has been adjusted, the timer can measure from minutes to hours. The disadvantage of this timer is that the time it measured is only limited in one day. The experiment designed in Figure 87 seems too complex to find a rule.

To find a rule, a simpler experiment has been designed. The input end of the channels are the same, which is more easy to find the rule between each channel. In Figure 87a, from left to right are square pads, square pads and line and line. The width of the line is

0.2mm, and the square pads are 5mm. In Figure 87b, when the food color was injected to it, the food color in the line is the fastest one and the square pads and line is the slowest one. The shape of the paper has the potential to control the speed of food color in the channel, which can be used to build a timer.

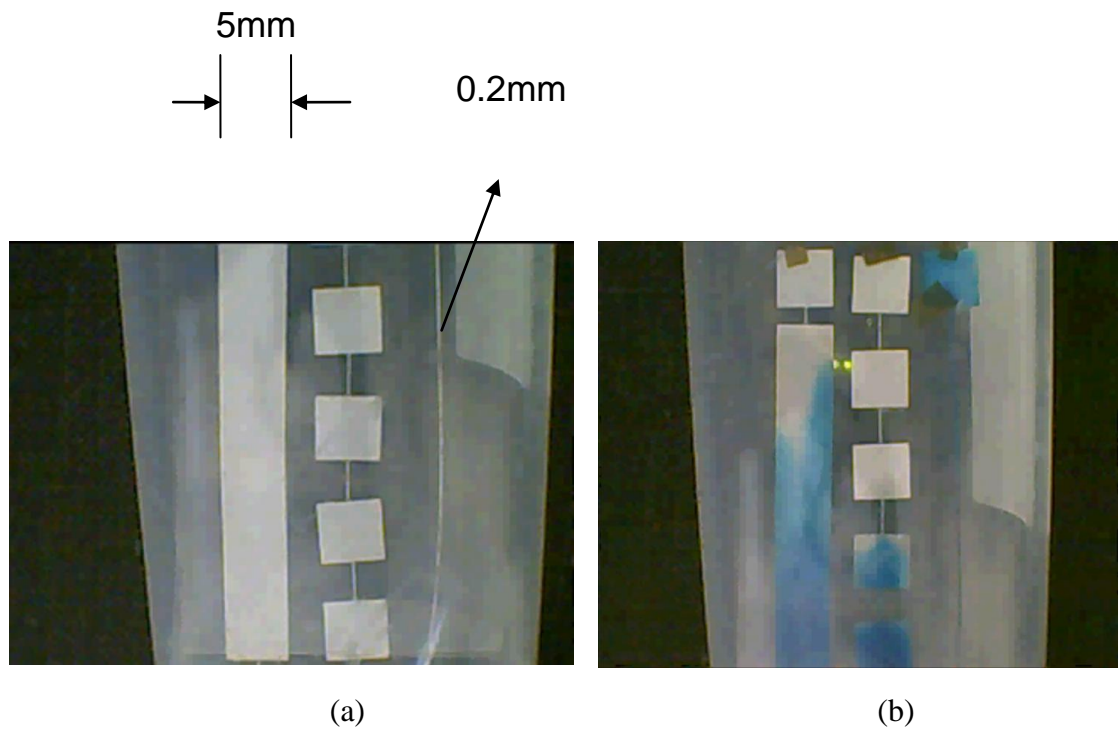**6.8 Paper based sandglass like microfluidic**

(a)   (b)

Figure 89: rectangle pad, line, square pad-line comparison. (a) Three kind of channels. (b) The channels dipped in food color.

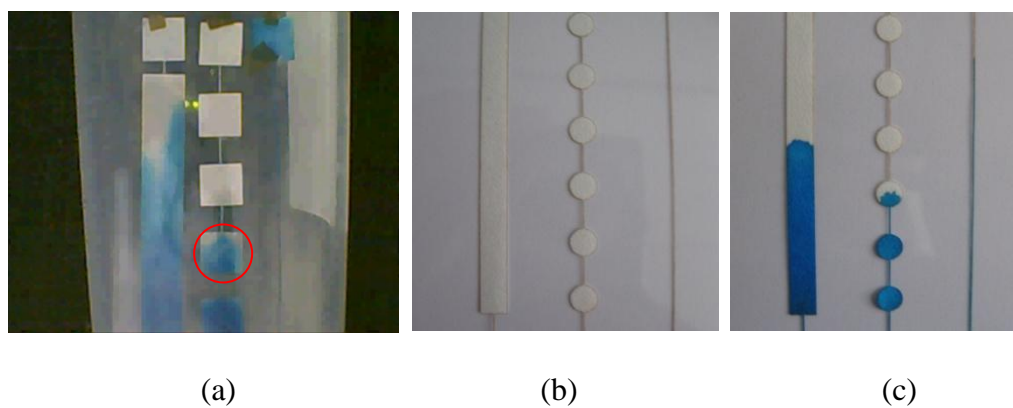(a)   (b)   (c)

Figure 90: rectangle and cycle pads channel comparison. (a) The rectangle pads. (b) and (c) are cycle pads channel.

a) In the red cycle, the square pad cannot be fulfilled with food color. b) There are three filter paper based strips, which input end is the same. The width of the left one is 3mm, the width of the right one is 0.2mm. The diameter of the pads of the middle strip is 3mm and the width of the stem is 0.2mm.   c) Three paper slips have been put into the food color. The middle slip turns to be the slowest one

In Figure 90a, the channel is fabricated with square pad and line. In the red cycle, the square pad can't be fulfilled with the food color, especially at the corner of the pads. To make it better, a cycle pad with line channel has been designed in Figure 3bc. With this design, there is no corner in the pads.

In Figure 90b, there are three filter paper strips, whose input ends are the same. The width of the left trip is 3mm, and the width of the right one is 0.2mm. The diameter of the pads of the middle strip is 3mm and the width of the stem is 0.2mm. In Figure 3c when the strips dipped into food color, the middle one is the slowest, and the food color can fulfilled in the pads. The middle one is just like an invertible sandglass, the difference is that if we change a two bubbles sandglass to three bubbles sandglass, it doesn't extend the time which sandglass measured, but this device does. To predict precise results, the simulation of the experiment had been done in further work.

6.9 Results and discussion
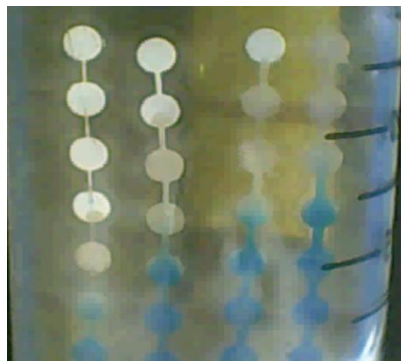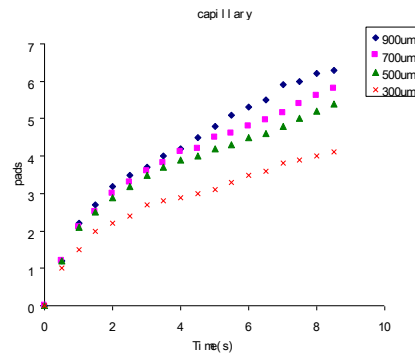
(a)   (b)

Figure 91: Results of paper channel pumped with capillary. (a) 4 paper channels with different width of the stems. (b) The results of 4 channels comparison

The diameter of the pads is 3mm; the widths of the stem are 300μm, 500μm, 700μm, 900μm respectively. The food color has been pumped with capillary to find that the stem with 900μm is the fast one. It takes 9 minutes to reach the 7 pads.
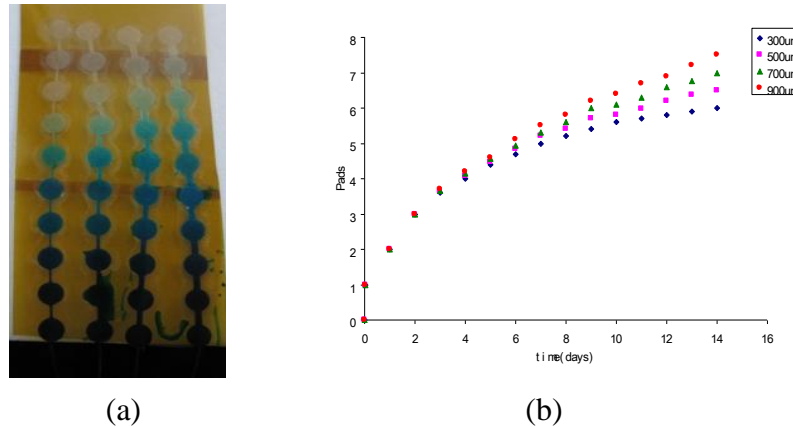

(a)   (b)

Figure 92 Results of paper channel pumped with diffusion. (a) Pre-wet paper channel with food color. (b) The results of 4 channels comparison

The diameter of the pads is 3mm; the width of the stem is 300μm, 500μm, 700μm, 900μm. The food color has been pumped with diffusion. It is found that the stem with 900μm is the fast one. It takes 12 days to reach the 7 pads.

Experiment has been done to optimize the structure of the pads. In Figure 91 the diameter of the pads has been kept as 3mm and the width of stem are 300μm, 500μm, 700μm, 900μm. The input end of the dry strips has been put into food color. The food color has been pumped into the strips with capillary force to find that the speed increased with the stems increased.

Even though, it can differentiate time, but it is still limited in hours. To extend the time scale, diffusion method has been introduced. Figure 92 shows the paper timer, which is pre-wetted with colorless DI water before the dye solution is introduced via diffusion process. The results show that diffusion process is much slower than the capillary forces. In the diffusion way, the timer can measured from hours to months. Both capillary and

diffusion methods show that the stem is thinner and the speed is slower. Therefore, these parameters can be used to control the speed of food color on the strips include: the quantity of the pads, the proportion between the diameter of the pads and the width of the stem, and capillary or diffusion. The experiment has been repeated for 5times, and Figure 92 is one of the results.
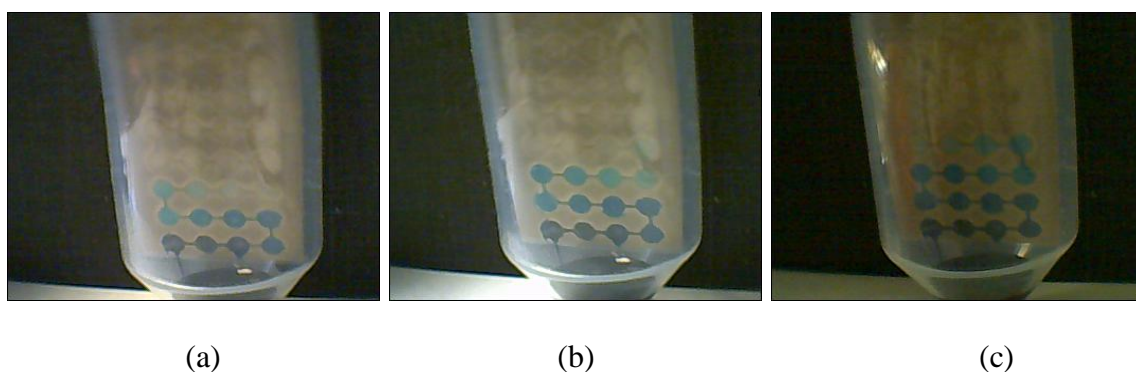

(a)   (b)   (c)

Figure 93 long term paper based microfluidic timer. (a) is the first day, (b) is the fifth day and (c) is the 20th day.

The food color takes about half a month to reach the end of the channel. The channel has been extended to extend the time it can measure in Figure 93. The channel contains 32 pads which is pre-wetted. One end of the channel has been dipped in the food color and the channel has been put in a tube which is sealed to prevent evaporation.

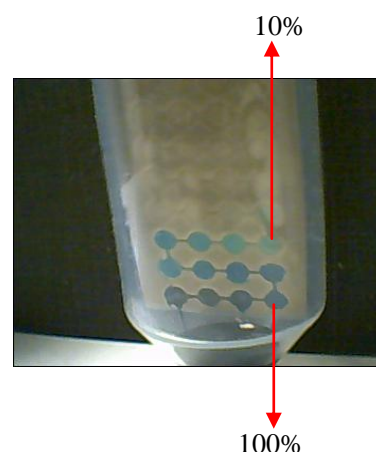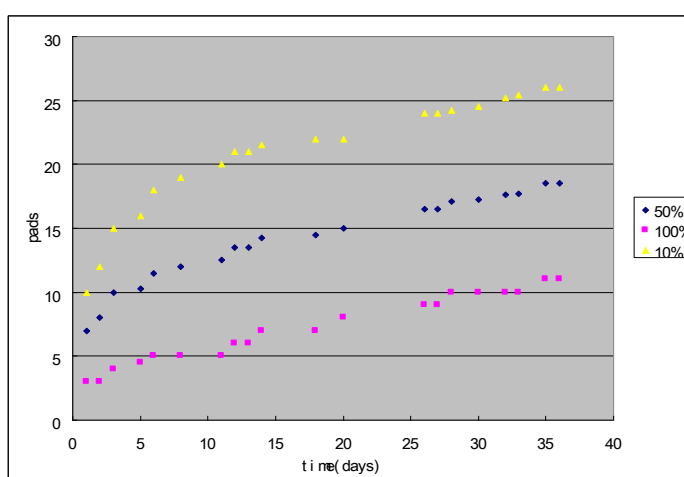(a)   (b)

Figure 94: results of long term paper timer. A) the results of the paper timer. B) the way to measure 10% and 100% of food color.

Figure 94 shows that photoshop has been used to obtain the color from the picture. With these data, a graph has been drawn to show the relationship between the time and the speed of the paper timer. As to the line 10%, it increased sharply in the first five days, then the speed seems slower. On the other hand, the 100% line increased slowly at the same speed, it seems that the relationship between the time and speed is linear. It has the potential to make a timer which can last for more than one month.

| 1day | 2days | 4days | 6days |

| 7days | 9days | 10days |
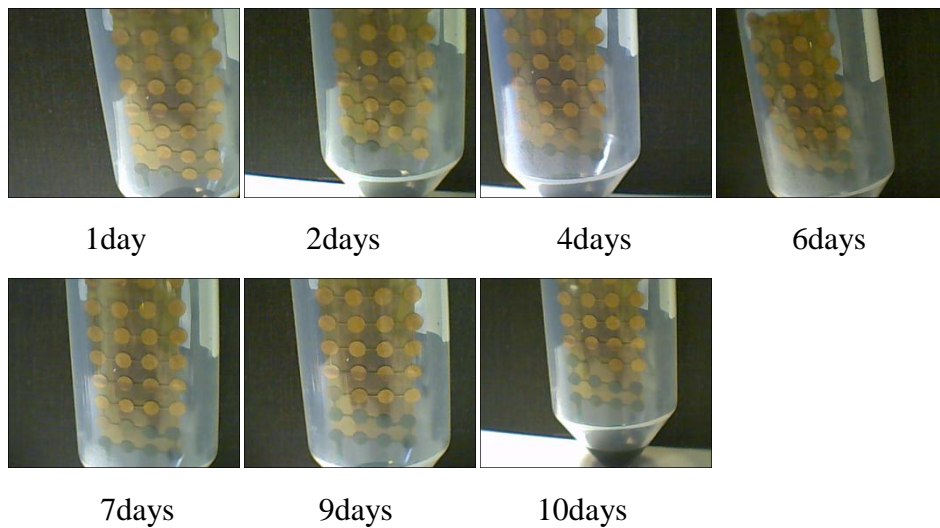
Figure 95: polyimide sealed paper timer

(a)   (b)
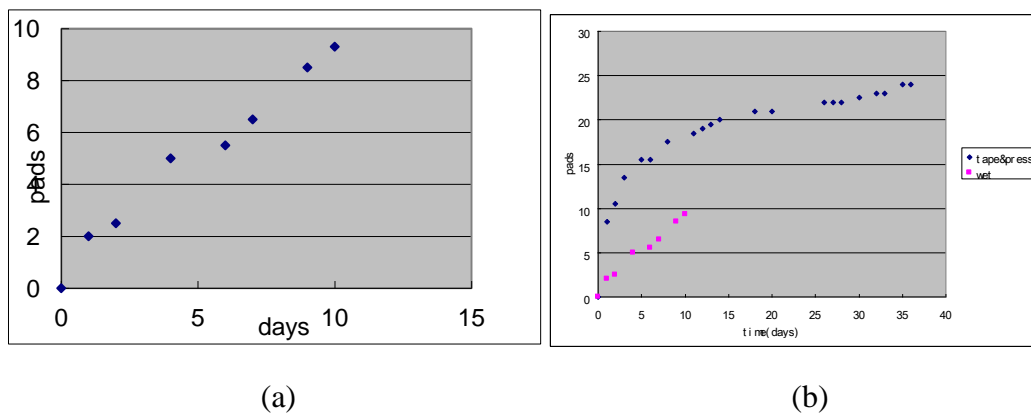
Figure 96: (a) Results of polyimide sealed paper timer. (b) Comparison of sealed paper and pre-wet paper timer.

Figure 95 shows that the timer has been sealed with polyimide tape on double sides, which is not pre-wetted. One end of the timer has been dipped in food color to find that the food color pumped by capillary force. It takes 10 days to run about 10 pads. In

Figure 96, it has been compared with the timer pumped by diffusion. The timer sealed with tape pumped by capillary is slower than the timer pumped by diffusion. If a more slower timer is needed, the timer sealed with tape can be pre-wetted, which may run much longer.

6.10   Simulation

6.10.1 Numerical method

Recently, the lattice Boltzmann method is known as a promising computational fluid dynamics model. The LBE model is presented as a useful method to simulate the diffusion process in fluid system [16]. In this thesis, we implement the multi-component LBE model (2D) with external forces to describe the motion of fluid in the paper micro-fluidic system. One component represents the motion of the fluid called fluid lattice or σ component and another component simulates the concentration field called concentration lattice or $\bar{\sigma}$ component.

The distribution function for each component are governed by lattice Boltzmann equations with the lattice BGK (Bhatnagar-Gross-Krook) collision algorithm,

$$f_i^{\sigma}(x+e_i\Delta t, t+\Delta t) = f_i^{\sigma}(x,t) - \frac{1}{\tau_{\sigma}}[f_i^{\sigma}(x,t) - f_i^{\sigma,eq}(x,t)] \tag{1}$$

where f_i^{σ} is the distribution function of σ th component in the i th velocity direction, i is a direction index. For the fluid lattice, we use the D2Q9 model, $i = 0, 1, 2, 3, 4, 5, 6, 7, 8$. e_i represents the vectors of the lattice basis as shown in Figure 102. e_i is given as

$$e_i = (0,0) \qquad\qquad i = 0$$

$$e_i = \left(\cos\frac{(i-1)\pi}{2}, \sin\frac{(i-1)\pi}{2} \right) \qquad\qquad i = 1-4 \tag{2}$$

$$e_i = \sqrt{2}\left(\cos\left(\frac{(i-5)\pi}{2} + \frac{\pi}{4}\right), \sin\left(\frac{(i-5)\pi}{2} + \frac{\pi}{4}\right) \right) \qquad i = 5-8.$$

The superscript eq denotes the equilibrium state, τ_σ is the relaxation time parameter, related with macroscopic kinematic viscosity of the fluid lattice by the equation

$$\upsilon_\sigma = c_s^2 \left(\tau_\sigma - \frac{1}{2} \Delta t \right)$$

(3)

And for the concentration lattice, the 4 velocities model is sufficient to describe the diffusion phenomena [17]. Thus D2Q4 model is used to $\bar{\sigma}$ component. The e_i represents 4 velocity vectors i=0,1,2,3,4. The relaxation time for this lattice is controlled by the diffusivity $D_{\bar{\sigma}}$ as below

$$D_{\bar{\sigma}} = c_s^2 \left(\tau_{\bar{\sigma}} - \frac{1}{2} \Delta t \right)$$
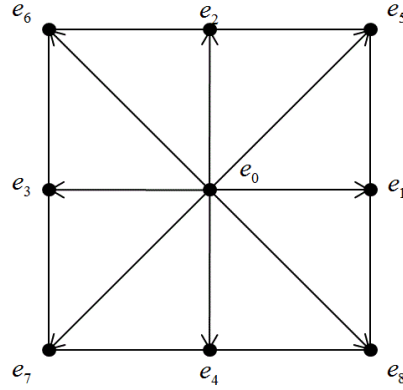
(4)

Figure 97: Velocity vectors of D2Q9 model

The equilibrium distribution function for different component can be described by

$$f_i^{\sigma,eq}(x,t) = \omega_i^\sigma \rho_\sigma \left[1 + \frac{e_i \cdot u_\sigma^{\sigma,eq}}{c_s^2} + \frac{\left(e_i \cdot u_\sigma^{\sigma,eq}\right)^2}{2c_s^4} - \frac{u_\sigma^{\sigma,eq\,2}}{2c_s^2} \right]$$

(5)

$$f_i^{\bar{\sigma},eq}(x,t) = \omega_i^{\bar{\sigma}} \rho_{\bar{\sigma}} (1 + \frac{e_i \cdot u_{\bar{\sigma}}^{eq}}{c_s^2})$$

(6)

where the weight ω_i^σ is 4/9 for the particles $i = 0$, is 1/9 for $i = 1, 2, 3, 4$ and 1/36 for $i = 5, 6, 7, 8$, and $c_s = c/\sqrt{3}$, c is the basic speed on the lattice ($c = \Delta x / \Delta t$), since in

LBM method, $\Delta x = \Delta t = 1$, and $c_s = 1/\sqrt{3}$ is the velocity of sound for D2Q9 model. The weight for the concentration lattice is $\omega_i^{\bar{\sigma}} = 1/3$ for i=0 and $\omega_i^{\bar{\sigma}} = 1/6$ for i=1,2,3,4.

The equilibrium velocity in Eq. 5 is determined by the force acting on the σ th component in the momentum equation, which is described by

$$u_\sigma^{eq} = u^{'} + \frac{\tau_\sigma F_\sigma}{\rho_\sigma} \tag{5}$$

F_σ is the total force acting on the σ th component, including the long range interparticle fluid-fluid forces F_σ^f, the fluid-surface force F_σ^s and external force such as gravity F_σ^g. All of them cause the momentum (velocity) change in the equilibrium distribution function, in the multi-component SC model the fluid-fluid force is given by

$$F_\sigma^f(x) = -\psi_\sigma(x)\sum_{x^{'}} G_{\sigma\bar{\sigma}}(x,x^{'})\psi_{\bar{\sigma}}(x^{'})(x^{'} - x) \tag{6}$$

where ψ_σ and $\psi_{\bar{\sigma}}$ are the "effective mass", which are the function of density. $G_{\sigma\bar{\sigma}}$ is the Green's function to describe the interaction strength and the same for two components.

Based on the Fick's law

$$J = -D\frac{\partial \phi}{\partial x} \tag{7}$$

where J is the diffusion flux, D is the diffusivity(m²/s), φ is the concentration in dimension (mol/m³), x is the position. $\frac{\partial \phi}{\partial x}$ indicates the concentration gradient, which is the driving force for the diffusion. The driving force for the diffusion process is classified in the external force in LBM model. We assume that the density for concentration lattice is linear with the concentration, namely $\rho / \rho_\infty = 1 + (c - c_\infty)$, c is the fluid concentration. The buoyancy force is therefore $\rho \cdot g(c - c_\infty)$.

The simulation model for the $\bar{\sigma}$ component obeys the following equation

$$\frac{\partial \rho_{\bar{\sigma}}}{\partial t} + \nabla \cdot \left(\rho_{\bar{\sigma}} u\right) = \nabla \cdot \left(D \nabla \rho_{\bar{\sigma}}\right) \tag{8}$$

The concentration field is simulated by the density field for the $\bar{\sigma}$ component. The diffusivity is given in Eq(4).

6.10.2 Simulation results

We present the simulation results in this section. The simulation are performed in a 650*100 lattice with the initial concentration on the bottom is 1. The width of channel 1 and 3 are 60 lattices and 6 lattices separately. And for case 2, the bubble diameter is 60 and the width of the channel between the bubbles is 6 lattices. The characteristic parameters are Ra=100, Pr=0.71

Ra is abbreviation of Rayleigh number, which is for a fluid is a dimensionless number associated with buoyancy driven flow (also known as free convection or natural convection). Pr is abbreviation of the Prandtl number which is a dimensionless number; the ratio of momentum diffusivity (kinematic viscosity) to thermal diffusivity.

The simulation results for these 3 cases are compared on time step 48000 in Figure 98.
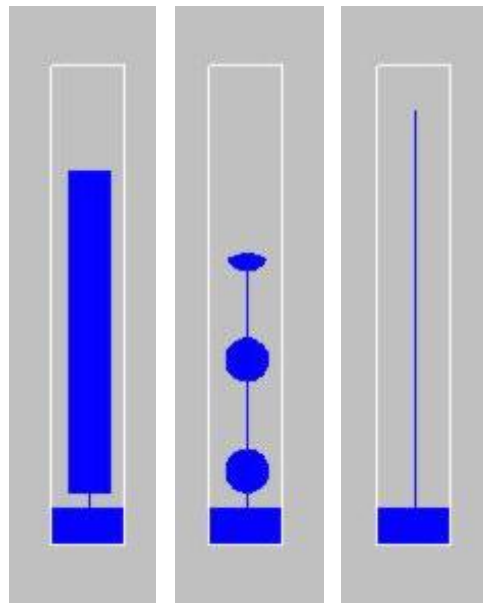
Figure 98: simulation results for paper based microfluidic

It means that the data from the experiment can match the simulation results. For the long term timer, the simulation method has the potential to predict the results.

6.11   Application for biochemical reaction kinetic assay I
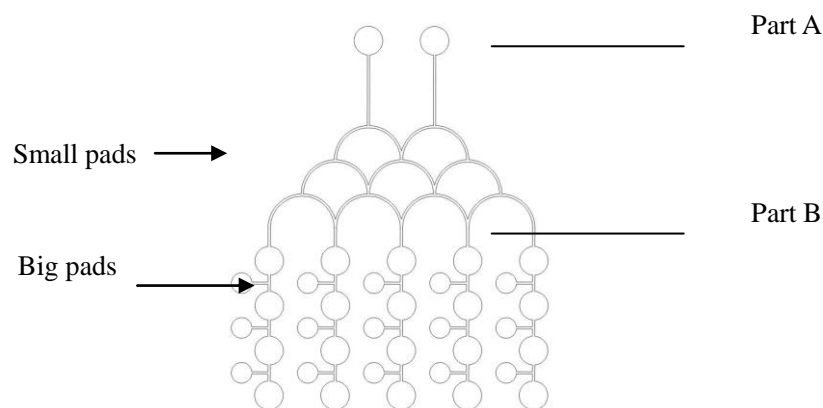

Part A

Small pads ⟶

Part B

Big pads ⟶

Figure 99: design of microfluidic mixing paper timer

Figure 99 shows the new device which integrate the microfluidic mixing and paper timer. Part A is a paper microfluidic mixing and Part B is a paper timer. Part B has combined with small pads and big pads. The small pads are used to detection and big pads are part of the timer which are used to measure time. With this device, concentration gradient and time gradient can be obtained for reaction. It has the potential to apply for
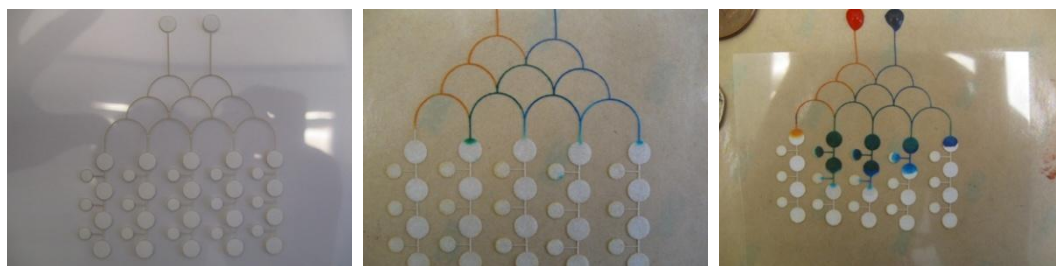
biochemical reaction kinetic assay.

Figure 100: microfluidic mixing paper timer.

Yellow and blue food color has been dipped to the device. The color has been changed from yellow to blue. One of the problem is that the middle one run faster than others. The flux is just like a pyramid in Figure 101. The input end are the same, but the output end are quite different. The middle one is six times than the one on the edge. As the flux is different, the input end of the timer is different and the timer doesn't work in this device.

$$
\begin{array}{ccccccccc}
 & & & & 1 & & 1 & & \\
 & & & 1/2 & & 1 & & 1/2 & \\
 & & 1/4 & & 3/4 & & 3/4 & & 1/4 \\
 & 1/8 & & 4/8 & & 6/8 & & 4/8 & & 1/8 \\
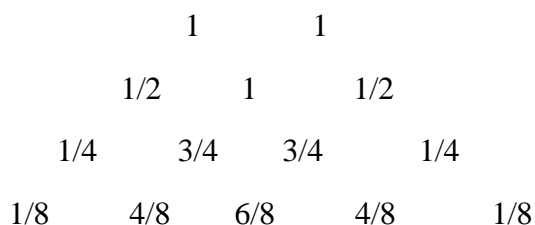\end{array}
$$

Figure 101: the flux pyramid

However, the middle channel should be the fast one, but the results we obtained are that the second and the third are fast. To solve the problem a new device has been designed and fabricated in Figure 102. With the new design, a rectangle structure replaces the pyramid structure.
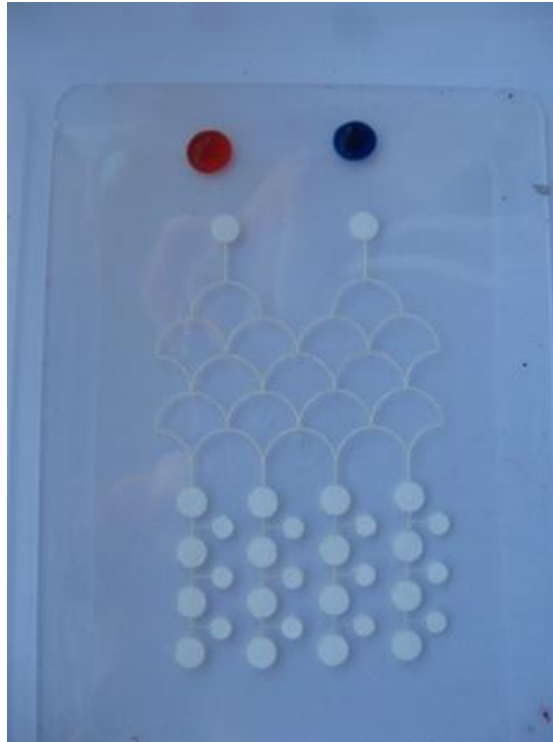
Figure 102: microfluidic mixing paper timer version II

$$1 \qquad\qquad 1$$
$$1/2 \quad 1/2 \qquad 1/2 \quad 1/2$$
$$1/4 \quad 2/4 \quad 2/4 \qquad 2/4 \quad 1/4$$
$$4/8 \quad 4/8 \quad 4/8 \quad 4/8$$
$$4/16 \quad 8/16 \quad 8/16 \quad 8/16 \quad 6/16$$
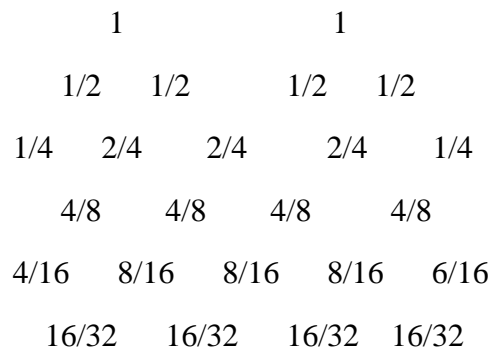$$16/32 \quad 16/32 \quad 16/32 \quad 16/32$$

Figure 103: flux rectangle

Figure 103 shows the flux mixing from two input ends to four output ends. The food color has been mixed and the total flux is the same. When the liquid come to the end of the mixing output end which is the starting of the timer input end. They should run with the same speed and start at the same line. Figure 104 show the yellow and blue food color has been dipped on the two input ends, and they come through the mixing part and timer part. The result is not as good as we expected. The blue food color may run faster than the orange one in the filter paper. The food color used in this experiment are origin one whose concentration may be too high to affect the speed. In Figure 105, the food color has been diluted to 10 times and the blue and yellow food color can run in the

same velocity and reach the timer pads at the same time. Therefore, if the concentration is not too high, the device is suitable.
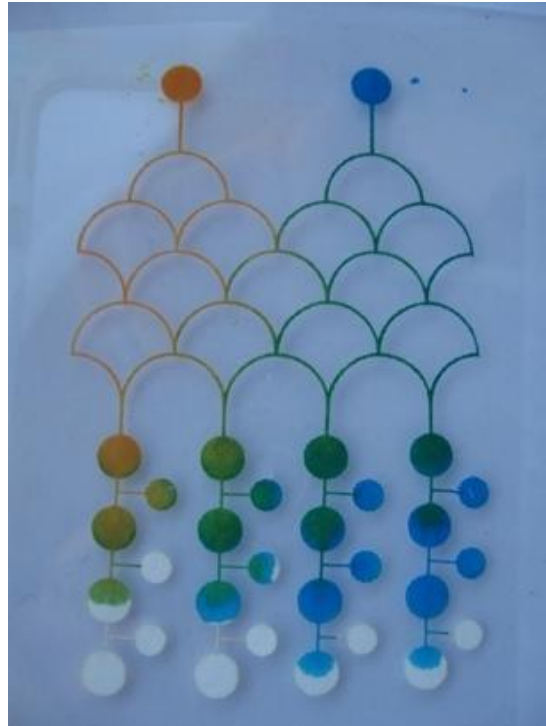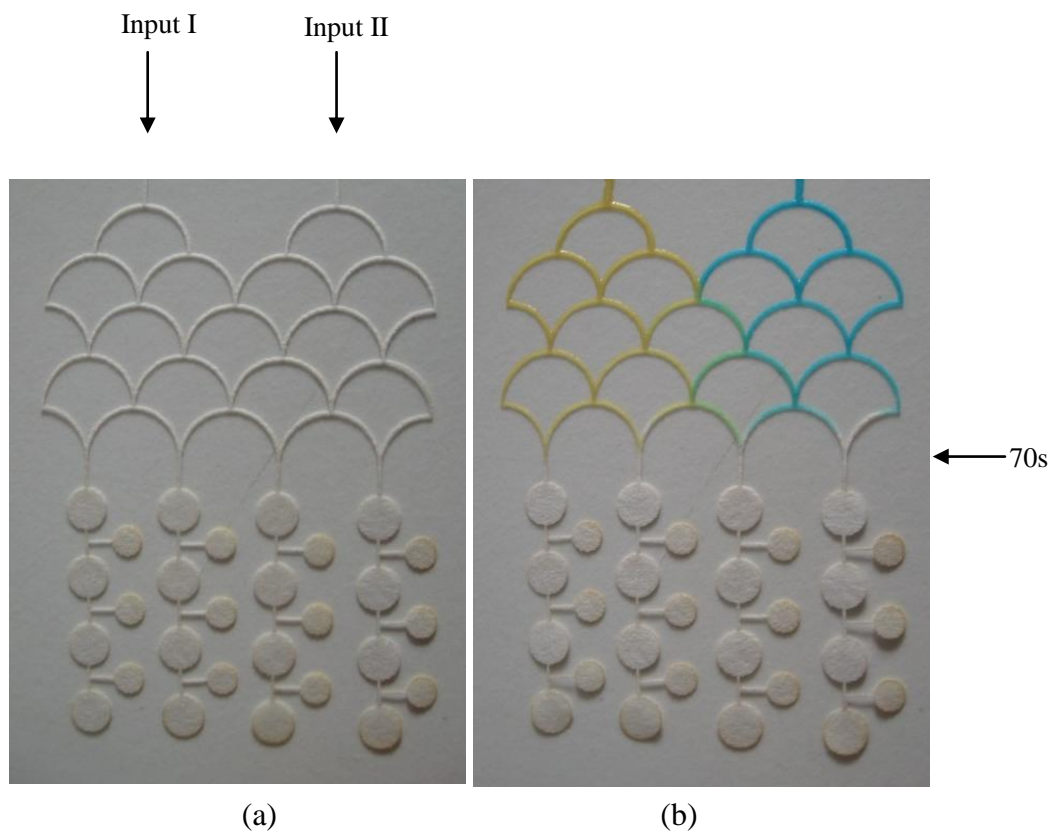

Figure 104: results of microfluidic mixing paper timer with original food color

Input I   Input II

70s

(a)   (b)

(c)　　　　　　　　　　　　　　　　(d)

(e)　　　　　　　　　　　　　　　　(f)

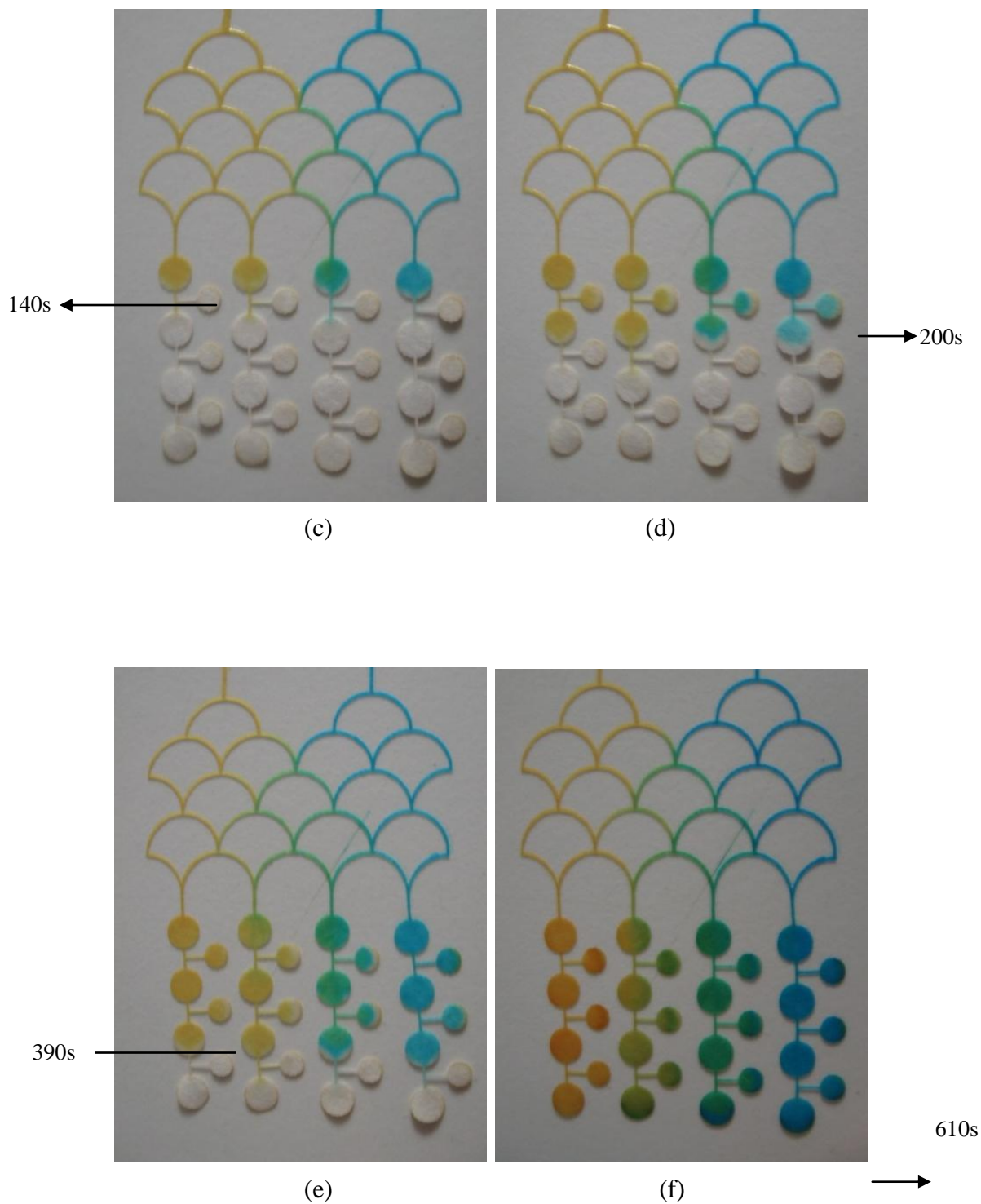Figure 105: From (a) to (f) are results of microfluidic mixing paper timer with diluted food color

Our devices add a time dimensional to paper microfluidic, therefore, time-related reaction can be easily controlled on the device. In Figure 18, time, concentration-related optimum reaction conditions can be obtained via orthogonal experiments with this device. The device can be divided into two parts: part A is used for concentration

proportion, part B is used to control time. Chemical reagent R is printed on small pads, chemical reagent P and Q can come into the device through input I and input II. There are 12 pieces of small pads, in each row, the proportion between P and Q are different, but the time that P-Q reacts with R is the same. On the other hand, in each line, the proportion between P and Q are the same, however, the time that P-Q reacts with R is different. If the device is not pre wet, it will take about 600 seconds, and if the device is pre wet it will take about 4 days. The time can be further controlled with the size of the pads. The device is not limited to 3x4 pads array, which can be expanded to more pads, for different concentration proportion and time gradient.

6.12   Application for biochemical reaction kinetic assay II

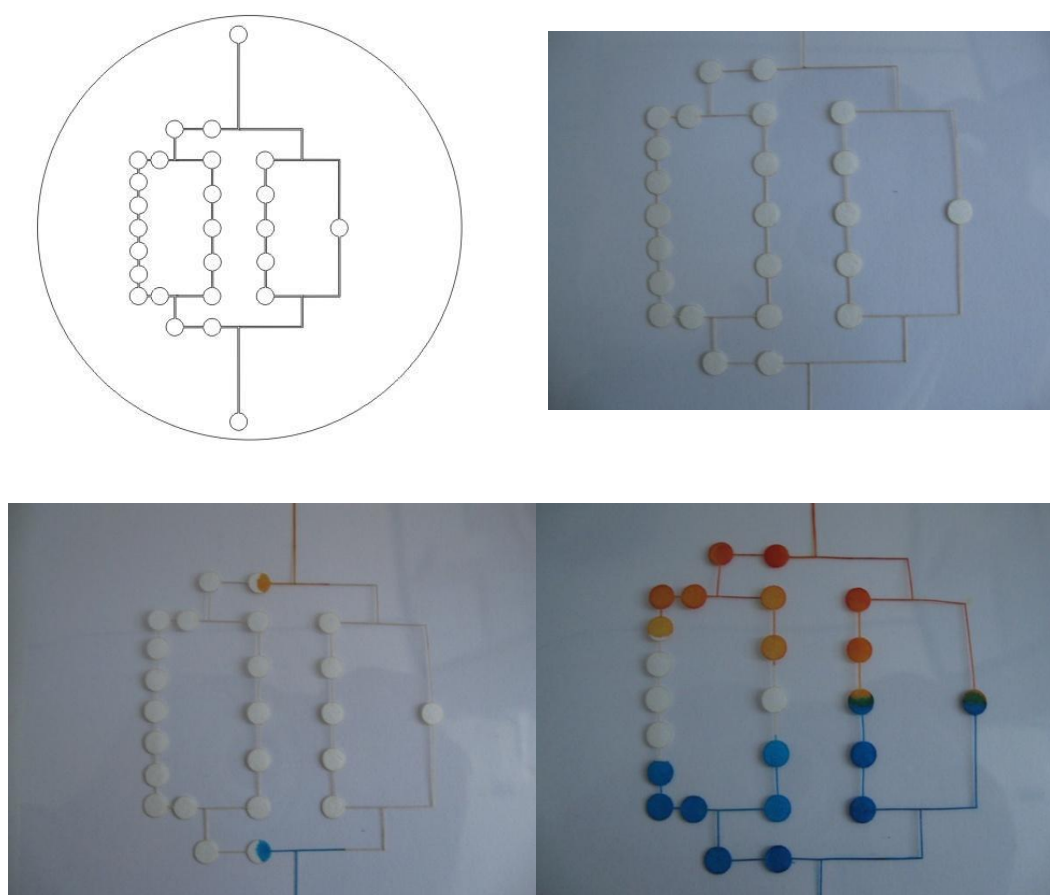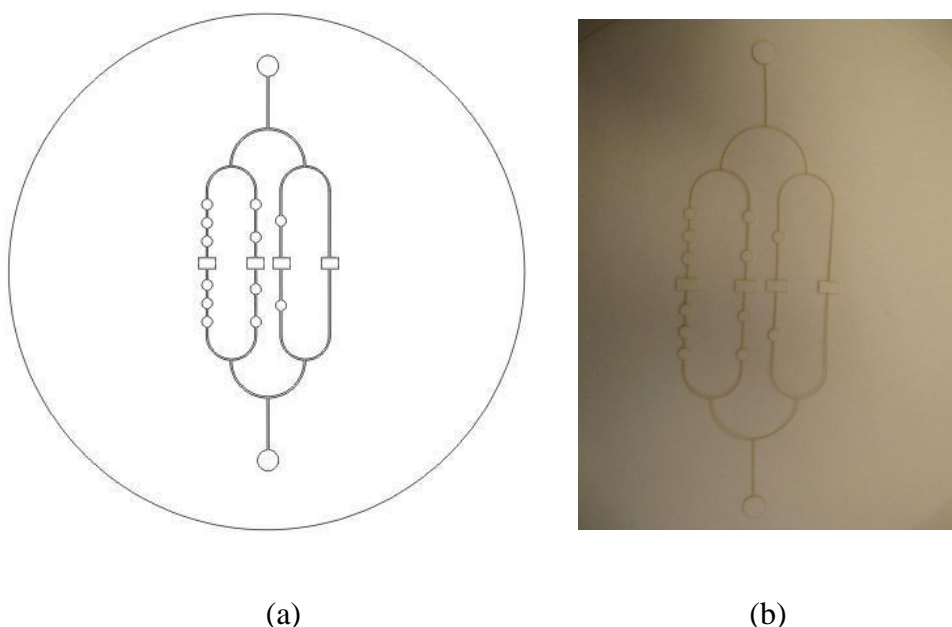Figure 106: The time control reaction device was designed with four channels. From right to left the pads increased from 0 to 6, the middle pad is used for reaction.

In Figure 105, P or Q are time depended reagent, but R is not. If both P and R are time depended reagents, the device will be designed like Figure 106. Figure 106 is a symmetrical structure, which contain four channels. From bottom to top, the number of

cycle pads is increased, which are used to differentiate time. The square in the middle is used for reaction. When reagent P and R are pumped into the device through Input I and II, in each channel, they can reach the middle square at the same time, however, in different channel the reaction time are different. The reaction time can be precise controlled by the number and size of the cycle pads. The reaction time array is also not limited in 4 channels. To make it more reasonable, the time control device has been designed in which the right angle can be changed to semicircle as shown in Figure 107.

(a)   (b)

Figure 107: another version of time control reaction device. A) is designed with autoCAD. B) is fabricated with laser.

6.13 Application for reaction kinetic assay III

(a)

(b)

(c)

(d)

(e)

(f)

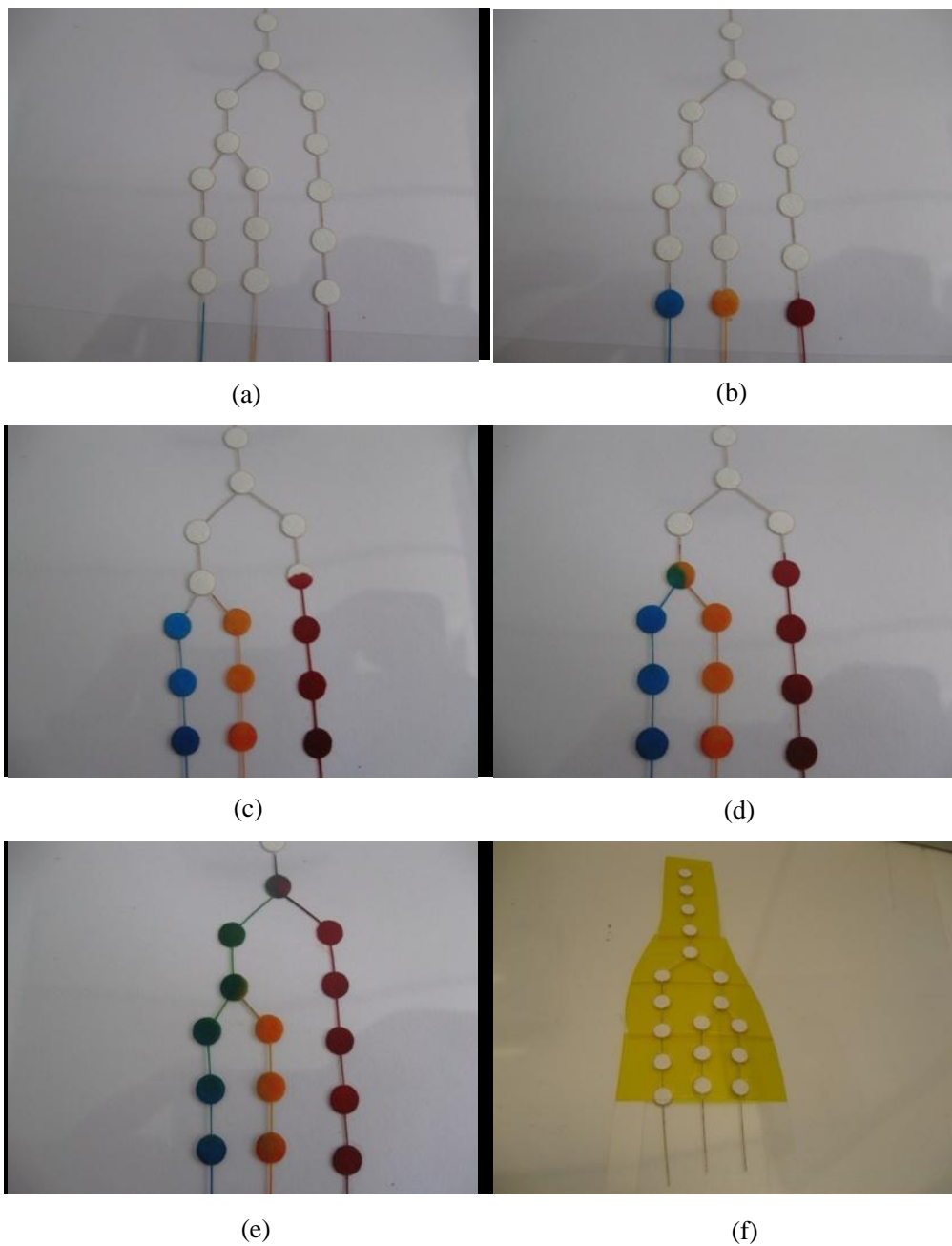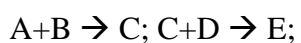Figure 108: application for reaction kinetic assay. From (a) to (e), it shows three food color mixed together. (f) the device packaged in polyimide tape.

In the biochemistry and chemistry experiment, this kind of experiment always required.

A+B → C; C+D → E;

To deal with this kind of experiment, A should be added to B and wait for a few minutes to add C in it. With our device, it can be operated in one step. In

Figure **108** shows a simple device for the reaction. The blue, orange and red food color added on the device on the same time, which can be treated as three different reagents. With the quantity of the pads and the proportion between the line and the pads, it can be controlled that when the blue one and orange one react. When the blue reagent and orange reagent react, and it takes few minutes to react with reagent red. The device can be re-designed more complex to cope different reaction. It has the potential to apply in the test paper. Traditionally, there is only one step reaction in the test paper. If the timer is introduced in the paper, the test paper can carry out multistep with time control reaction.

6.14   Timer for food label.
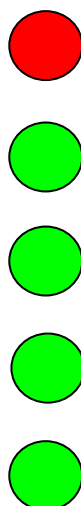
Figure 109: green and red light for food

Over £11bn of food is wasted every year in the UK alone. This is equivalent of £680 per family, much of which is food thrown out whilst still edible and safe to consume. The unique labeling system could have a significant impact on both the amount of food being unnecessarily discarded and in saving people money on their shopping by no longer needing to replace products as often.

The timer can be used as a label to apply at the point of production. When the consumer picks the jar of food off the shelf in the supermarket, the timer is already there and is only activated when the jar is opened for the first time. The timer can display how long

it has been opened since the first opening by a series of squares turning green indicating that it is still safe to use. Once it has reached its "use within" period, the final square turns red warning you that it is no longer safe to consume and can now be discarded. These lights are illustrated in Figure 109.

6.15   Single channel label

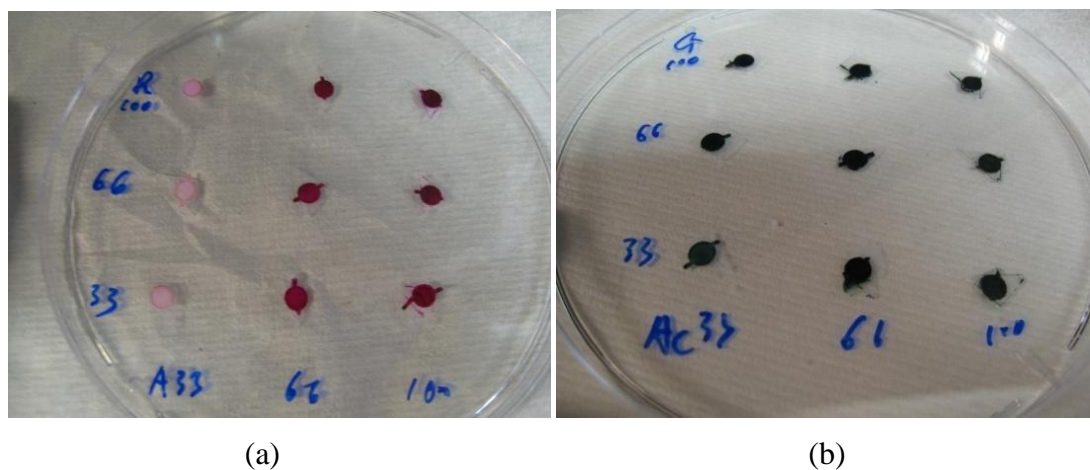(a)   (b)

Figure 110: Red and green pads array. (a) The red pads array. (b) The green pads array.

Pergascript green and Pergascript red are dissolved in 75% ethanol, and the saturated solution are treated at 100%. To find which parameter is suitable for both green and red dye, 18 pads have been put in two Petri dishes (3x3 arrays). On each row the concentration of the dye are 33%, 66% and 100%, respectively. In each line, the concentration of acetic acid varies from 33%, 66% and 100%. In Figure 110A, the red dye seems not very red, the color is near pink, and when the concentration of acetic acid is 33%. The color changed to pink very slowly (about 10mins). As to the green dye, there seems little difference in each line and row.

Figure 111: The color of the pads with 10% acetic acid

If the concentration of acetic acid is too high, it may not be suitable for paper timer. Therefore 10% acetic acid has been tried. As shown in Figure 111, the right pad turns to green, but the left one turns to very light pink. 10% acetic acid may be too low for this experiment.

(a)   (b)   (c)

Figure 112: Single channel label. (a) The channel are coated with the green and red dye. (b) The channel dipped in acetic. (c) The color faded in 3hours later

In Figure 112 the paper timer has been dipped in Pergascript green and pergascript red which concentration is 100%. The first two pads were dipped in the red dye and others were dipped in green dye. When the solutions are dried, one end of the timer has been dipped into 33% acetic. When the acetic comes through the channel, the color changed from green to red in Figure 112B. However 4hours later, the color fades in Figure 112C. The green and red are not very bright. The concentration of the acetic is 33%, which is a hazard to the user. The pergascript green and red are expensive, which are not edible. To solve these problems, a new method has been developed.
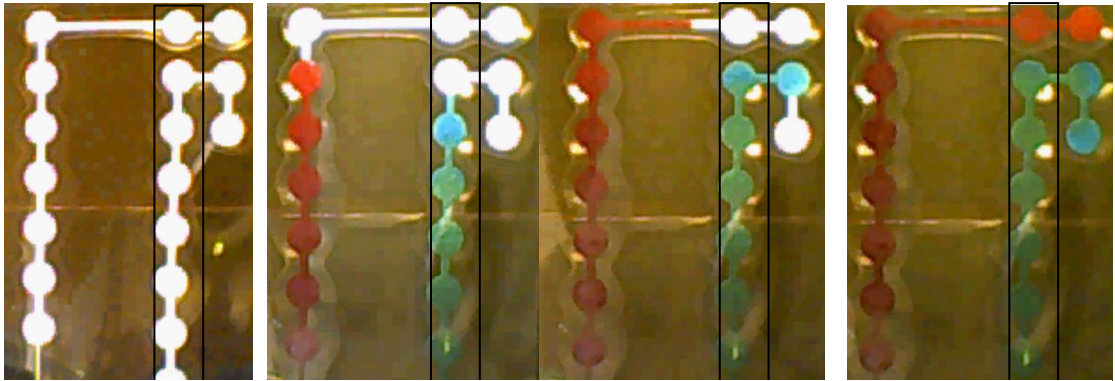
6.16   Multi-channel timer for food label.

Figure 113: Two timers had been injected into the red and green food color at the same time. The back box has been shown to the customer, then they will only see the red and green pads.

Figure 113 shows the timer which has been designed with two channels, each one is with 9 pads. When the jar opened on for the first time, it will triggered the food color to come into the timer. The food color will then run at the same velocity and reach the end at the same time. There is a black box which is used to show to customer. When the green color come to the end, the customer will see the red color just as that shown in Figure 112. The speed can be controlled with different method from minutes to months, which has been mentioned in this chapter. If this label used for milk, a 3-5days timer can be chosen.

Figure 114: green red and yellow light for food label
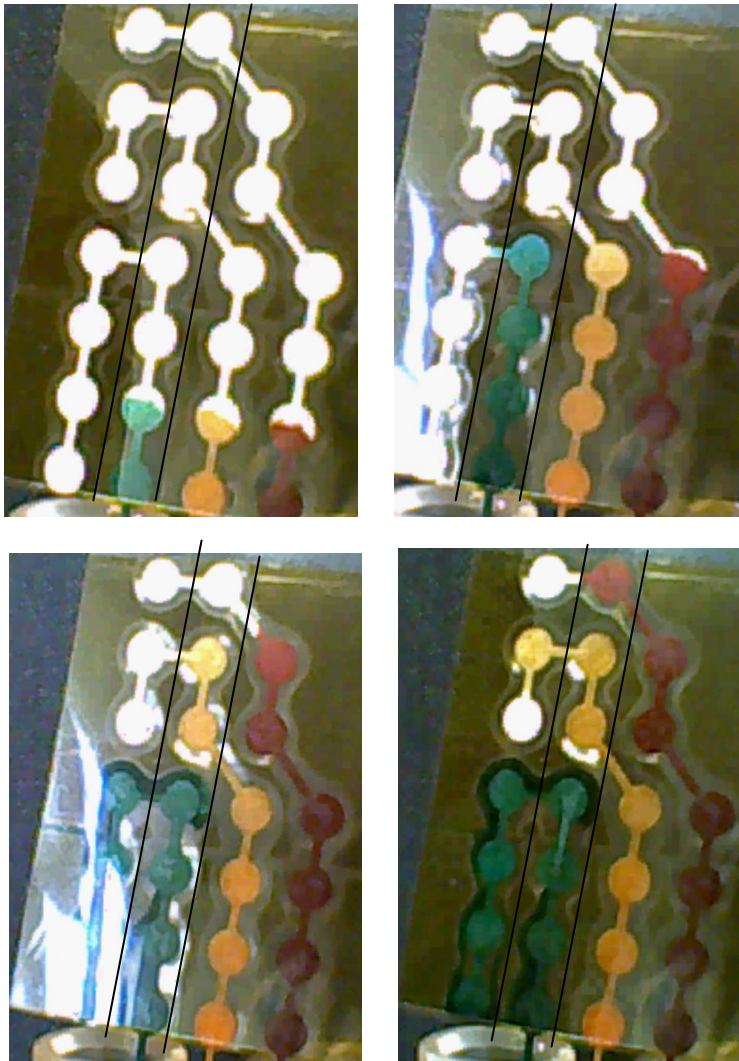

Figure 115: three channels label with red, green and yellow. Between the black lines, the color shows change from green to red.

Figure 114 shows the yellow pad, which is important just like the yellow light is important for the traffic light. When the label turns yellow, it means that the food is still fresh, but it will be not safe to eat. It is quite difficult for the single channel method to make it, but it is easy for the multichannel method to do it. In Figure 115, a three channels label has been fabricated. When the jar is opened on for the first time, it will trigger the three kind of food color to come into the timer at the same time. There is two black lines in each picture of Figure 115, which are used to show to the customer. There are four green pads, two yellow pads, and one red pad between the two black line. The advantage of the device is that it is more considerate than the two color pads, but it need the trigger device to inject three kind of food color at the same time. The trigger device will be discussed in this chapter.

6.16.1 Trigger device version I

When the jar is opened on for the first time, a device will triggered the food color to come into the timer. The device is made of 5 layers in Figure 116. The blue layers (layer 1,2,4,5) are 2mm PMMA, and the yellow layer (layer 3) is membrane. These layers are combined with double side tape.

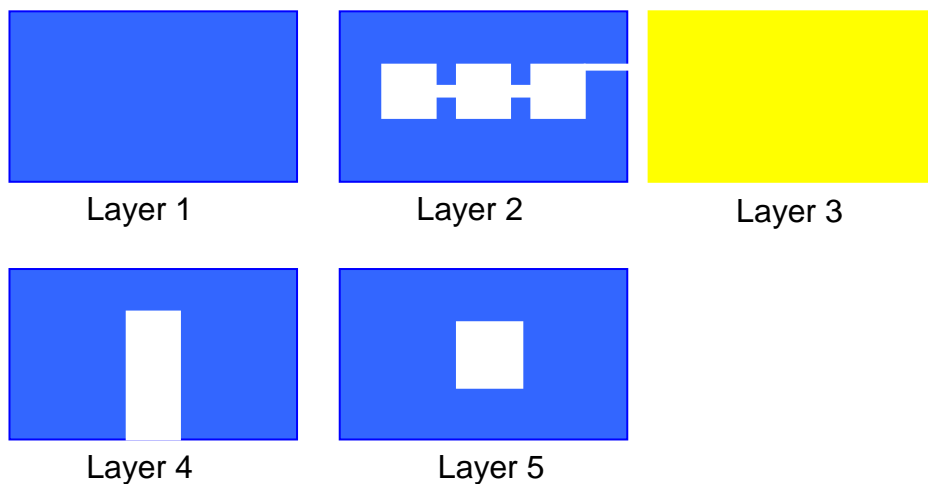**Version I**

Materials

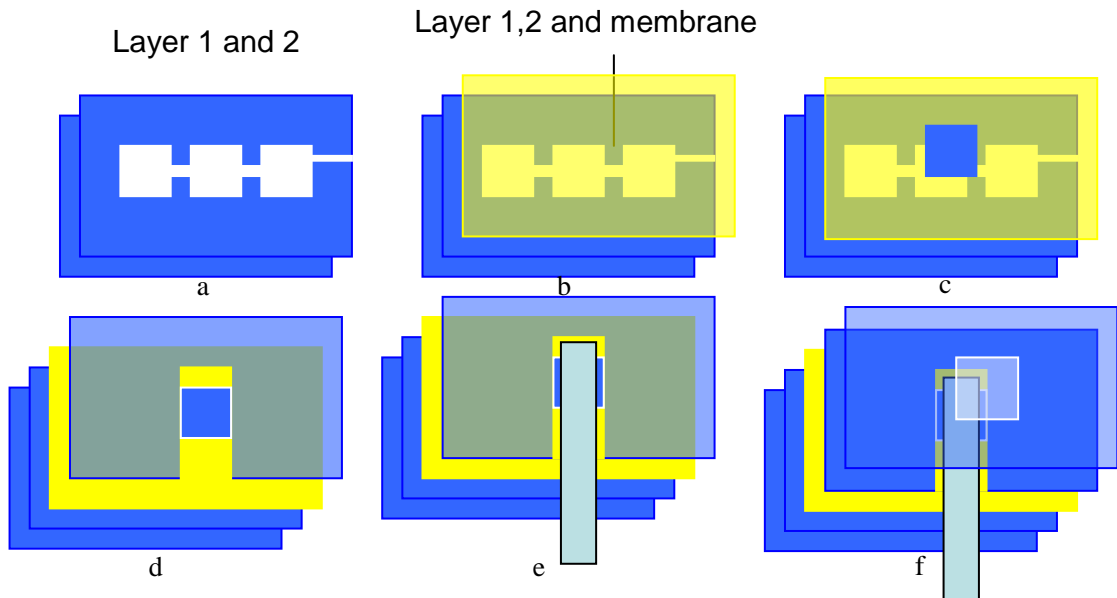

Figure 116:   5 layers for chamber

Scheme

Figure 117: scheme for chamber

Figure 117a shows the layer 1 and layer 2 is combined together with double side tape. The layer 2 is used to contained food color. In Figure 117b, a membrane is attached to seal the chamber. As shown in Figure 117c, a PMMA button is put on the membrane, which is not attached with double side tape. The thickness of the button is 2mm as well. In Figure 117d, Layer 4 is attached the membrane. In Figure 117e, the blue bar which used to turn on the button is to trigger the system. Figure 117f shows the last layer was attached to layer 4, but not the blue bar. In this way, the button can block the middle chamber, but it will be moved away, when the blue bar was removed. When the food color moves to the chamber on the right, the food color will come into the paper timer.

The system is made of PMMA, the width of it is the same as the two pences. Food color was injected into the system with a syringe. When the bar was taken out from it, the food color will be sucked into the middle chamber. However the food color can't go into the third chamber. Therefore, the version II system was made.

6.16.2 Trigger device version II
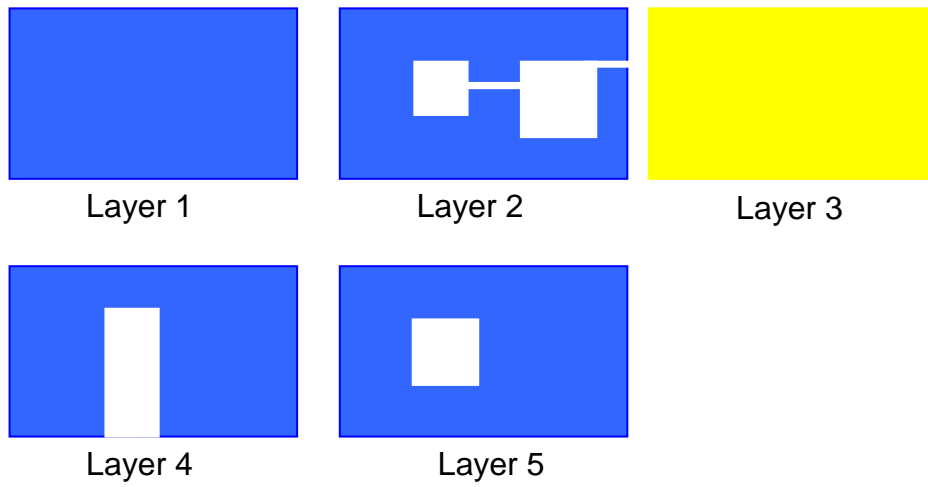
Figure 118: 5 layers for chamber version II

The device was designed with two chambers. It is also fabricated with 2mm PMMA and membrane. Each layer was designed like Figure 118. The blue layer is made of 2mm PMMA, the yellow layer is membrane.

Figure 119: scheme for chamber version II

Figure 120: chamber version II fabricated with laser

In version II, the channel between the two chamber was made narrower than that in version I , therefore it can prevent the ink coming into the second chamber. When the bar was taken out form the system, ink can go into the second chamber.

6.16.3 Trigger device version III

(a)

(b)

(c)

(d)
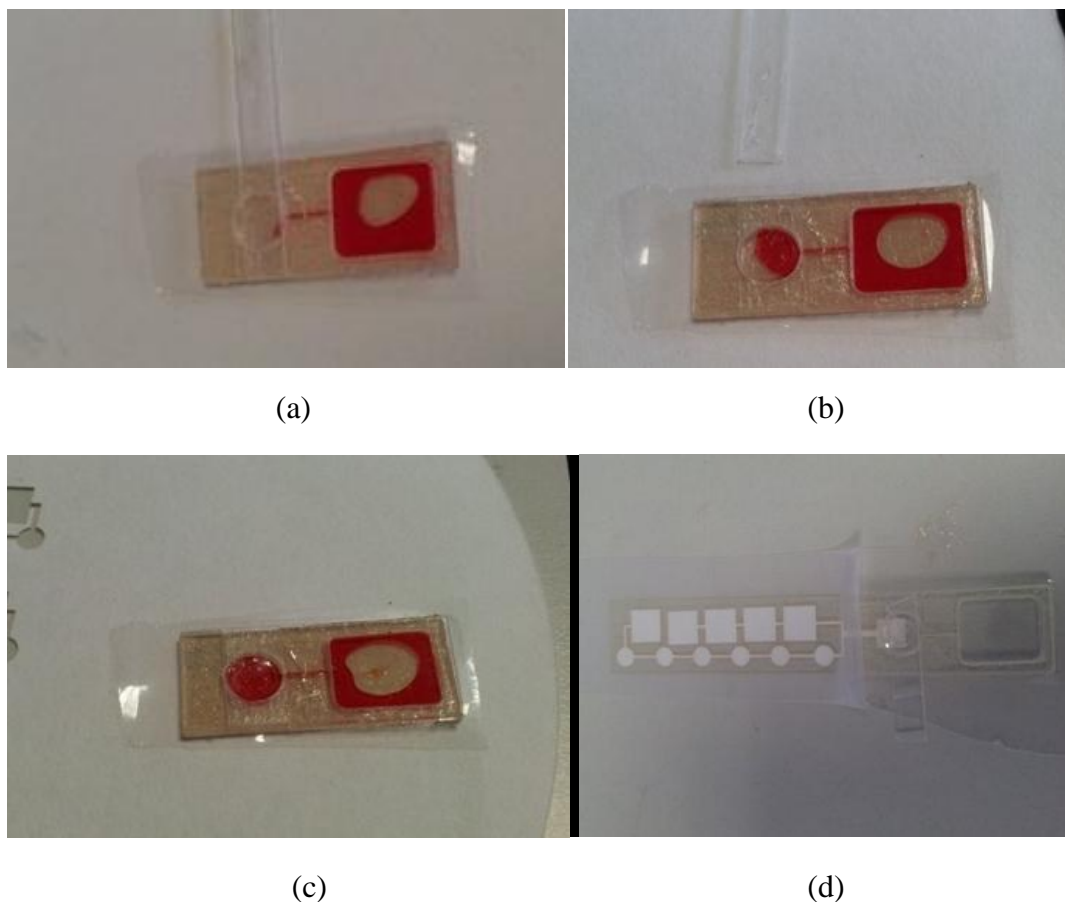
Figure 121: chamber version III (a) The device before triggered. (b) and (c) the device was triggered and the liquid flew form rectangle chamber to cycle chamber. (d) The device jointed with paper timer.
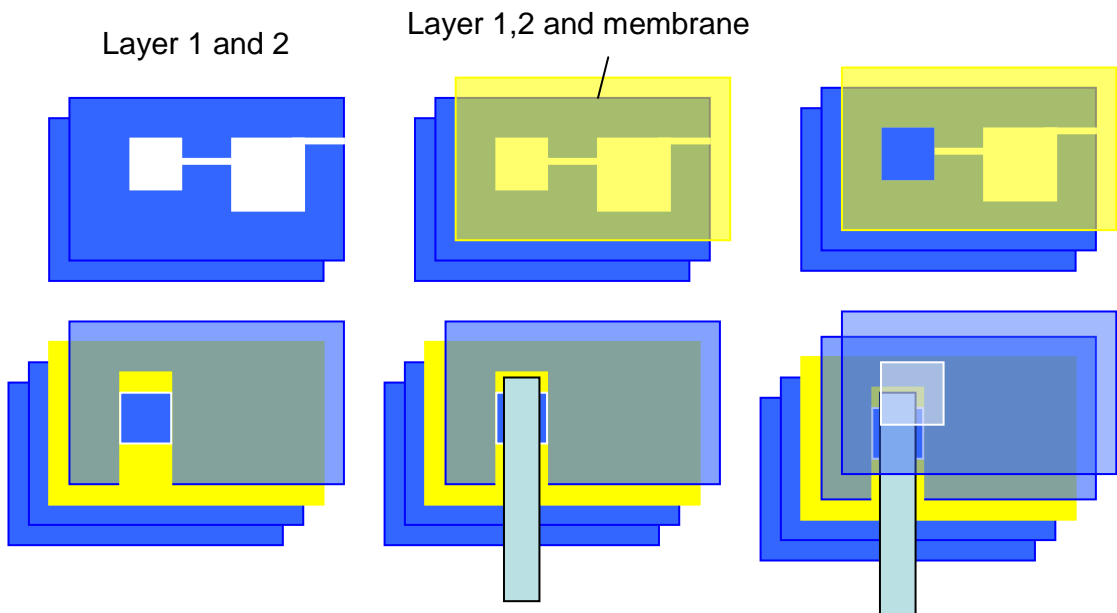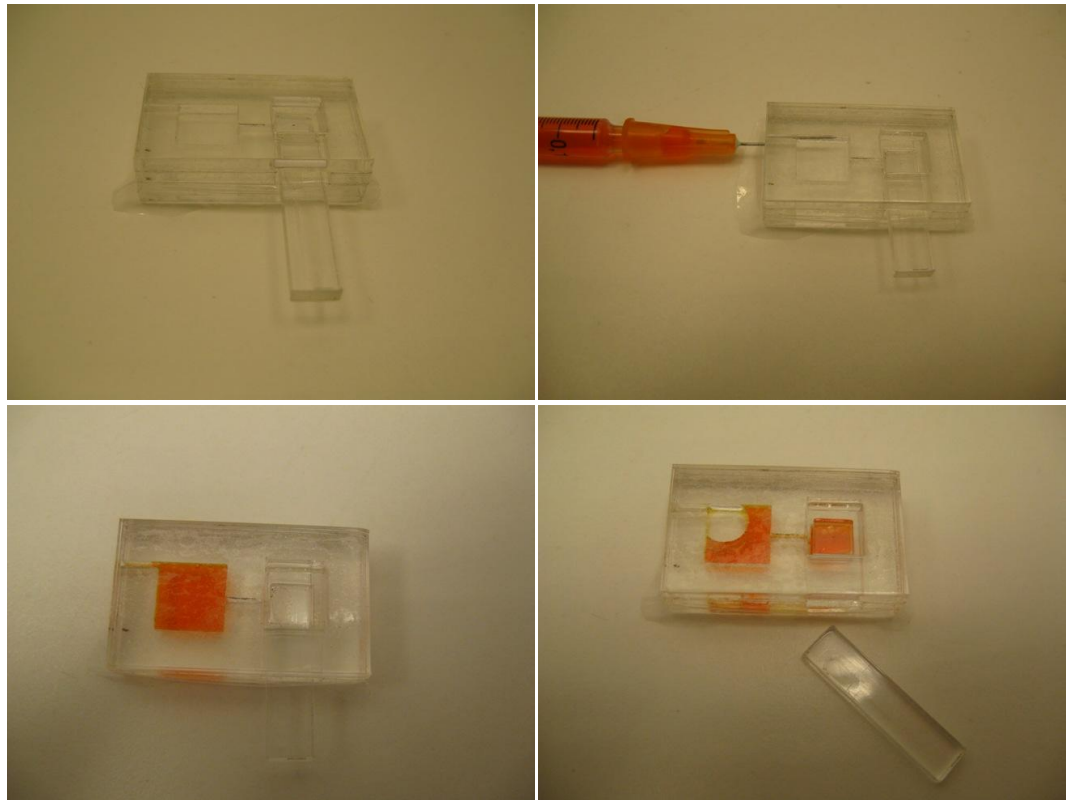
In Figure 121 , it is a new version. The PMMA has been changed to 0.2mm thickness, and the food color has been injected in the chamber when it has been fabricated. In this way, the device became very thin and it needn't needles to inject the food color in it. In Figure 121a, the device was fabricated and a PMMA bar is used to prevent the food color from coming in to the cycle chamber. In Figure 1b, when the bar was taken away through the device, the food color will come into the second chamber.

Few minutes later, the cycle chamber can be filled with food color in Figure 121c. In Figure 121d, the device can connect with the paper microfluidic timer device, which can use as a label for food.

6.17   Summary

❖ A paper microfluidic based device has been developed, which can be used as a timer, time dependent reaction.

❖ Different shape of paper has been tested to find that the paper fabricated like sandglass is the slowest one.

❖ The sandglass like structure has been optimized to find that the thinner the conjunction the slower the timer is. Diffusion and capillary have also been considered to control the speed.

❖ The liquid pumped with diffusion is much slower than capillary. With these conditions, the paper microfluidic based timer can be set from minutes to months.

❖ These parameters have been simulated to predict the situation for long time timer.

❖ A paper microfluidic based mixing and timer device as an application has been developed, which has the potential to be used for biochemical reaction kinetic assay.

❖ A device used to trigger the smart label has been developed with microfluidic technology.

6.18   References for Chapter 6

1.   Andersson, H. and A. Van den Berg, *Microfluidic devices for cellomics: a review.* Sensors and Actuators B: Chemical, 2003. **92**(3): p. 315-325.

2.   Kim, P., et al., *Soft lithography for microfluidics: a review.* 2008.

3.   Duffy, D.C., et al., *Rapid prototyping of microfluidic systems in poly (dimethylsiloxane).* Analytical Chemistry, 1998. **70**(23): p. 4974-4984.

4.   Ocvirk, G., et al., *Electrokinetic control of fluid flow in native poly (dimethylsiloxane) capillary electrophoresis devices.* Electrophoresis, 2000. **21**(1): p. 107-115.

5.   Chin, C.D., V. Linder, and S.K. Sia, *Lab-on-a-chip devices for global health: Past studies and future opportunities.* Lab Chip, 2006. **7**(1): p. 41-57.

6.   Martinez, A.W., et al., *Patterned Paper as a Platform for Inexpensive, Low-Volume, Portable Bioassays.* Angewandte Chemie International Edition, 2007. **46**(8): p. 1318-1320.

7.   Martinez, A.W., et al., *Simple telemedicine for developing regions: camera phones and paper-based microfluidic devices for real-time, off-site diagnosis.* Analytical Chemistry, 2008. **80**(10): p. 3699-3707.

8.   Martinez, A.W., et al., *FLASH: A rapid method for prototyping paper-based microfluidic devices.* Lab Chip, 2008. **8**(12): p. 2146-2150.

9.   Maisel, A.S., et al., *Utility of B-natriuretic peptide as a rapid, point-of-care test for screening patients undergoing echocardiography to determine left ventricular dysfunction.* American heart journal, 2001. **141**(3): p. 367-374.

10.   Tefferi, A. and J.W. Vardiman, *Classification and diagnosis of myeloproliferative neoplasms: the 2008 World Health Organization criteria and point-of-care diagnostic algorithms.* Leukemia, 2007. **22**(1): p. 14-22.

11.   Wang, J., *Electrochemical biosensors: towards point-of-care cancer diagnostics.* Biosensors and Bioelectronics, 2006. **21**(10): p. 1887-1892.

12.   Price, M.J., et al., *Prognostic significance of post-clopidogrel platelet reactivity assessed by a point-of-care assay on thrombotic events after drug-eluting stent implantation.* European heart journal, 2008. **29**(8): p. 992-1000.

13.   Kottke, P.A., F.L. Degertekin, and A.G. Fedorov, *Scanning mass spectrometry probe: A scanning probe electrospray ion source for imaging mass spectrometry of submerged interfaces and transient events in solution.* Analytical Chemistry, 2009. **82**(1): p. 19-22.

14.   Liu, W. and D.A. Saint, *A new quantitative method of real time reverse transcription polymerase chain reaction assay based on simulation of polymerase chain reaction kinetics.* Analytical biochemistry, 2002. **302**(1): p. 52-59.

15.   Chen, C.S., et al., *Quantitative analyses of biochemical kinetic resolutions of enantiomers.* Journal of the American Chemical Society, 1982. **104**(25): p. 7294-7299.

16.   Shan, X. and G. Doolen, *Diffusion in a multicomponent lattice Boltzmann equation model.* Physical Review E, 1996. **54**(4): p. 3614.

17.   Michael, C., T. Daniel, and J. Thome, *Lattice Boltzmann Modeling; An*

Introduction for Geoscientists and Engineers. 2006, Springer Berlin.

Chapter 7 Conclusions and Future work

7.1 Conclusions

In this thesis, different methods have been investigated in order to improve the performance of microcantilever sensors by amplifying the sensing signals. Alternative materials such as polyimide and paper with lower Young's modulus than silicon/silicon nitride have been studied in this thesis. According to the Stoney's equation, the sensitivity or the bending signal of polymer and paper cantilevers are higher than the silicon ones thanks to the lower Young's modulus of the cantilever. Double-side coated receptors polyimide based microcantilever sensor has been used to build an internally referenced microcantilever system. A polymer based microcantilever sensor with embedded microfluidic channel system has also been developed, and found it can not only improve the detection sensitivity but also need the tiny amount of sample.

Compared to QCM and SPR, cantilevers have some advantages, but there are still several problems to be solved, such as expensive, time-cost to fabricated, reference, signal need to be amplified etc. Our objectives are focused on solving some of these problems. Polyimide films have been used to fabricate cantilevers, which is much cheaper than silicon, and it is more sensitive due to the oung's module is lower. It is easy to fabricate and hundreds of cantilevers can be fabricated within few minutes.

An internally referenced polyimide based cantilever system has been developed, with the receptor and reference receptor immobilized evenly on both the top and the bottom of each cantilever without cross contamination. The surface quality and the thickness of the gold layer are controlled to be identical on both sides of each chip. The problems of unwanted bimetallic effects and cross contamination of receptors on each side can be solved perfectly in addition to other advantages, including: (1) the reference receptors on one side are used as a control to adjust the difference between each cantilever, therefore cancelling the system errors among cantilevers. (2) With this method, thousands of double sided functionalised cantilevers can be fabricated within a few

148

minutes, and the receptors on each side do not cross contaminate each other. (3) Polymer based cantilevers are more sensitive and have lower cost than traditional silicon based cantilevers. DNA hybridization experiments have been performed to show the application of the method, and DNA concentration and single mismatch detection will be presented in our work.

Paper based microfluidic timing device has been developed with paper based microfluidics technology. Many reactions are also time dependent, for example, biochemical reaction kinetic assay. We describe a method for time control reaction, which can control time from minutes to months. It has many potential applications, for example, reaction kinetic assay, timer label for food.

Previously, cantilevers have been embedded within microfluidic systems; The Manalis group have developed microfluidics upon cantilevers, manufactured from silicon and employed in the resonance mode. This highly successful strategy has lead to the weighing of single cells in fluid. In this thesis, smaller-scale microfluidics, which fits onto the cantilever surface itself, has been demonstrated. The main advantage of the system presented here is that since the device is made entirely of polyimide it is both cheaper and easier to manufacture.

7.2 Future work

The cantilever can be coated on each side with different receptors in this thesis, but current study is limited to small number of functionalised cantilevers. Further work could include the use of ink-jet printing for large array of functionalised cantilever sensors, further applications. The thickness of the polymer we have investigated is 7.8µm, thinner microcantilevers can be fabricated to further increase the sensitivity.

The performance of microfluidic channel based cantilever system could be improved by using thinner polyimide carrier, more reliable adhesive layer and photoresist. The polyimide carrier is 7.8µm, the polyimide tape is 25µm, and the photoresist is 20um. All of them can be much thinner, if sensitivity needs to be increased. The magnetic field can

be increased to improve the sensitivity, and we need not worry that it will break the bond between the receptors and analyte to affect the results, because the magnets are in the channel, even when the bonds have been broken, the results are not affected. Electromagnets can be used in the future, and we need not to move the magnet field away and move it back physically. It will be easy to manipulate. The system has the potential to detect cell and other biological species in the future. We have used the system to detect liquid density using buffer solutions. In the future, we can study the details of this experiment for more meaningful fluids.

The limitation of paper microfluidic base microcantilever sensors is the magnetic beads are pumped very slowly in the paper microfluidic channel. It may be improved with different kinds of paper or magnetic beads. The device for timer needs the liquid much slower if we want to label it for longer time period. Chemical reagent can be added to the channel to slow down the speed of the food colour in the channel. The device used to trigger the paper timer system can be improved by using thinner materials. The alternative membrane can be found which is not only waterproof but also not permeable to air, because the liquid in the chamber can be evaporated within a few months' time. Therefore, for the development of longer timing device, the membrane for packaging need to be changed.